ISSN 1916-6117 (online)
ISBN 978-1-4435-9958-0 (PDF)

ISSN 0826-9580 (print)
ISBN 978-1-4435-9958-0 (print)

It is recommended that reference to the Content be made in the following form:

Gao, C. 2012. Results of regional till sampling in the Cobalt–New Liskeard–Englehart areas, northern Ontario; Ontario Geological Survey, Open File Report 6259, 87p.

Contact:

FOR FURTHER INFORMATION ON	PLEASE CONTACT:	BY TELEPHONE:	BY E-MAIL:
The Reproduction of the Content	MNDM Publication Services	Local: (705) 670-5691 Toll-Free: 1-888-415-9845, ext. 5691 (inside Canada, United States)	Pubsales.ndm@ontario.ca
The Purchase of MNDM Publications	MNDM Publication Sales	Local: (705) 670-5691 Toll-Free: 1-888-415-9845, ext. 5691 (inside Canada, United States)	Pubsales.ndm@ontario.ca
Crown Copyright	Queen's Printer	Local: (416) 326-2678 Toll-Free: 1-800-668-9938 (inside Canada, United States)	Copyright@gov.on.ca

Ontario

Ontario Geological Survey
Open File Report 6259

Results of Regional Till Sampling in the Cobalt–New Liskeard–Englehart Areas, Northern Ontario

2012

Ontario

ONTARIO GEOLOGICAL SURVEY

Open File Report 6259

Results of Regional Till Sampling in the Cobalt–New Liskeard–Englehart Areas, Northern Ontario

by

C. Gao

2012

Parts of this publication may be quoted if credit is given. It is recommended that reference to this publication be made in the following form:

Gao, C. 2012. Results of regional till sampling in the Cobalt–New Liskeard–Englehart areas, northern Ontario; Ontario Geological Survey, Open File Report 6259, 87p.

Users of OGS products are encouraged to contact those Aboriginal communities whose traditional territories may be located in the mineral exploration area to discuss their project.

Open File Reports of the Ontario Geological Survey are available for viewing at the John B. Gammon Geoscience Library in Sudbury and at the regional Mines and Minerals office whose district includes the area covered by the report (see below).

Copies can be purchased at Publication Sales and the office whose district includes the area covered by the report. Although a particular report may not be in stock at locations other than the Publication Sales office in Sudbury, they can generally be obtained within 3 working days. All telephone, fax, mail and e-mail orders should be directed to the Publication Sales office in Sudbury. Purchases may be made using cash, debit card, VISA, MasterCard, American Express, cheque or money order. Cheques or money orders should be made payable to the *Minister of Finance.*

John B. Gammon Geoscience Library 933 Ramsey Lake Road, Level A3 Sudbury, Ontario P3E 6B5	Tel:	(705) 670-5615
Publication Sales 933 Ramsey Lake Rd., Level A3 Sudbury, Ontario P3E 6B5	Tel: Toll-free: Fax: E-mail:	(705) 670-5691 (local) 1-888-415-9845 ext. 5691 (705) 670-5770 pubsales.ndm@ontario.ca

Regional Mines and Minerals Offices:

Kenora - Suite 104, 810 Robertson St., Kenora P9N 4J2

Kirkland Lake - 10 Government Rd. E., Kirkland Lake P2N 1A8

Red Lake - Box 324, Ontario Government Building, Red Lake P0V 2M0

Sault Ste. Marie - 875 Queen St. E., Suite 6, Sault Ste. Marie P6A 6V8

Southern Ontario - P.O. Bag Service 43, 126 Old Troy Rd., Tweed K0K 3J0

Sudbury - 933 Ramsey Lake Rd., Level A3, Sudbury P3E 6B5

Thunder Bay - Suite B002, 435 James St. S., Thunder Bay P7E 6S7

Timmins - Ontario Government Complex, P.O. Bag 3060, Hwy. 101 East, South Porcupine P0N 1H0

Cette publication est disponible en anglais seulement.

Parts of this report may be quoted if credit is given. It is recommended that reference be made in the following form:

Gao, C. 2012. Results of regional till sampling in the Cobalt–New Liskeard–Englehart areas, northern Ontario; Ontario Geological Survey, Open File Report 6259, 87p.

Contents

FIGURES

TABLES

Miscellaneous Release—Data 284

Till Sample and Indicator Mineral Data for the Cobalt, New Liskeard and Englehart Areas, Northern Ontario

by C. Gao

This release presents the results of a regional till sampling and surficial mapping project undertaken in the Cobalt, New Liskeard and Englehart areas in northern Ontario between 2007 and 2009. The results consist of geochemical and compositional data of kimberlite indicator minerals (KIMs), metamorphic/magmatic massive sulphide indicator minerals (MMSIM®) and gold grains recovered from till and glaciofluvial sand and gravel samples. The data are being released in conjunction with Open File Report 6259, available separately. Files in this release contain information on sample site locations; a list of abbreviations; sample processing data; KIMs picked and picking remarks; microprobe analyses of KIMs; gold grain data; MMSIM® data; pebble lithology data; and adjusted KIM and MMSIM® results. The data are available on 1 CD.

These digital data are available separately from this report.

Abstract

More than 1700 gold and 14 000 kimberlite indicator mineral (KIM) grains were counted or estimated from 151 till and 16 glaciofluvial sand and gravel samples collected in the Cobalt, New Liskeard and Englehart areas in northern Ontario during regional till sampling and surficial mapping conducted between 2007 and 2009. Up to 58 gold grains were recovered from individual samples with some containing relatively abundant pristine gold grains indicating possible proximity to source areas. There are quite a few samples that contain anomalous numbers of KIM grains with 871 being recovered from a single sample. The KIM assemblages are dominated by ilmenite and pyrope garnets. Some samples contain harzburgitic G10D, pyroxenitic/lherzolitic, pyroxenitic/eclogitic and eclogitic G5D, G4D and G3D garnets, as well as chromites classified in the diamond inclusion and intergrowth field, indicating diamondiferous source areas. Most of the anomalies do not appear to be associated with the known kimberlite pipes, suggesting a high potential for finding new kimberlite pipes in the study area. The presence of large concentrations of low-Cr diopside in conjunction with chalcopyrite grains suggests the potential for magmatic nickel and copper mineralization in this region.

Results of Regional Till Sampling in the Cobalt–New Liskeard–Englehart Areas, Northern Ontario

C. Gao[1]

Ontario Geological Survey
Open File Report 6259
2012

[1]Geoscientist, Sedimentary Geoscience Section, Ontario Geological Survey

Introduction

Thick and extensive surficial deposits have hampered mineral exploration in parts of the Abitibi greenstone belt. The New Liskeard and Englehart areas, represented by the 1:50 000 National Topographic System (NTS) map sheets 31 M/12 and 31 M/13, were identified for surficial mapping and till sampling for indicator minerals (Figure 1). The adjacent Cobalt area (NTS 31 M/5) located in Precambrian terrain was also mapped because of the presence of known kimberlite pipes and the high potential for diamond mineralization (Ayer et al. 2006). This area used to be a major silver producing camp in Ontario following the discovery of high-grade silver veins near the town of Cobalt in 1903 (Nichols 1988). However, the silver mines remain closed due to the low price of this commodity. The recent discovery of a boulder containing high grade gold in the Cobalt area indicates the potential for significant gold mineralization in this region (Temex Resources Corporation 2011).

Modern alluvium sampling projects were previously conducted in the western and southern parts of the current project area (Reid 2002, 2004; Guindon and Reid 2005). The results of the previous studies show anomalous concentrations of indicator minerals and high potential for finding new kimberlites and gold mineralization. The till sampling in the current project corroborates the indicator mineral data generated previously and also provides further information on mineral potential in this region. Till deposits at the base of ice sheets contain rock fragments and minerals that are closely related to and, generally, not far from their source areas in the up-ice direction. Indicator minerals from basal till can thus provide important information on locating the source areas for mineral exploration follow-up.

Additional sampling was undertaken in 2008 and 2009 after the first sampling summer in 2007 which showed prominent anomalies in some areas. Sampling over the three years has generated the 07CG-, 08CG- and 09CG-series of sample numbers in the report (Figure 2; Appendix 1). This report summarizes the results of this work and is being released in conjunction with Miscellaneous Release—Data (MRD) 284 that contains all of the study data in digital format (Gao 2012). The Appendix numbering in this report is consistent with the data description in MRD 284; however, only a select number of data tables are included in the Appendixes. The Table of Contents (*see* "Contents") indicate which tables and/or data are available in this report. The Quaternary geology maps from this project area were released previously (Baker, Gao and Perttunen 2010; Gao 2010a, 2010b).

Bedrock Geology

The study area encompasses the Cobalt kimberlite field where more than 15 kimberlite pipes of Jurassic age have been discovered to date, mostly along the western flank of the Lake Timiskaming Structural Zone that is defined by the northwest-trending Paleozoic Lake Timiskaming graben and a group of faults in the same alignment across the map area (*see* Figure 1). As well, the northern part of the study area is located adjacent to the Kirkland Lake kimberlite field where many kimberlite pipes have been identified. Lamprophyre dikes of Proterozoic age occur within the study area and some contain macrodiamonds (Grabowski and Wilson 2005). Within the study area, the Archean bedrock occurs north of Englehart and the Proterozoic in the southwest, whereas Paleozoic carbonate rocks occur in the the centre of the Lake Timiskaming graben (*see* Figure 1).

The Archean bedrock consists of mafic flow-dominated volcanic rocks with mafic, ultramafic and granitic intrusives (Ayer et al. 2006). In the southwestern part of the report area, it is overlain by thick, flat-lying Proterozoic sedimentary rocks consisting of argillite, arkose, greywacke, conglomerate and

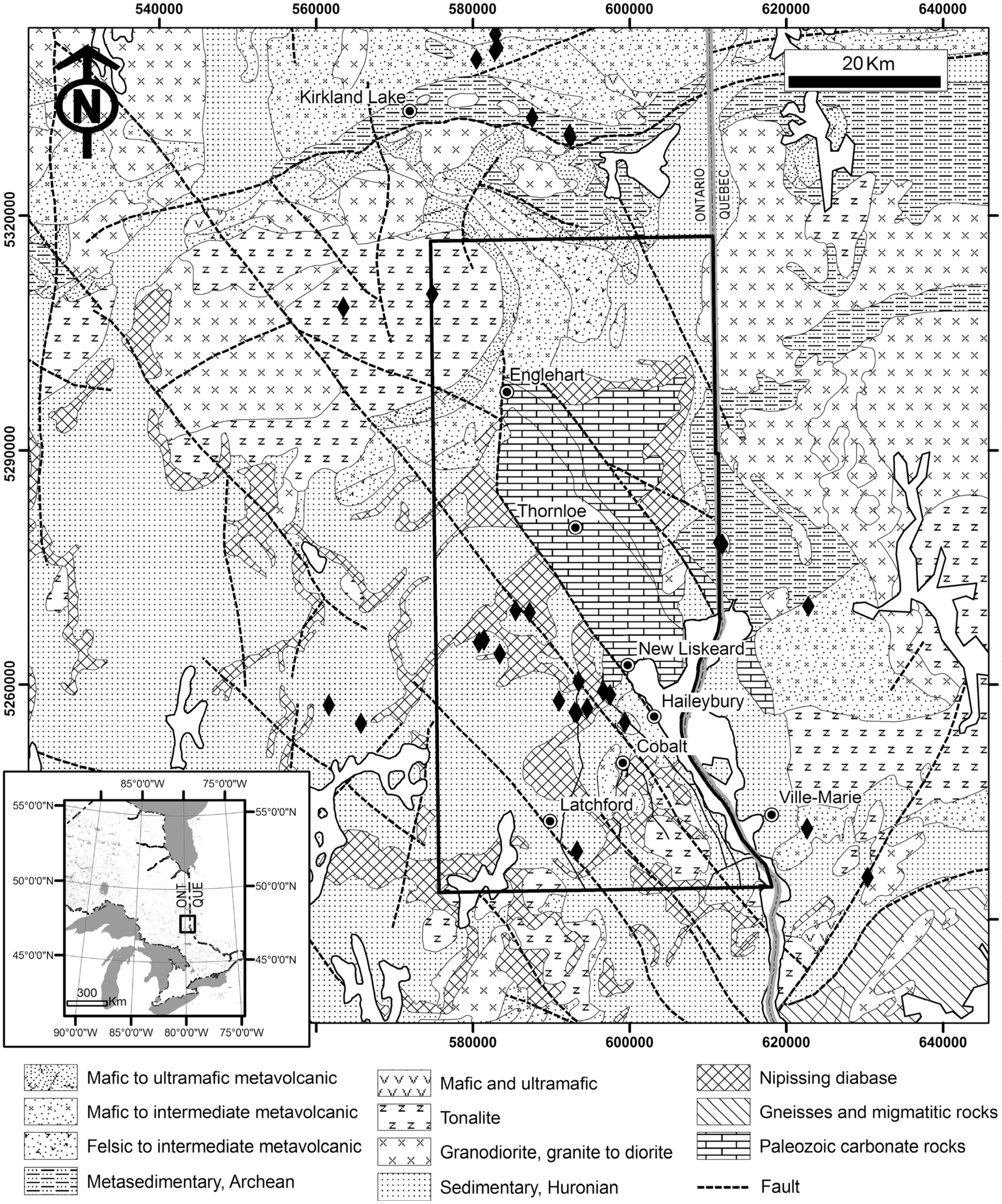

Figure 1. Location map and bedrock geology of the study area (*after* OGS 1991).

tillite of the Cobalt Group within the Huronian Supergroup. The Archean and Proterozoic rocks were later intruded by a 300 m thick Nipissing gabbro sill of Neoproterozoic age (Ayer et al. 2006). Silver and cobalt mineralization often occurs in calcite veins in the Proterozoic sedimentary rocks, in particular, in the lower part of the Cobalt Group (Nichols 1988). Recent studies suggest that such veins may have the potential for hosting high grade gold deposits in this region (Temex Resources Corporation 2011). During the Paleozoic Era, the Lake Timiskaming Structural Zone, a northwest-trending rift system, developed, forming a large graben within which thick deposits of Paleozoic carbonate rocks accumulated (Russell 1984). The emplacement of the kimberlite pipes within this region appears to be closely related to this structure (Sage 2000).

Quaternary Geology

The major Quaternary or surficial deposits in this region include till, glaciofluvial sand and gravel and glaciolacustrine silt and clay (Figure 3) (Baker, Gao and Perttunen 2010; Gao 2010a, 2010b). The till deposits show distinct compositional variability closely reflective of the underlying bedrock. Deposits on the Precambrian bedrock terrain are commonly less than 1 m thick although accumulations of 3 to 5 m thick occur locally in bedrock depressions or on the lee sides of rock ridges and hillocks. The deposits are usually noncalcareous and have a sandy texture with numerous boulders of Precambrian affinity. In contrast, till deposits on the Paleozoic carbonate bedrock usually exceed 2 m in thickness, are calcareous and have a sand to silt texture with abundant carbonate clasts. The 2 tills were likely emplaced during a single ice advance during the Late Wisconsinan and can probably be correlated to the Matheson Till mapped in the adjacent areas (Hughes 1965; Baker 1985; Gao and Kodors 2009).

The regional ice flows, as indicated by striae, exhibit a south-southwest (180 to 220°) direction which later changes to the south-southeast (130 to 170°) (McClenaghan and Veillette 2001; Baker, Gao and Perttunen 2010; Gao 2010a, 2010b). There is little evidence to suggest that the cross striations are associated with more than one major ice advance during the Late Wisconsinan in this region (Baker, Gao and Perttunen 2010; Gao 2010a, 2010b). They probably resulted from the same ice mass that deposited the Matheson Till but were subjected to a change in the general flow direction from the south-southwest to the southeast (Veillette 1986).

Prominent glaciofluvial deposits occur in the study area. The largest one commences south of Charlton and runs to the southeast, passing between Cobalt and Latchford (*see* Figure 3). This glaciofluvial system contains eskers and numerous kettle holes, especially in its northernmost part, south of Charlton. North of Englehart, an elongated glaciofluvial deposit consists mainly of a southward-aligned esker that makes up the southern extension of a large esker system referred to as the Munro Esker, to the north (Baker 2000). It is noteworthy that, at the intersection between Highway 11 and Sharpe Lake Road, a small, south-trending esker referred to as the Sharpe Lake Esker occurs along the western shore of Sharpe Lake. Although this esker has undergone intense extraction for sand and gravel material in the past, a segment about 50 m long remains intact in its northernmost part where a southward-aligned narrow ridge stands about 10 m high above the lake. Kimberlite boulders from this esker, have been reported in the past (Kjarsgaard et al. 2004), and many more collected recently (Baker, Gao and Perttunen 2010).

During the Late Wisconsinan deglaciation, proglacial lakes Barlow–Ojibway developed in front of the retreating ice margin, inundating a large portion of the study area and extending northward across the continental drainage divide (Vincent and Hardy 1979; Baker 1985; Baker, Gao and Perttunen 2010; Gao 2010a, 2010b). The resultant glaciolacustrine clay and silt mantles the till and associated deposits within the Lake Timiskaming graben and discontinuously veneers the Precambrian bedrock terrain elsewhere

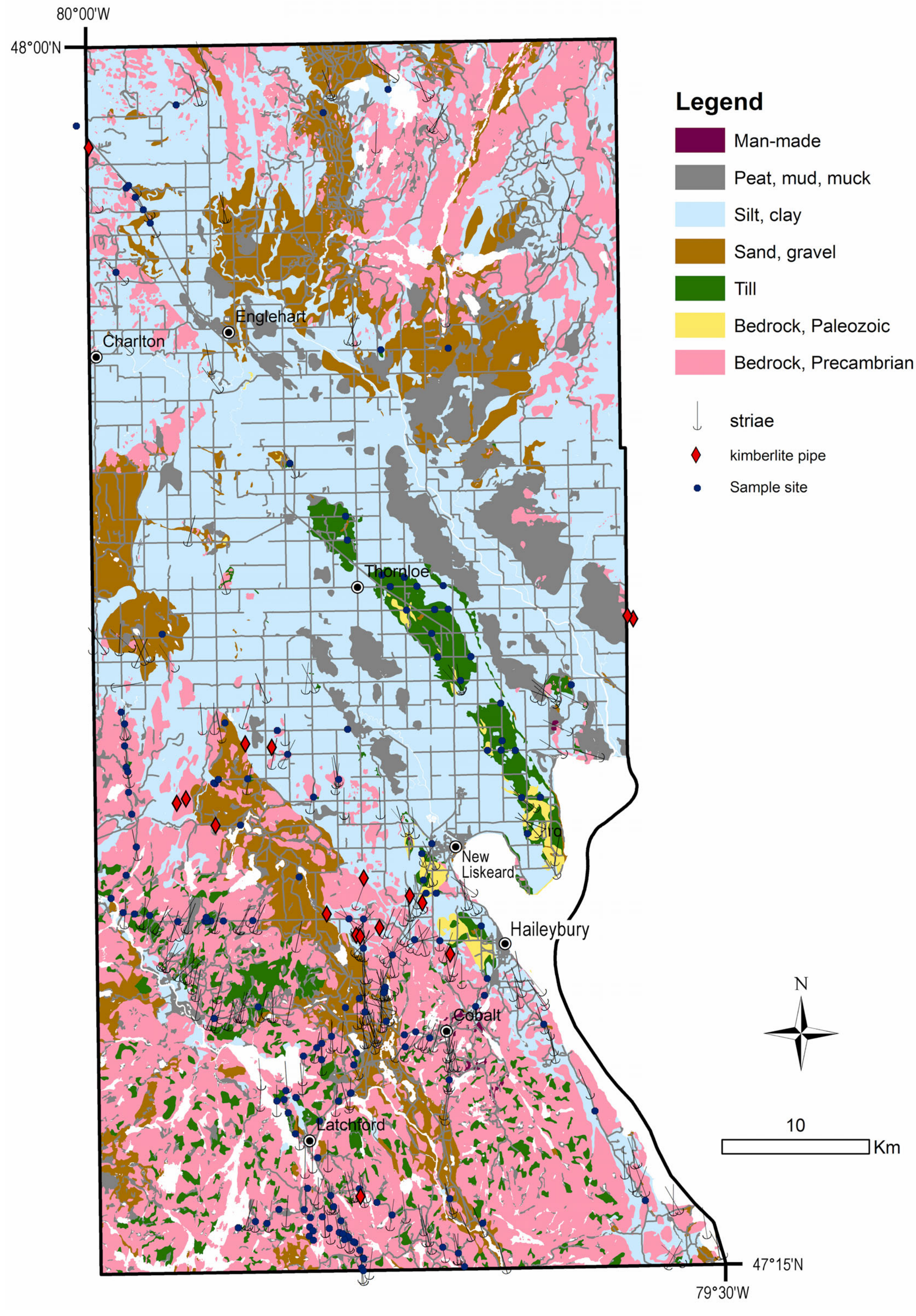

Figure 3. Quaternary geology of the study area (*after* Baker, Gao and Perttunen 2010; Gao 2010a, 2010b).

Methods

Samples were mainly collected in well-exposed sections along the roads and in gravel pits, which resulted in an irregular sample grid (*see* Figure 2). Apart from till, glaciofluvial sand and gravel deposits were also collected from eskers. At each site, the material was screened to remove the fraction larger than 7 mm and a 10 to 20 kg sample collected. Where possible, till samples were collected near the till–bedrock contact. Sample locations were determined using a global positioning system unit Garmin GPSmap60Cx. Sample locations are tabulated in Appendix 1 in Universal Transverse Mercator (UTM) projection and grid system, zone 17, North American Datum 1983 (NAD1983).

The samples collected in the field were processed by Overburden Drilling Management (ODM) to extract heavy mineral concentrates and pick kimberlite indicator minerals (KIM), gold and metamorphic/magmatic massive sulphide indicator mineral (MMSIM®[1]) grains. In the laboratory, each sample was wet-sieved to remove the >2 mm fraction, and the <2 mm fraction was subjected to gravity tabling for the initial separation of a heavy mineral preconcentrate. Appendix 2 summarizes the description and weight distribution of the clasts (>2 mm) and matrix (< 2 mm) obtained from the tabling phase. During the tabling phase, gold grains were counted. If gold was observed during the tabling stage, the <0.25 mm preconcentrate was micropanned to refine the gold grain count. The size and shape of gold grains were determined and recorded at this stage. Appendixes 3 and 4 summarize the data from the gold grain counts and details on the gold grains, respectively.

The preconcentrate underwent further separation using density-dependent settling in methylene iodide, a heavy liquid with a specific gravity of 3.2. Ferromagnetic mineral grains were then removed from the resultant heavy mineral concentrate using a magnet. The nonferromagnetic heavy mineral concentrate was sieved into 3 size fractions (0.25 to 0.5 mm, 0.5 to 1.0 mm and 1.0 to 2.0 mm). Appendix 5 summarizes the size distribution of each fraction of the heavy mineral concentrate following sample processing. Under a binocular microscope, indicator minerals in each size fraction were counted on the basis of their physical properties including colour, grain morphology and/or the presence of adhering kimberlite matrix material. Minerals counted or picked include reddish pyrope garnet, apple green chromium diopside (Cr-diopside, a pyroxene), black magnesium ilmenite (Mg-ilmenite) and chromite, and yellowish to light-coloured forsterite (olivine) grains, as well as some MMSIM® grains. Appendixes 6 and 7 summarize the KIM counts and KIM picking remarks.

Electron microprobe analysis of the KIM grains was conducted at the Geoscience Laboratories (Geo Labs) of the Ontario Geological Survey to determine their geochemical compositions (Appendix 8). The geochemical compositions of the pyrope grains are imperative for classification of garnets and evaluation of diamond potential of the source areas or kimberlite pipes. Because of the large number of the picked KIM grains, only portions of them were analyzed for this project. Consequently, the original data set of KIMs was adjusted to incorporate the changes in garnet classification (Appendix 9). MMSIM® grains were not analyzed by electron microprobe except for the low-Cr diopside mineral. This mineral is common in the till samples from the study area. It was picked as a pseudo KIM because of its similarity in colour and physical appearance to those of a kimberlitic orgin. The microprobe data for KIM and MMSIM® grains are being released together with other data in digital format as MRD 284, and are available separately from this report (Gao 2012).

[1] MMSIM is a registered trademark of Overburden Drilling Management Limited, Nepean, Ontario

Gold Grain Data

Significant numbers of gold grains in the heavy mineral fraction of till samples indicate the presence of gold mineralization in the up-ice direction. Where anomalously high yields of gold grains occur in till samples that are adjacent, clustered or aligned along a fault zone, it is likely that the source is not very far. Because of the low sampling density in this study, single sample anomalies should be investigated to determine their significance.

Gold grains are described as pristine, modified and reshaped according to their surface morphology. Such morphometric information can help infer their transport history. Pristine gold grains in till may indicate negligible mechanical abrasion. As such, large numbers of pristine grains in till indicate short transport distance from the source area. Sulphide grains that contain particulate gold may also generate *in situ* pristine gold grains in till deposits through weathering. In this case, although the style of mineralization involving sulphide-hosted gold can be inferred, little information is available on the transport history of the gold grains.

More than 1700 gold grains were counted from the samples (*see* Appendix 3). Gold counts in individual samples range from 0 to 58 (Figure 4), comparable to the results of the modern alluvium sampling surveys conducted previously in this region (Reid 2004; Guindon and Reid 2005). Samples having 20 or more gold counts came from sites underlain by a variety of bedrock types but with the most located in the Precambrian bedrock terrain (Table 1, *see* Figure 4). In a previous study, more than 80 gold grains were recovered from a 10 kg modern alluvium sample south of Mowat Landing in the middle west of Barr Township (Reid 2004; also *see* Figure 2 for the sample site locations). In comparison with other areas where significant anomalous gold counts exist (Bajc 1997), this number appears less prominent. However, given that the regional background concentration of gold grains is estimated to be no greater than 20 per 10 kg bulk till sample for this region (Bajc 1996, 1997), and the presence of large gaps in the sampling grid in this study, it does not preclude the possibility for finding significant gold mineralization in this region.

Pristine gold counts of 0 to 13 were found in individual samples (Table 2). Generally, the greater the number of total gold grains, the greater the number of pristine ones in a sample (*see* Tables 1, 2). However, it is not always the case. For instance, sample 09-CG-109 which has a total of 41 gold counts contains only 4 pristine grains, whereas, with the same number of pristine grains, 09-CG-102 has a total of 10 gold grains (*see* Table 2). The till samples in the Precambrian terrain have a much higher ratio of pristine to total gold grains than those collected in the Lake Timiskaming graben basin (Figure 5). This probably suggests a local source for some of the gold grains in the samples collected in the Precambrian terrain, whereas the gold grains from the latter-mentioned location are likely brought in by glaciers from a more distant source (*see* Figures 4, 5).

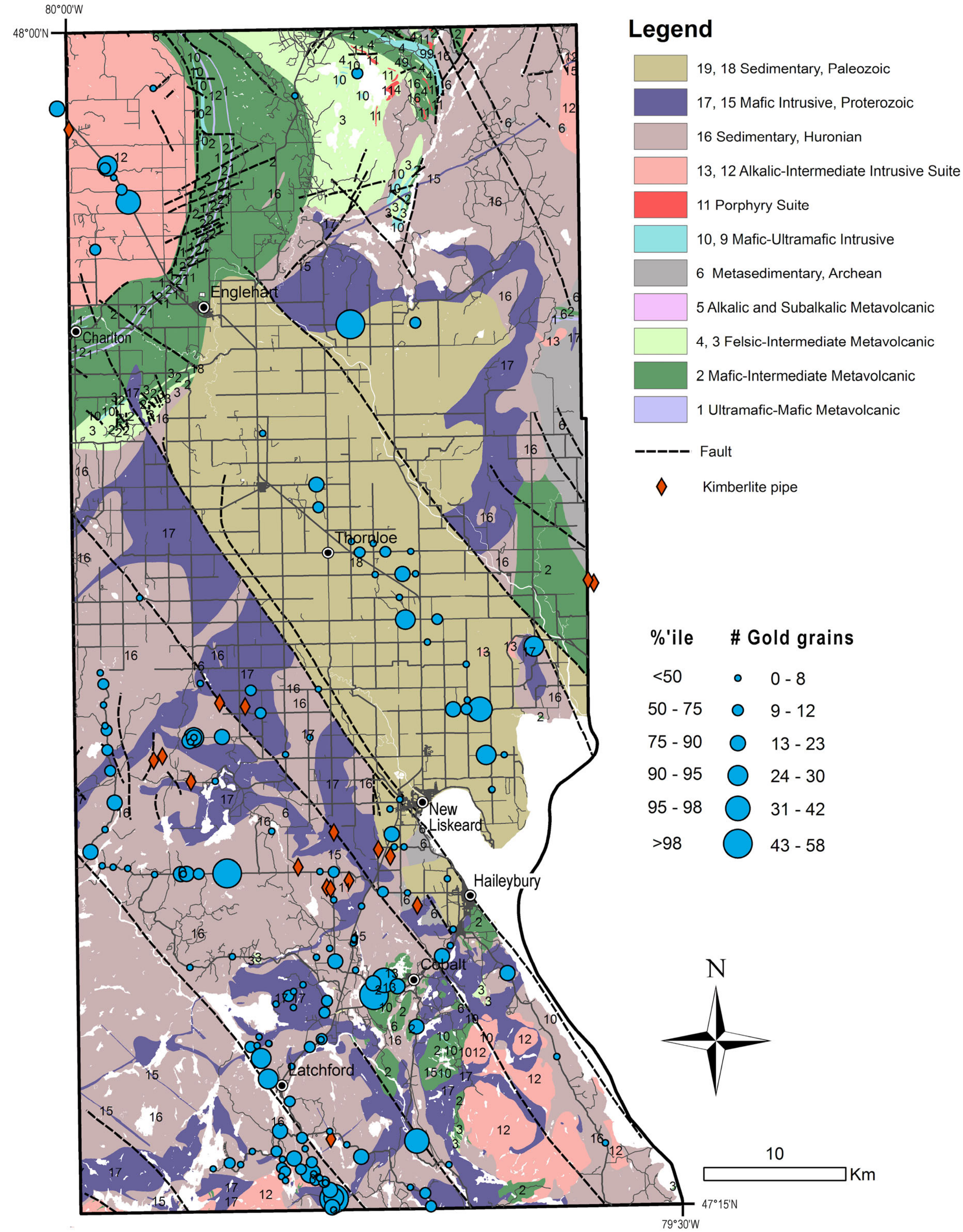

Figure 4. Regional distribution of gold grains. Bedrock geology *after* OGS (1991) and Ayer et al. (2006).

Table 1. Summary of samples containing 20 or more gold grains.

Sample Number	Number of Visible Gold Grains				Bedrock
	Total	Reshaped	Modified	Pristine	
09-CG-058	58	36	13	9	Huronian Sedimentary
09-CG-027	57	40	9	8	Mafic Intrusive
09-CG-065	50	34	10	6	Huronian Sedimentary
09-CG-110	43	22	8	13	Mafic Intrusive
09-CG-109	41	30	7	4	Felsic to Intermediate Intrusive
08CG-47	38	34	1	3	Paleozoic Sedimentary
09-CG-135	35	18	10	7	Huronian Sedimentary
09-CG-142	31	11	10	10	Huronian Sedimentary
09-CG-045	30	24	4	2	Huronian Sedimentary
09-CG-051	30	25	3	2	Paleozoic Sedimentary
09-CG-028	29	16	12	1	Mafic Intrusive
08CG-48	28	26	2	0	Paleozoic Sedimentary
09-CG-108	27	18	6	3	Felsic to Intermediate Intrusive
08CG-53	26	15	6	5	Paleozoic Sedimentary
08CG-39	26	25	0	1	Mafic Intrusive
09-CG-043	26	17	9	0	Huronian Sedimentary
08CG-31	24	21	3	0	Huronian Sedimentary
08CG-34	23	22	1	0	Mafic Intrusive
08CG-51	21	17	2	2	Huronian Sedimentary
07CG-024	21	16	4	1	Paleozoic Sedimentary
08CG-19	21	19	1	1	Huronian Sedimentary
07CG-143	20	19	1	0	Huronian Sedimentary

Table 2. Summary of samples containing 4 or more pristine gold grains.

Sample Number	Number of Visible Gold Grains				Pristine to total gold grains (%)	Bedrock
	Total	Reshaped	Modified	Pristine		
09-CG-110	43	22	8	13	30	Mafic Intrusive
09-CG-142	31	11	10	10	32	Huronian Sedimentary
09-CG-058	58	36	13	9	16	Huronian Sedimentary
09-CG-027	57	40	9	8	14	Mafic Intrusive
09-CG-135	35	18	10	7	20	Huronian Sedimentary
09-CG-143	15	8	0	7	47	Huronian Sedimentary
09-CG-069	12	4	1	7	58	Huronian Sedimentary
09-CG-065	50	34	10	6	12	Huronian Sedimentary
08CG-53	26	15	6	5	19	Paleozoic Sedimentary
08CG-17	7	0	2	5	71	Huronian Sedimentary
09-CG-109	41	30	7	4	10	Felsic to Intermediate Intrusive
07CG-081	16	11	1	4	25	Paleozoic Sedimentary
09-CG-102	10	5	1	4	40	Felsic to Intermediate Intrusive

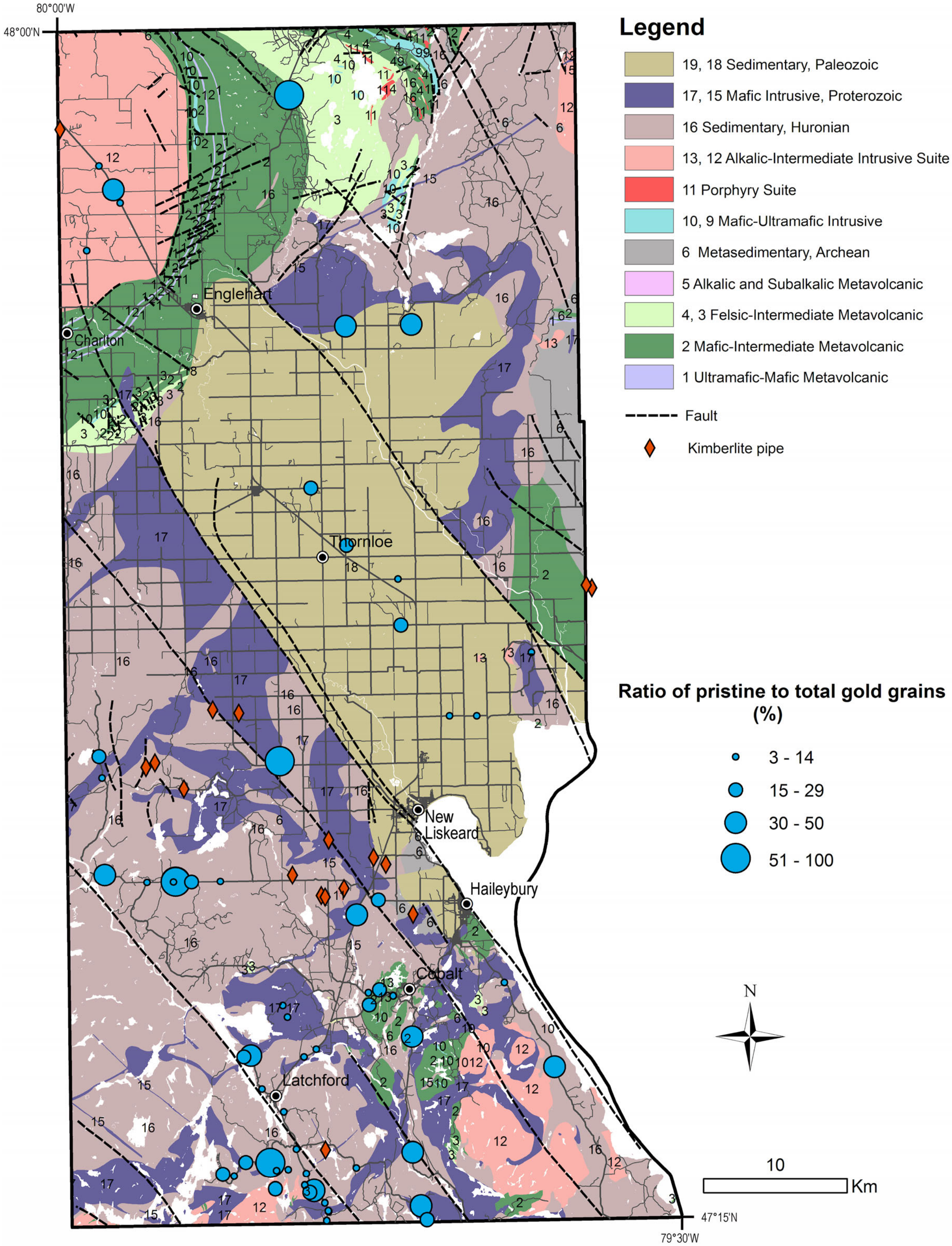

Figure 5. Regional distribution of the ratios of pristine to total gold grains. Bedrock geology *after* OGS (1991) and Ayer et al. (2006).

Kimberlite Indicator Minerals

Kimberlite is the primary host rock for natural diamonds (Helmstaedt 1993). During volcanic eruptions, kimberlitic magmas, often originating greater than 150 km below the Earth's surface, entrain various xenoliths including diamonds from the upper mantle and transport them to the surface. The most important source rocks for diamonds are peridotite and certain eclogitic rocks in the upper mantle. Harzburgite, lherzolite and wehrlite are the most common types of peridotite. Garnet harzburgite is the dominant source for diamonds, followed by chromite harzburgite and lherzolite.

Kimberlite indicator minerals (KIMs) are a unique group of heavy minerals with distinct physical and geochemical properties, that can be isolated with relative ease from minerals of other origins. They often coexist with diamonds in the upper mantle and are far more abundant than diamonds. As such, in exploration, focus is placed on the recovery of the indicator minerals rather than diamonds. The kimberlite indicator suite of minerals include, apart from diamond, pyrope garnet, chromite, Mg-ilmenite, Cr-diopside (pyroxene) and forsterite (olivine), derived from both xenoliths of mantle rock and kimberlite magmas.

Indicator minerals from xenoliths of upper mantle rock include diamond, peridotitic and eclogitic pyrope garnets, chromite and Cr-diopside. Because they coexist with diamonds, their presence can be used to evaluate the source rocks or kimberlite pipes for diamond potential. Those minerals derived from kimberlite magmas include Mg-ilmenite and titanian pyrope garnet. Commonly, they are large in size and often referred to as megacrysts. It is believed that these crystals are precipitated from protokimberlitic melts at mantle depths (Mitchell 1986). Although these megacrysts can not be used to evaluate the diamond potential of the source rocks, they are very important indicator minerals for kimberlite pipes.

GARNET

Garnets of purple to red wine colour are generally of a peridotitic origin, and the orange colour variety are of eclogitic and megacrystic origin (Averill 1999). These 2 groups of garnets are coded in the laboratory as GP and GO, respectively (*see* Appendix 6). The presence of a large number of GP garnets in a till sample indicates a high potential for the source rock for diamonds because of their association with peridotite. In a recent classification of garnets, GP and GO garnets also include those of a pyroxenitic origin (Grütter et al. 2004).

The picked GP and GO grains were submitted for electron microprobe analysis to determine major oxide geochemical compositions which were used in their identification and classification. Because of the large numbers of garnets picked, only some of the grains were analyzed. Using the multiple variables proposed by Grütter et al. (2004), the garnets were classified into harzburgitic G10, lhezolitic G9, wehrlitic G12, metasomatised peridotitic G11, eclogitic G3, megacrystic G1, and pyroxenitic G4 and G5 (Table 3; Figures. 6, 7; *see* Appendix 8). In this classification, there is some overlap between G9 and G5, as well as between G3 and G4. Apart from G10, G9, G12 and G11, the GP should include G5. Similarly, in addition to eclogitic and megacrystic G3 and G1, the GO should include G4.

Of the 1806 GP grains analyzed, 90% were confirmed and about 10% were reclassified as GO garnets (Table 4). There were 11 misidentified crustal garnets which accounted for less than 0.6% of the total of grains analyzed. Of the 904 GO grains analyzed, 90% were confirmed and the remainder reclassified as GP (4%) and crustal garnets (6%) (*see* Table 4). Almandine garnets in some samples were also picked. Of the 13 grains analyzed, more than half were reclassified as GO garnets (*see* Table 4). Subsequently, the GP and GO garnet data sets were adjusted to incorporate these changes in garnet classification and plotted on a bedrock geology map (Figures 8 to 13; Appendix 9).

Among harzburgitic G10 garnets, only those above the diamond/graphite boundary indicate a diamondiferous source area. As well, statistically, those classified as diamond inclusions have concentrations of MnO lower than 0.36 weight % (Grütter et al. 2004). Harzburgitic G10 garnets that satisfy either of these constraints are considered to be derived from diamond-bearing kimberlite pipes and a suffix 'D' is added (G10D). Statistically, eclogitic garnets occurring as diamond inclusions have elevated concentrations of Na_2O (>0.07 weight %) (McCandless and Gurney 1989; Schulze 1997, 2003). If this value is surpassed, the garnets are labelled as G3D; the same threshold value is also applied to pyroxenitic garnets and those from diamondiferous source rocks can be labelled as G4D and G5D (Grütter et al. 2004). There are 8 G10D and about 40 G3D, G4D and G5D grains in the garnets that were classified by microprobe analysis (Table 5; *see* Figures 8 to 13).

CHROMITE

Chromite harzburgite is an important host rock for diamonds. Chromites occur in mafic to ultramafic rocks; however, those with a kimberlitic origin often have elevated concentrations of Cr_2O_3 and MgO (Griffin et al. 1994; Fipke, Gurney and Moore 1995). Chromites in the diamond inclusion and intergrowth field typically have Cr_2O_3 and MgO greater than 60 and 9 weight %, respectively (Fipke, Gurney and Moore 1995). Using these variables, such grains can be isolated from chromites of other origins (Figure 14). In addition, Fipke, Gurney and Moore (1995) used concentrations of Cr_2O_3 and TiO_2 to further classify chromites into a diamond inclusion and intergrowth field, a field unique to kimberlites and lamproites, a non-kimberlitic/lamproitic field, and an overlap field (Figure 15). Of the chromites that were analyzed, 16 grains from 13 samples were classified into the diamond inclusion and intergrowth field (Table 6; Figure 16).

More than 3300 chromite grains were counted or estimated from the heavy mineral concentrates of the till samples (*see* Appendix 6). Of the 1240 grains analyzed, 82% were confirmed with 10% reclassified as Mg-ilmenite and 3% crustal ilmenite (Table 7). Using the microprobe data, the data set of chromite was adjusted to incorporate these changes in mineral reclassification and plotted on a bedrock geology map (Figure 16; Appendix 9). Although corresponding, to certain extent, with the pryope garnets, the chromites are also abundant at many other sites (Figure 16; *see* Figures 8, 11). This suggests that the wide distribution of chromites may also represent the occurrence of mafic rocks of crustal origin common in this region (*see* Figure 16).

Mg-ILMENITE

Ilmenite grains derived from kimberlite are typically enriched in MgO and Cr_2O_3 with concentrations greater than 4 and 0.11 weight %, respectively (Mitchell 1986; Schulz 1997). Those from crustal sources are, in general, depleted in chromium and have concentrations of MgO less than 4 weight % (Figure 17). More than 5700 Mg-ilmenites were counted or estimated from the heavy mineral concentrates of the samples (Appendix 6). Of the 2182 grains analyzed, 89% were confirmed to be kimberlitic with the remainder reclassified as either crustal ilmenites (4 %) or chromites (6%) (*see* Table 7).

Crustal ilmenite grains were occasionally picked from the heavy mineral concentrates. Of the 34 grains analyzed, 30 were reclassified as kimberlitic (*see* Table 7). Using the microprobe data, the counts of Mg-ilmenite grains were adjusted to incorporate these changes in mineral reclassification and plotted on a bedrock geology map (Figures 18 to 20; Appendix 9). The Mg-ilmenite data exhibit a striking similarity in number to the pyrope garnet data (*see* Figures 8, 11), providing further evidence for a kimberlitic origin.

Cr-DIOPSIDE

Cr-diopside grains have a bright apple green colour and are easily isolated from heavy mineral concentrates. This clinopyroxene mineral is a key component of lherzolitic peridotite and also occurs in wehrlitic peridotite and pyroxenite. Because harzburgitic peridotite is the primary host rock for diamonds and contains no clinopyroxene, this mineral provides limited information for assessing the source rocks for diamond potential. Although Cr-diopside may be derived from rocks at crustal depths, this mineral has been used as an important indicator mineral in exploration for kimberlite pipes (Morris et al. 2002; Crabtree 2003).

More than 800 Cr-diopside grains were counted or estimated from the heavy mineral concentrates of the samples (*see* Appendix 6). Of the 392 Cr-diopside grains analyzed by electron microprobe, only one was reclassified as andradite. Based on the data from known kimberlites worldwide, Crabtree (2003) was able to define a field for kimberlites on a scatter plot of Na_2O vs. Ca/Ca+Mg (atomic). Plotting of the microprobe data showed that a dominant portion of the analyzed Cr-diopside grains were within the kimberlitic field (Figure 21). This suggests that the majority of the Cr-diopside grains counted by ODM are of kimberlitic origin. As such, the estimated total Cr-diopside grains were plotted on a bedrock geology map to highlight the general trend of this indicator mineral (Figure 22). It is notable that the samples with elevated counts of Cr-diopside also contain large numbers of pyrope garnets, consistent with the interpretation for a kimberlitic origin for this mineral (*see* Figures 8, 11).

There are more than 4800 low-Cr diopside grains counted or estimated from the heavy mineral concentrates of the samples and classified as metamorphic/magmatic massive sulphide indicator minerals or pseudo KIMs (*see* Appendix 6). Of the grains analyzed by electron microprobe, most are located outside the kimberlitic field with only a few reclassified into this field (Table 8, *see* Figure 21), confirming that the majority of these pyroxene grains identified as low-Cr diopside have a non-kimberlitic origin.

OLIVINE (FORSTERITE)

Forsteritic olivine occurs in a variety of mafic and ultramafic rocks and it does not have compositions that can be definitively linked to kimberlites based on major oxide chemistry (Crabtree 2003). However, if large numbers of olivine grains are recovered from heavy mineral concentrates in association with other KIMs, there is a strong possibility that these minerals have a kimberlitic origin. Although olivine is abundant in kimberlites, this grain is easily weathered and broken down during transport by glaciers and rivers.

More than 1400 forsteritic olivine grains were counted or estimated from the heavy mineral concentrates of the samples (*see* Appendix 6). Their regional distribution shows certain similarities with that of pyrope garnets, suggesting that most of the olivine grains are likely of kimberlitic origin (Figure 23; *see* Figures 8, 11). For instance, in addition to abundant olivine grains in sample 08CG-22 at Mowat Landing at the western end of Municipal Road, other KIMs are also present in this sample, suggesting a kimberlitic origin for the olivine grains (Figure 23; *see* Figure 2 for sample location). Abundant olivine grains are also present in a nearby sample 08CG-23 collected from an esker (*see* Figure 23; *see* Figure 2 for sample location). However, their connection to kimberlites remains less definitive because of few pyrope and ilmentite grains present at this site (*see* Figures 10, 13, 20).

Discussion of KIM Results

With exception of 09-CG-035, all samples collected as part of this project contain various amounts of KIMs (Figure 24; Appendix 9). Samples that contain greater than 100 KIMs are mostly located in the Precambrian bedrock terrain in the southern part of the report area (Table 9; Figures 25, 26). In the Precambrian bedrock terrain in the northern and northeastern part of the report area, the till samples are scant and a large portion of this area was not sampled because of the lack of accessibility and well exposed road cuts that contain till deposits (*see* Figure 24). However, a sample collected in this area contains anomalous concentrations of KIM grains. In a previous modern alluvium sampling program, anomalous KIM grains were counted in 10 kg samples collected north of Englehart (Guindon and Reid 2005). Similarly, in the southwestern corner of the report area in Kittson and Brigstocke Townships (*see* Figure 2 for locations), no till samples were obtained but previous studies indicate anomalous concentrations of KIM grains in 10 kg modern alluvium samples (Reid 2004). As such, future high density till sampling in these areas is warranted.

It is noteworthy that, in a previous study, an anomalous number of pyrope garnets (>30) were recovered from a 10 kg modern alluvium sample (JR-MA-018) collected between Latchford and Cobalt on Highway 11 (Reid 2004). However, a couple of till samples collected from the current study, e.g., 09-CG-012 and 09-CG-021, in the adjacent area showed low concentrations of KIM grains (*see* Figures 9, 12; *see* Figure 2 for locations). Furthermore, abundant KIM grains (>80) were counted in quite a few modern alluvium samples collected previously south of Cobalt (Reid 2002). Till samples collected in this study are sparse in this area and they all show low to moderate numbers of KIM grains (*see* Figure 24). To track the source of the KIM anomalies in the modern alluvium deposits, resampling in this area is highly recommended.

In the Lake Timiskaming graben basin, many till samples are present but they generally contain low to moderate concentrations of KIMs (*see* Figure 24). This feature may indicate a lack of kimberlite pipes in the vicinity. Alternatively, the low number of KIMs in the till may have resulted from increased dilution of KIM grains as the ice sheet passed from resistant Precambrian rock types to the north onto less durable Paleozoic carbonate rocks in the graben. Although this process is difficult to quantify, the current work shows that most of the samples that have anomalous numbers of KIM counts come from till deposits no more than 2 m thick on Precambrian bedrock. If this observation is correct, then the samples collected in the graben basin with moderate concentrations of KIMs may also be important follow-up targets for diamond exploration.

Ilmenite and pyrope grains dominate at many sample sites. However, the mineral compositions as indicated by the samples containing greater than 100 KIM grains vary across the study area, suggesting different source areas and transport history (*see* Table 9; Figures 25, 26). The presence of G10D, G5D, G4D and G3D garnets, as well as chromites in the diamond inclusions and intergrowth field suggests a high potential of the source rocks or kimberlite pipes for diamonds. In the discussion below, some sites were selected for further discussion because they contain clustered samples that exhibit anomalous concentrations of KIMs or where individual samples are in the vicinity of known kimberlite pipes and detailed discussion of them may provide insights into the dispersal feature and the adjacent kimberlites. These sites or areas were outlined loosely, as areas A, B, C, D and E in the following figures, each containing a single sample or a cluster of samples. They were used for the convenience of the discussion only. They are not the follow-up targets.

Table 3. Classification scheme for garnets (Grütter et al. 2004).

Garnets	Cr_2O_3	CaO	TiO_2	MgO	CA_INT*	MgNum**
G1 Megacrystic	0 to <4		≥2.13-2.1MgNum; <4		≥3.375 to <6	≥0.65 to <0.85
G3 Eclogitic	0 to <1	≥6 to <32	<2.13-2.1MgNum; <2			≥0.17 to <0.86
G4 Pyroxenitic	<1		<2.13-2.1MgNum			≥0.3 to <0.9
G5 Pyroxenitic	≥1 to <4	≥2 to <6	<2.13-2.1MgNum		≥3.375 to <5.4	≥0.3 to <0.7
G9 Lherzolitic	≥1 to <20				≥3.375 to <5.4	≥0.7 to <0.9
G10 Harzburgitic	≥1 to <22				<3.375	<0.95
G11 Peridotitic, metasomatised	≥1 to <20	<28	≥2.13-2.1MgNum; <4		≥3	≥0.65 to <0.9
G12 Wehrlitic	≥1 to <20	<28		>5	>5.4	

* Ca_INT (garnet Ca_intercept value): If CaO ≤ 3.375+0.25Cr_2O_3, then Ca_INT=13.5CaO/(Cr_2O_3+13.5); Else Ca_INT=CaO-0.25Cr_2O_3

** MgNum=(MgO/40.3)/(MgO/40.3+FeOt/71.85)

Table 4. Summary of the statistics in the microprobe analysis of garnets that include GP, GO and almandine grains.

GP grains analyzed

Total	G9	G10	G11	G12	G5	G1	G3	G4	Other
1806	1341	89	180	8	8	160	3	6	11
	GP	**GO**	**Other**	**%GP**	**%GO**	**%Other**	**%Total**		
	1626	169	11	90	9.4	0.6	100		

GO grains analyzed

Total	G1	G3	G4	G9	G11	Other			
904	630	32	147	26	9	60			
	GO	GP	Other	%GO	%GP	%Other	%Total		
	809	35	60	89.5	3.9	6.6	100		

Almandine grains analyzed

Total	G3	G1	G4	Other
13	1	1	5	6
	GO	**Other**		
	7	6		

Table 5. Geochemistry (in weight %) of diamondiferous G10D, G5D, G4D and G3D garnets (*after* Grütter et al. 2004).

Sample	Grain Label	SiO_2	TiO_2	Al_2O_3	V_2O_3	Cr_2O_3	MgO	CaO	MnO	FeO*	Na_2O	K_2O	Total	Classification
07CG-564	07CG-564-070	41.406	0.646	21.672	0.059	0.151	17.592	5.231	0.473	13.164	0.074	0.001	100.47	G4D
07CG-734	07CG-734-107	40.596	0.688	22.266	0.027	0.062	14.426	8.838	0.261	12.398	0.158	0.000	99.72	G3D
07CG-737-3	07CG-737-3-003	41.697	0.485	22.121	0.033	0.431	20.253	4.194	0.358	10.366	0.079	0.000	100.02	G4D
08CG-10-3	08CG-10-3-104	41.452	0.465	22.428	0.033	0.368	19.089	4.241	0.378	10.941	0.071	0.000	99.47	G4D
08CG-10-3	08CG-10-3-108	41.888	0.472	22.372	0.028	0.330	19.588	4.300	0.384	11.117	0.079	0.000	100.56	G4D
08CG-17	08CG-17-249	39.535	0.157	22.266	0.008	0.058	10.544	6.936	0.434	19.948	0.072	0.000	99.96	G3D
08CG-17	08CG-17-269	39.586	0.142	22.354	0.013	0.064	10.739	6.996	0.440	19.989	0.071	0.001	100.39	G3D
08CG-17	08CG-17-272	39.850	0.149	22.302	0.018	0.041	10.593	7.009	0.433	20.053	0.071	0.000	100.52	G3D
08CG-17	08CG-17-200	41.334	0.578	22.355	0.030	0.215	18.575	4.531	0.421	11.761	0.075	0.000	99.88	G4D
08CG-17	08CG-17-235	41.569	0.584	22.401	0.039	0.243	18.638	4.710	0.439	11.968	0.085	0.000	100.67	G4D
08CG-17	08CG-17-240	41.543	0.471	22.797	0.033	0.151	18.845	3.982	0.446	11.613	0.075	0.000	99.96	G4D
08CG-18	08CG-18-136	41.819	0.343	20.637	0.031	3.369	20.308	4.927	0.404	8.247	0.084	0.017	100.19	G5D
08CG-19	08CG-19-105	40.182	0.584	22.484	0.021	0.060	12.662	7.771	0.346	16.110	0.168	0.000	100.39	G3D
08CG-19	08CG-19-108	40.389	0.382	22.490	0.016	0.226	12.267	8.670	0.305	15.509	0.116	0.000	100.37	G3D
08CG-19	08CG-19-132	40.428	0.563	22.364	0.020	0.055	12.614	7.763	0.347	16.193	0.161	0.000	100.51	G3D
08CG-19	08CG-19-112	42.052	0.545	22.340	0.041	0.321	19.269	4.497	0.395	11.261	0.079	0.000	100.80	G4D
08CG-30	08CG-30-195	42.243	0.430	22.191	0.034	0.866	20.130	4.660	0.333	9.526	0.073	0.000	100.49	G4D
08CG-31	08CG-31-112	41.865	0.467	22.476	0.034	0.280	19.360	4.341	0.384	11.187	0.073	0.001	100.47	G4D
08CG-31	08CG-31-114	41.573	0.515	22.248	0.041	0.332	18.371	4.416	0.443	12.391	0.073	0.000	100.40	G4D
08CG-31	08CG-31-122	41.505	0.563	22.082	0.041	0.363	18.353	4.497	0.447	12.431	0.074	0.000	100.36	G4D
08CG-32	08CG-32-167	41.308	0.574	22.344	0.049	0.341	18.448	4.453	0.430	12.451	0.073	0.000	100.47	G4D
08CG-32	08CG-32-185	41.921	0.424	22.061	0.036	0.970	20.308	4.693	0.329	9.442	0.072	0.000	100.26	G4D
08CG-33	08CG-33I-078	41.870	0.400	22.211	0.028	0.654	20.093	4.722	0.335	9.630	0.072	0.000	100.01	G4D
08CG-33	08CG-33R-030	41.271	0.625	21.906	0.049	0.175	17.843	4.842	0.457	12.975	0.072	0.002	100.22	G4D
08CG-35	08CG-35-002	41.776	0.072	21.395	0.041	2.778	20.597	3.113	0.248	9.666	0.020	0.000	99.70	G10D
08CG-35	08CG-35-020	41.387	0.209	18.681	0.040	6.382	21.254	4.851	0.309	6.387	0.044	0.000	99.54	G10D
08CG-54	08CG-54-006	41.006	0.179	15.221	0.044	10.664	20.174	5.931	0.321	6.206	0.034	0.000	99.78	G10D
09-CG-017	09-CG-017-005	41.478	0.491	22.710	0.022	0.024	19.133	3.449	0.303	12.249	0.079	0.000	99.94	G4D
09-CG-021	09-CG-021-010	41.369	0.557	21.881	0.038	0.190	18.169	4.544	0.467	12.726	0.071	0.000	100.01	G4D
09-CG-059	09-CG-059-042	42.296	0.009	21.002	0.032	4.139	24.678	0.898	0.336	6.148	0.009	0.001	99.55	G10D
09-CG-059	09-CG-059-048	41.374	0.448	18.481	0.035	6.516	21.855	4.255	0.295	6.272	0.047	0.000	99.58	G10D
09-CG-059	09-CG-059-087	41.387	0.432	21.816	0.033	0.780	18.440	3.864	0.299	13.078	0.097	0.000	100.23	G4D
09-CG-059	09-CG-059-106	41.811	0.516	22.362	0.032	0.221	19.852	4.000	0.445	10.945	0.078	0.000	100.26	G4D

Table 5. continued

Sample	Grain Label	SiO_2	TiO_2	Al_2O_3	V_2O_3	Cr_2O_3	MgO	CaO	MnO	FeO*	Na_2O	K_2O	Total	Classification
09-CG-063	09-CG-063-060	40.902	0.150	15.485	0.034	10.338	21.359	4.779	0.270	5.872	0.002	0.000	99.19	G10D
09-CG-063	09-CG-063-115	41.722	0.483	22.566	0.034	0.110	19.479	4.219	0.412	11.262	0.071	0.000	100.36	G4D
09-CG-086	09-CG-086-032	41.847	0.432	22.282	0.029	0.495	20.622	4.242	0.331	9.918	0.075	0.000	100.27	G4D
09-CG-086	09-CG-086-035	41.747	0.399	22.259	0.021	0.702	20.713	4.171	0.322	9.743	0.071	0.000	100.15	G4D
09-CG-108	09-CG-108-007	41.375	0.482	22.431	0.030	0.036	19.197	4.098	0.395	11.947	0.087	0.000	100.08	G4D
09-CG-134	09-CG-134-002	42.318	0.153	18.426	0.050	7.215	22.506	4.177	0.258	5.598	0.036	0.000	100.74	G10D
09-CG-135	09-CG-135-004	40.642	0.491	22.320	0.016	0.069	14.070	5.113	0.394	17.420	0.150	0.000	100.69	G4D
09-CG-136	09-CG-136-062	41.787	0.115	17.780	0.050	7.799	21.069	5.128	0.305	6.370	0.031	0.000	100.43	G10D
09-CG-137	09-CG-137-006	41.610	0.430	22.501	0.027	0.217	19.383	4.608	0.385	10.938	0.074	0.002	100.17	G4D
09-CG-137	09-CG-137-007	41.966	0.490	22.483	0.031	0.566	20.294	4.129	0.346	10.212	0.075	0.000	100.59	G4D
09-CG-137	09-CG-137-016	41.738	0.488	22.221	0.028	0.520	20.091	4.191	0.348	10.293	0.076	0.002	100.00	G4D
09-CG-137	09-CG-137-017	42.020	0.489	22.469	0.028	0.393	20.210	4.066	0.370	10.533	0.072	0.000	100.65	G4D

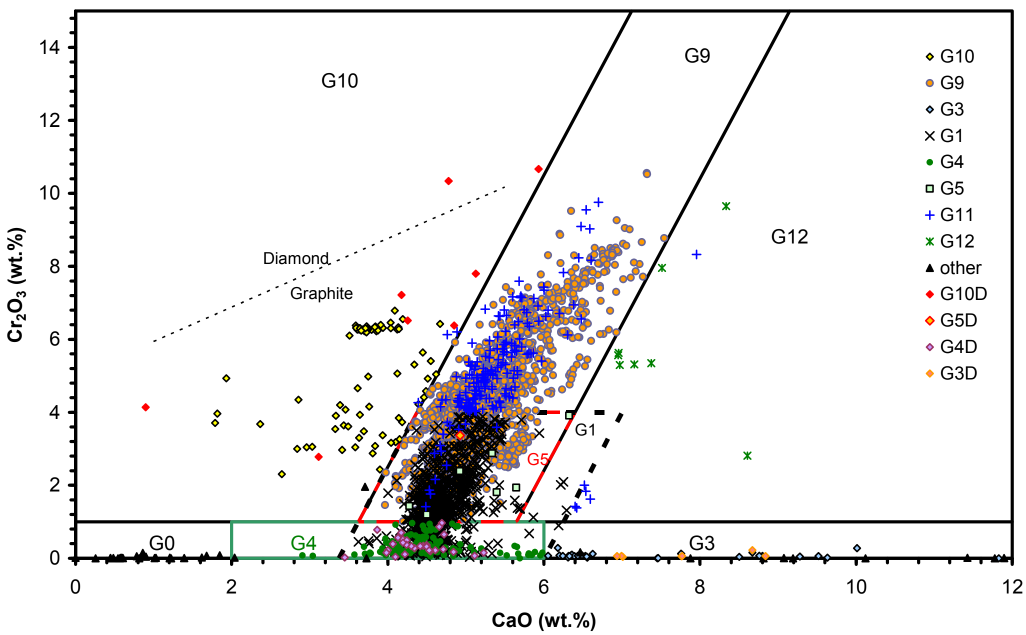

Figure 6. CaO versus Cr_2O_3 binary plot of pyrope garnet grains recovered from the study area (*after* Grütter et al. 2004). G10D, G5D, G4D and G3D are garnets classified as being derived from diamondiferous kimberlite pipes.

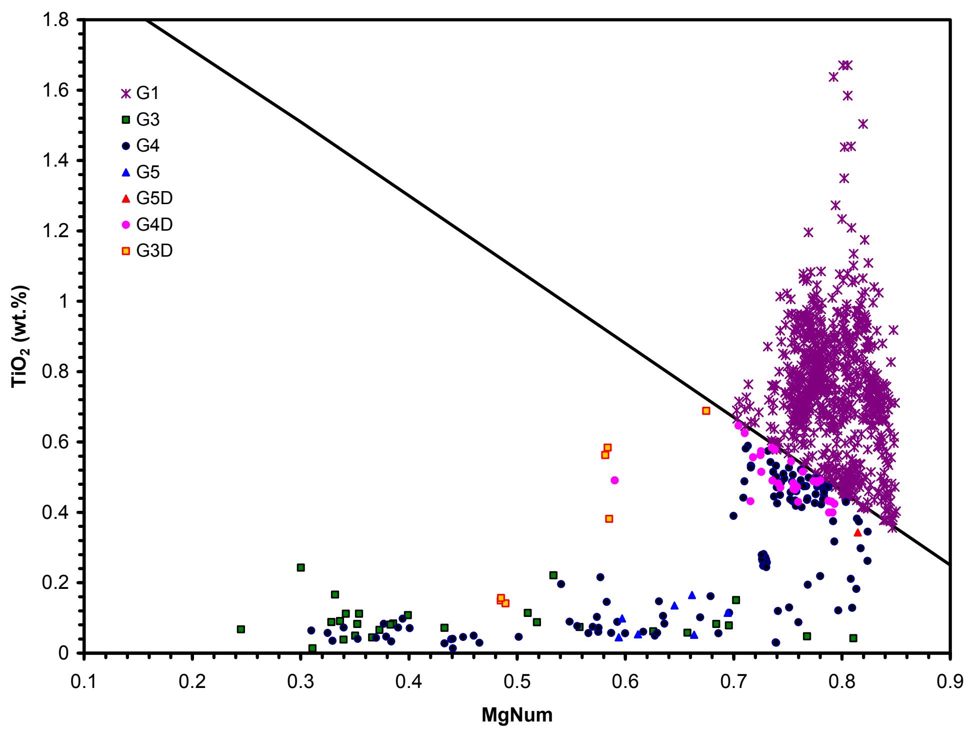

Figure 7. MgNum versus TiO_2 binary plot of megacrystic, eclogitic and pyroxenitic garnets recovered from the study area (*after* Grütter et al. 2004). G5D, G4D and G3D are garnets classified as being derived from diamondiferous kimberlite pipes. MgNum = (MgO/40.3)/(MgO/40.3+FeOt/71.85).

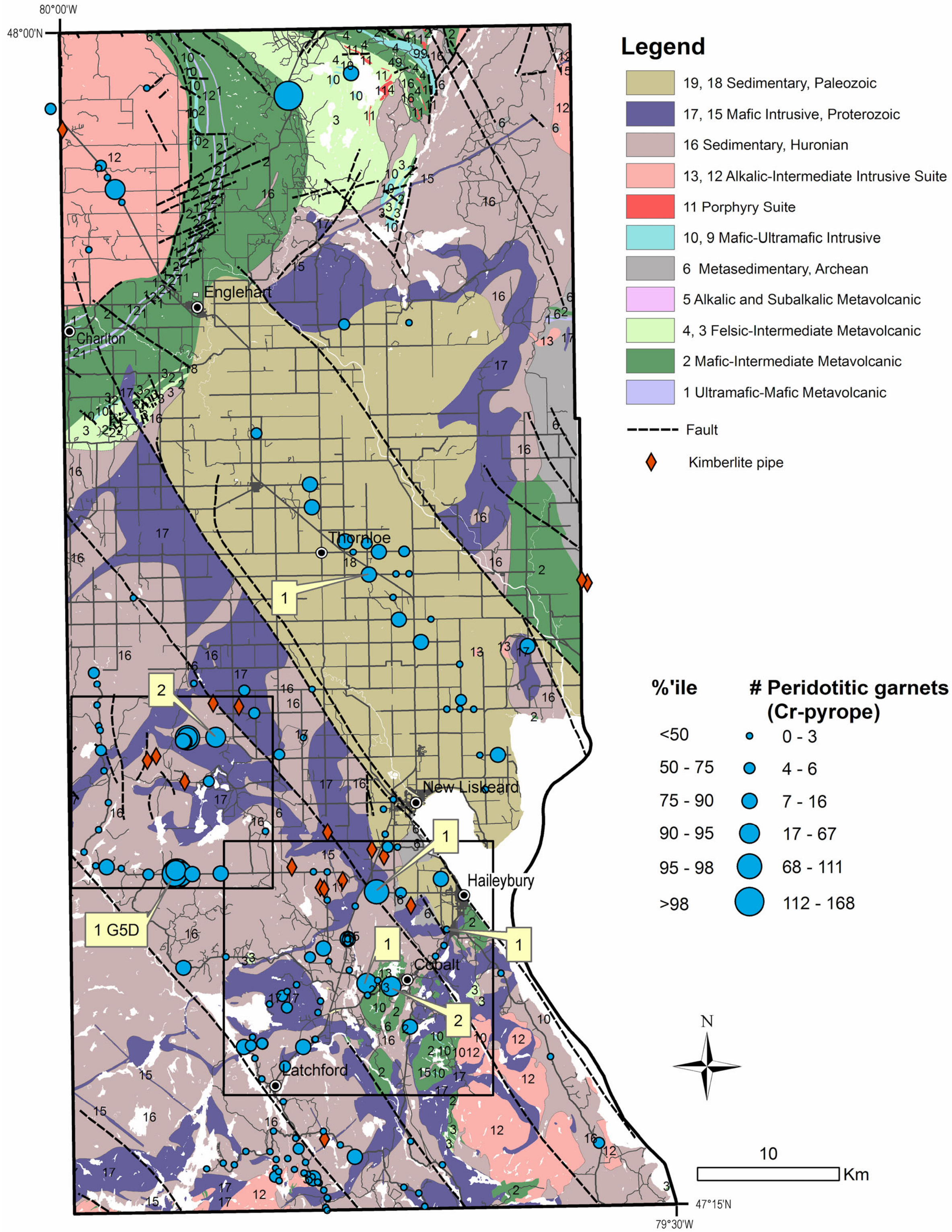

Figure 8. Regional distribution of peridotitic garnet grains. Annotation with numbers indicates G10D garnets unless it is specified, e.g., '1 G5D' indicative of 1 G5D garnet. Boxed areas are enlarged in Figures 9 and 10. Bedrock geology *after* OGS (1991) and Ayer et al. (2006).

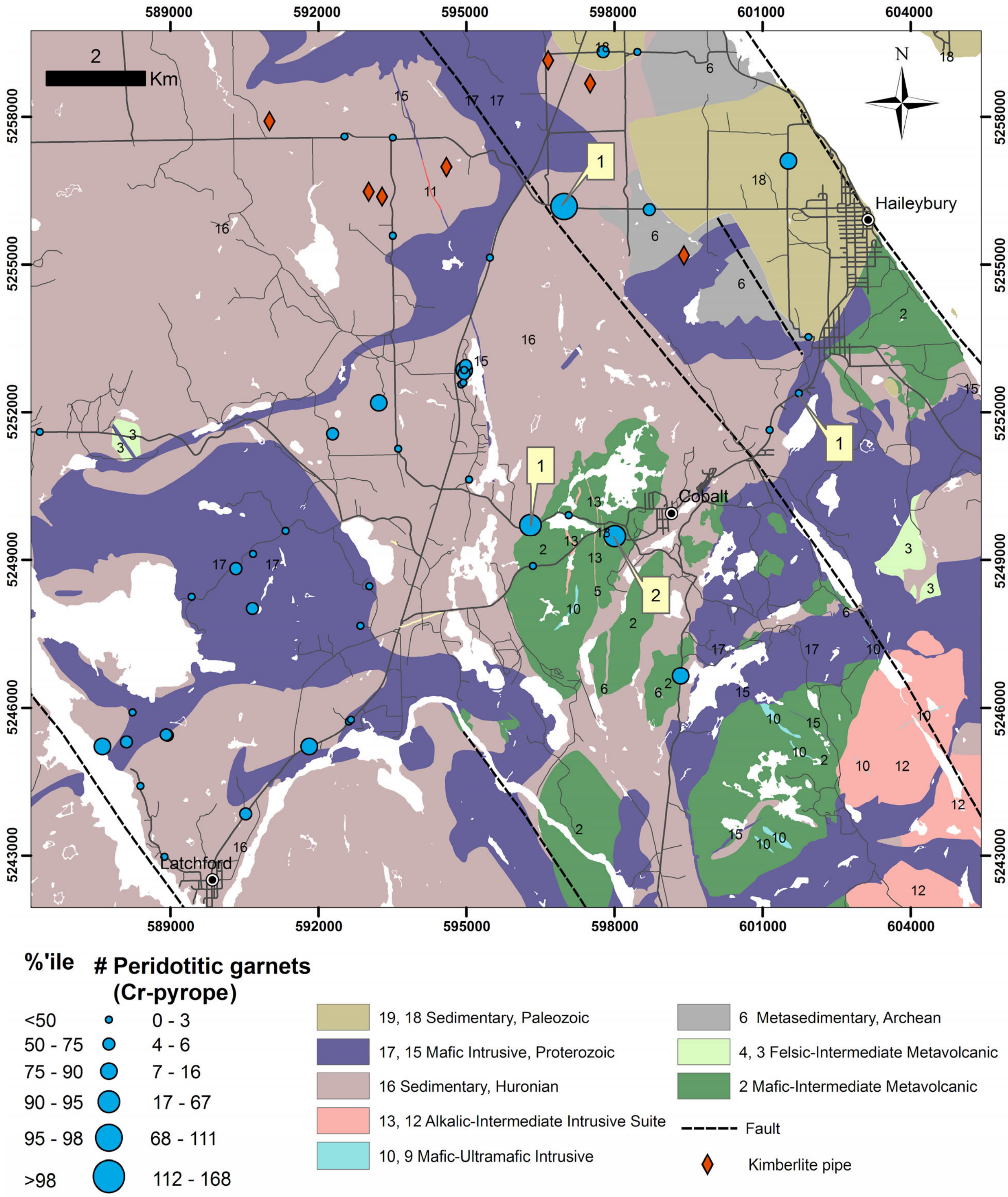

Figure 9. Enlarged view of regional distribution of peridotitic garnet grains in the Cobalt area. Annotation with numbers indicates G10D garnets.

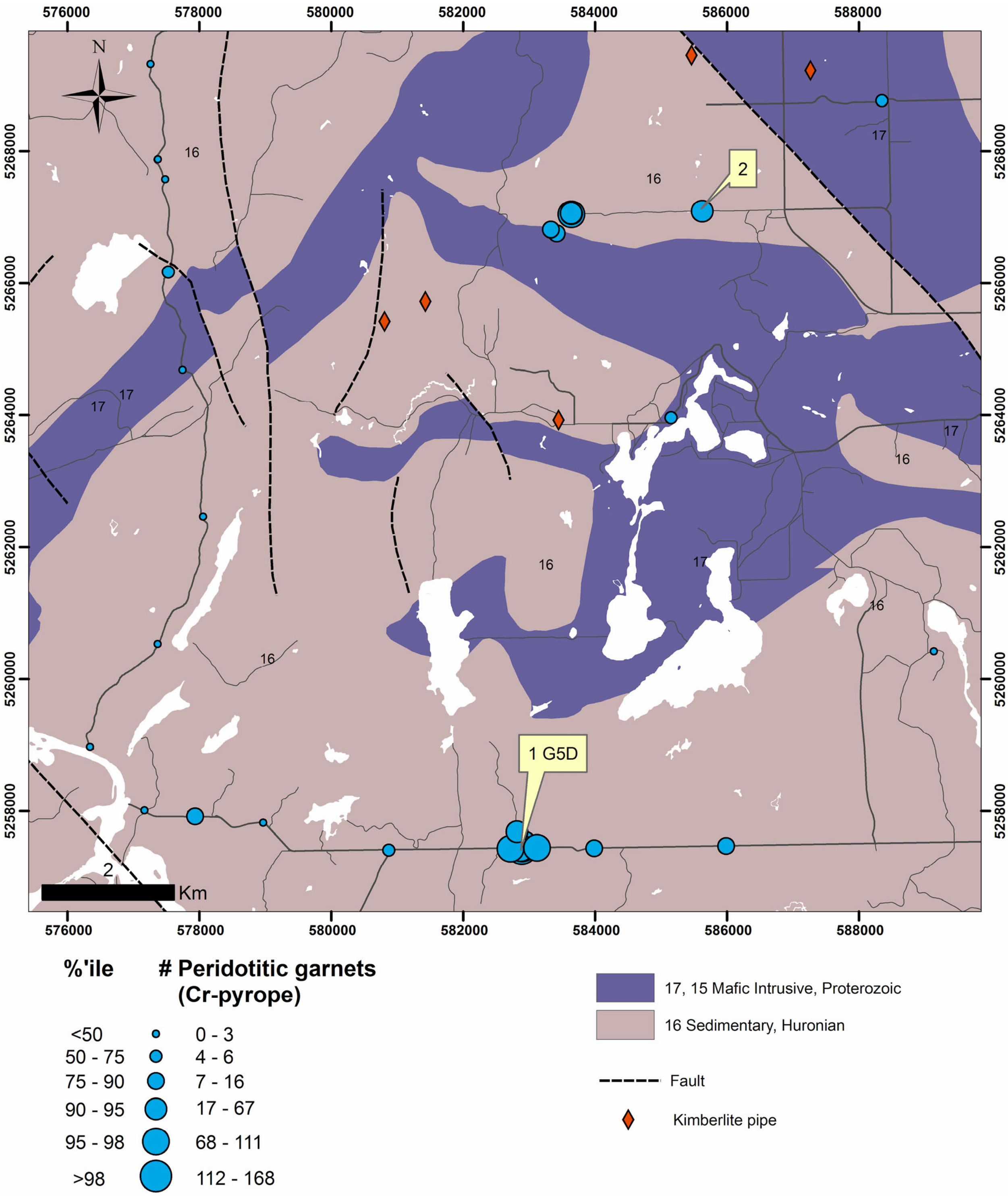

Figure 10. Enlarged view of regional distribution of peridotitic garnet grains in the western part of the New Liskeard area (*see* Figure 8 for location). Annotation with numbers indicates G10D garnets unless it is specified, e.g., ‘1 G5D’ indicative of 1 G5D garnet.

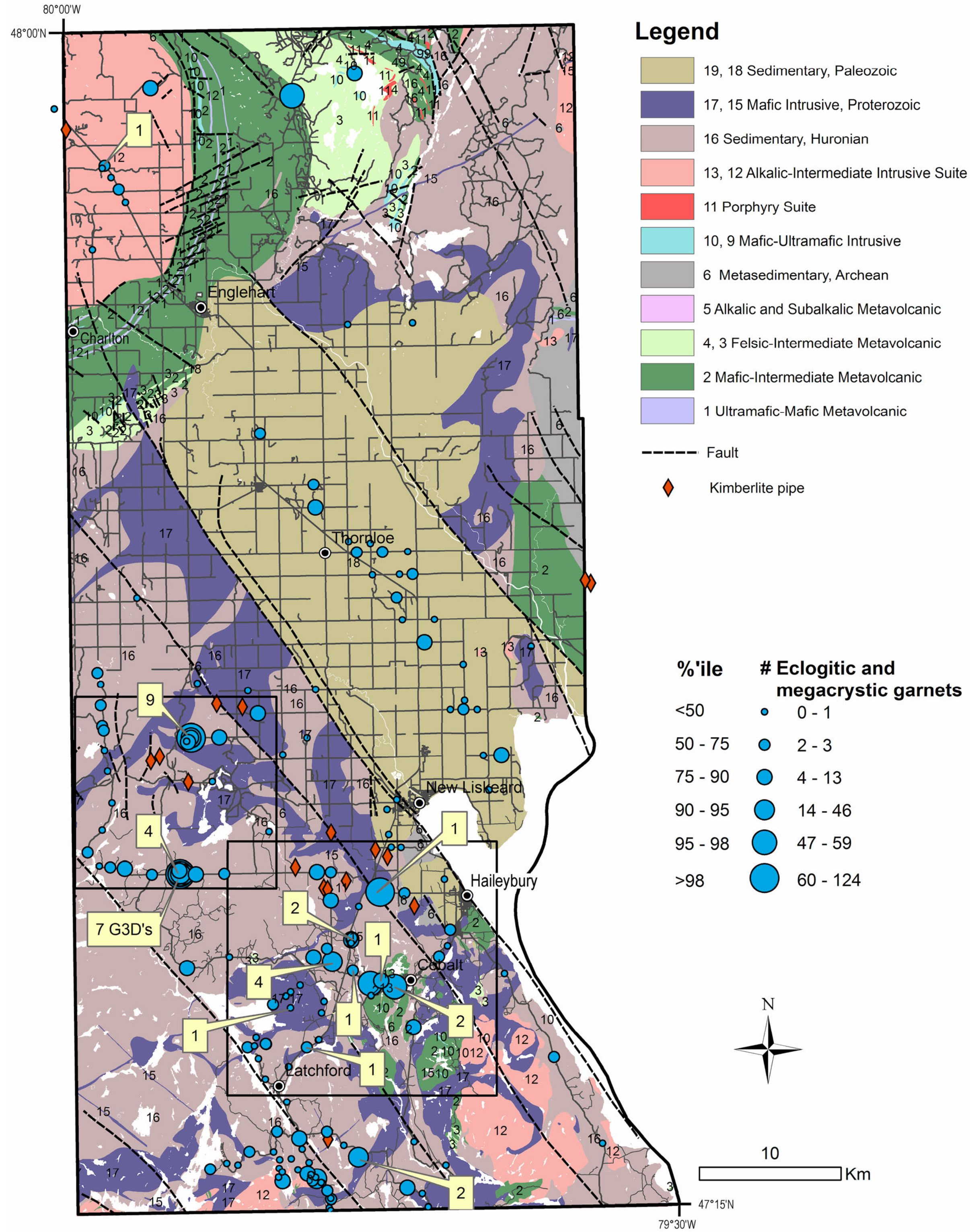

Figure 11. Regional distribution of eclogitic and megacrystic garnet grains. Annotation with numbers indicates G4D garnets unless it is specified, e.g., '7 G3D's' indicative of 7 G3D garnets. Boxed areas are enlarged in Figures 12 and 13. Bedrock geology *after* OGS (1991) and Ayer et al. (2006).

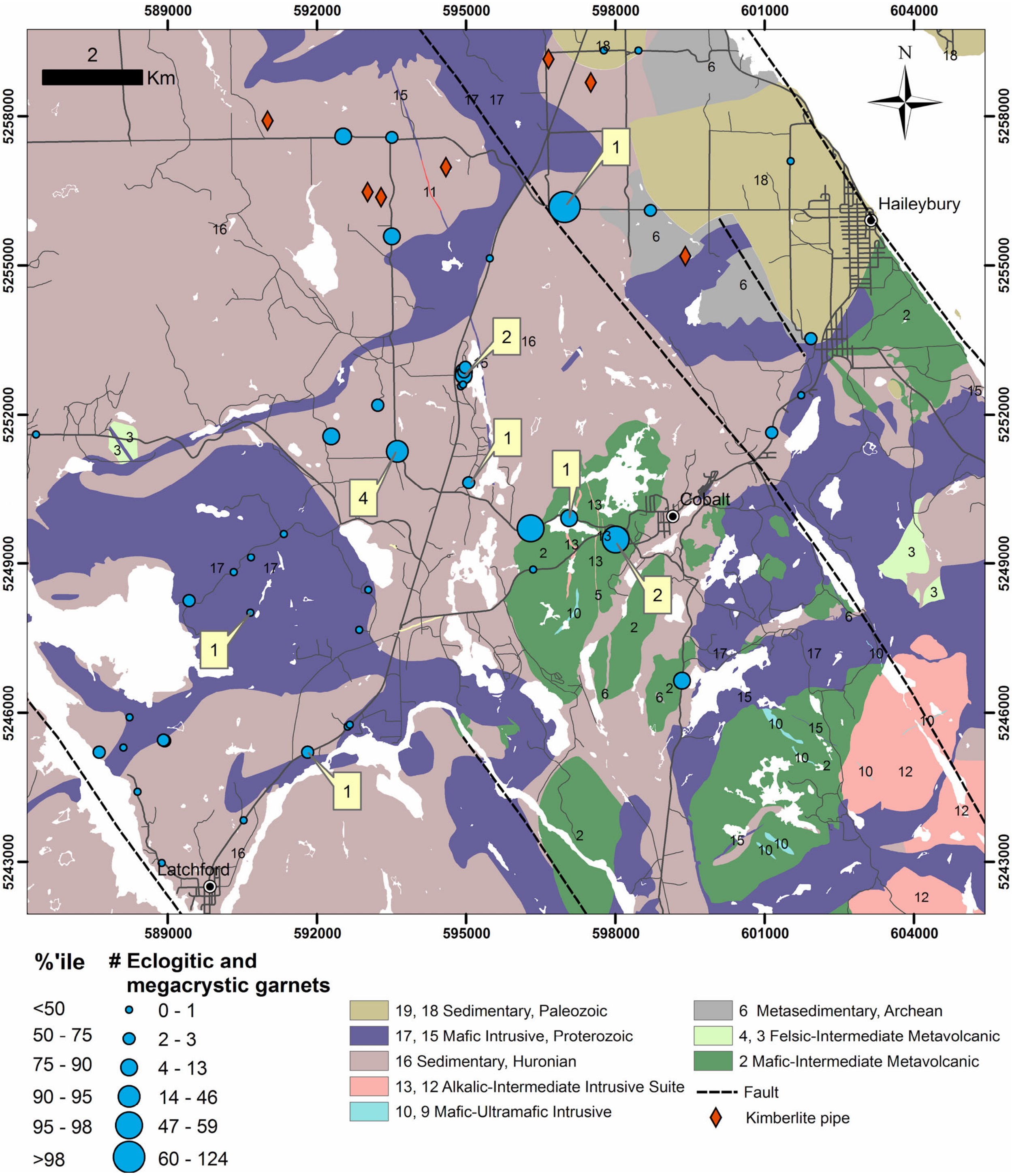

Figure 12. Enlarged view of regional distribution of eclogitic and megacrystic garnet grains in the Cobalt area. Annotation with numbers indicates G4D garnets.

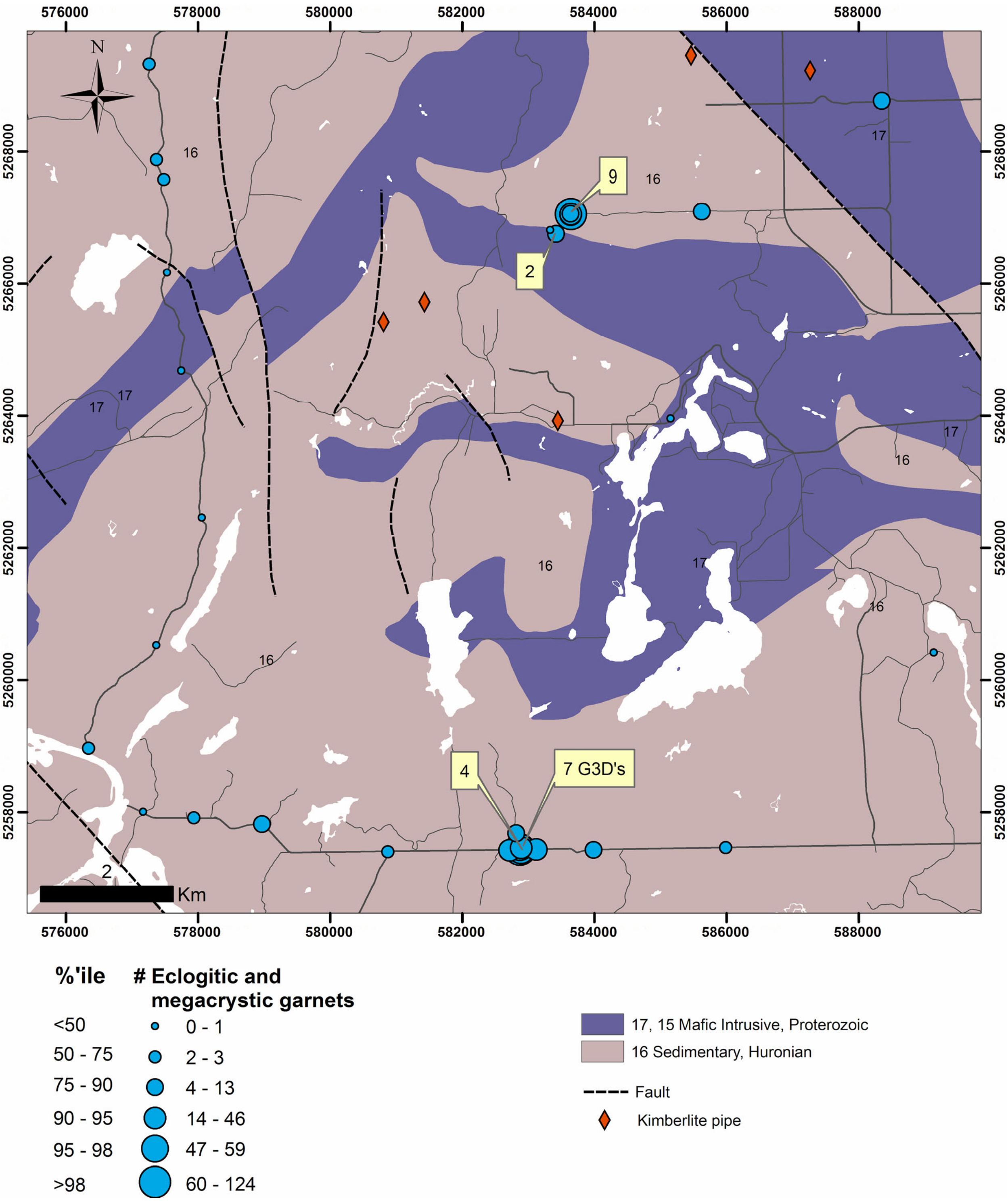

Figure 13. Enlarged view of regional distribution of eclogitic and megacrystic garnet grains in the western part of the New Liskeard area (*see* Figure 11 for location). Annotation with numbers indicates G4D garnets unless it is specified, e.g., '7 G3D's' indicative of 7 G3D garnets.

Table 6. Geochemistry (in weight %) of chromite grains classified into the diamond inclusion and intergrowth field (*after* Fipke et al. 1995).

Sample	Grain label	SiO_2	TiO_2	Al_2O_3	V_2O_3	Cr_2O_3	Nb_2O_3	MgO	CaO	MnO	FeO*	NiO	ZnO	Total	Fe_2O_3	FeO (new)	Total	Plot A	Plot B
07CG-332	07CG-332-012	0.07	0.00	9.02	0.17	61.61	0.00	11.28	0.00	0.22	16.98	0.05	0.15	99.54	1.30	15.81	99.67	1	1
07CG-332	07CG-332-013	0.17	0.16	6.85	0.04	60.41	0.00	11.93	0.00	0.21	19.54	0.16	0.05	99.52	5.27	14.80	100.05	0	1
07CG-699-2	07CG-699-2-026	0.04	0.66	1.16	0.30	63.28	0.00	9.04	0.00	0.33	24.16	0.08	0.12	99.17	6.42	18.39	99.81	1	1
07CG-734	07CG-734-173	0.05	0.05	8.28	0.17	60.15	0.00	11.87	0.00	0.24	18.40	0.06	0.13	99.40	3.99	14.81	99.80	0	1
07CG-734	07CG-734-158	0.05	0.06	9.49	0.16	61.51	0.00	12.00	0.00	0.20	15.96	0.05	0.13	99.61	1.22	14.86	99.74	0	1
07CG-749	07CG-749-011	0.12	0.25	3.08	0.02	64.09	0.00	8.10	0.00	0.95	22.86	0.18	0.14	99.80	3.97	19.29	100.20	0	1
08CG-18	08CG-18-226	0.03	0.02	9.15	0.14	62.31	0.01	12.10	0.00	0.24	15.56	0.04	0.14	99.75	1.09	14.59	99.85	1	1
08CG-18	08CG-18-194	0.13	0.34	7.96	0.24	61.08	0.00	13.03	0.00	0.20	16.38	0.11	0.06	99.54	3.30	13.41	99.87	1	1
08CG-31	08CG-31-084	0.06	1.54	1.72	0.12	63.21	0.00	9.90	0.00	0.38	21.98	0.10	0.17	99.19	4.60	17.85	99.65	1	0
09-CG-012	09-CG-012-001	0.15	0.26	8.15	0.06	60.67	0.00	12.64	0.00	0.20	17.93	0.15	0.06	100.29	4.14	14.21	100.70	0	1
09-CG-062	09-CG-062-016	0.04	0.06	9.00	0.19	61.39	0.00	12.15	0.00	0.23	16.18	0.06	0.11	99.40	1.90	14.47	99.59	0	1
09-CG-080	09-CG-080-008	0.09	0.02	9.25	0.16	62.06	0.00	12.22	0.00	0.22	15.86	0.08	0.05	100.01	1.34	14.66	100.15	1	1
09-CG-081	09-CG-081-007	0.12	0.17	5.81	0.04	63.09	0.00	13.50	0.00	0.40	15.71	0.17	0.02	99.05	4.33	11.82	99.48	1	1
09-CG-113	09-CG-113-118	0.04	0.01	8.60	0.19	60.52	0.00	9.82	0.00	0.34	19.68	0.04	0.22	99.45	2.13	17.76	99.67	0	1
09-CG-122	09-CG-122-006	0.07	1.52	4.76	0.15	62.46	0.00	11.21	0.00	0.30	18.15	0.10	0.08	98.80	2.06	16.30	99.00	1	0
09-CG-124	09-CG-124-011	0.09	1.84	5.34	0.13	63.27	0.01	13.20	0.00	0.21	15.19	0.10	0.07	99.45	1.36	13.97	99.59	1	0

Table 7. Summary of the statistics in the microprobe analysis of chromite and ilmenite grains.

CR grains							
Total	**Chromite**	**Mg-ilmenite**	**Crustal ilmenite**	**Other**			
				Fe-Oxide	**Fe-Ti oxide**	**Rutile**	**Hematite**
1240	1022	125	34	7	48	3	1
	%Chromite	**%Mg-ilmenite**	**%Crustal ilmenite**	**%Other**	**%Total**		
	82.4	10.1	2.7	4.8	100		
IM grains							
Total	**Mg-ilmenite**	**Crustal ilmenite**	**Chromite**	**Other**			
				Fe-Oxide	Fe-Ti oxide	Rutile	
2182	1949	83	135	9	3	3	
	%Mg-ilmenite	**%Crustal ilmenite**	**%Chromite**	**%Other**	**%Total**		
	89.3	3.8	6.2	0.7	100		
Crustal ilmenite grains							
Total	**Crystal ilmenite**	**Mg-ilmenite**	**%Crustal ilmenite**	**%Mg-ilmenite**	**%Total**		
34	4	30	11.8	88.2	100		

Table 8. Summary of the statistics in the microprobe analysis of pyroxene grains.

Cr-diopside grains						
Total	**Cr-diopside**	**Low-Cr-diopside**	**Andradite**	**% Cr-diopside**	**%Low Cr-diopside**	**%Other**
402	401	0	1	99.8	0	0.2
Low-Cr diopside grains						
Total	**Low Cr-diopside**	**Cr-diopside**	**Amphibole**	**%Low Cr-diopside**	**Pyroxene DC**	**%Other**
643	0	642	1	0	99.8	0.2
Enstatite grains						
Total	**Enstatite**	**Cr-diopside**				
12	0	12				

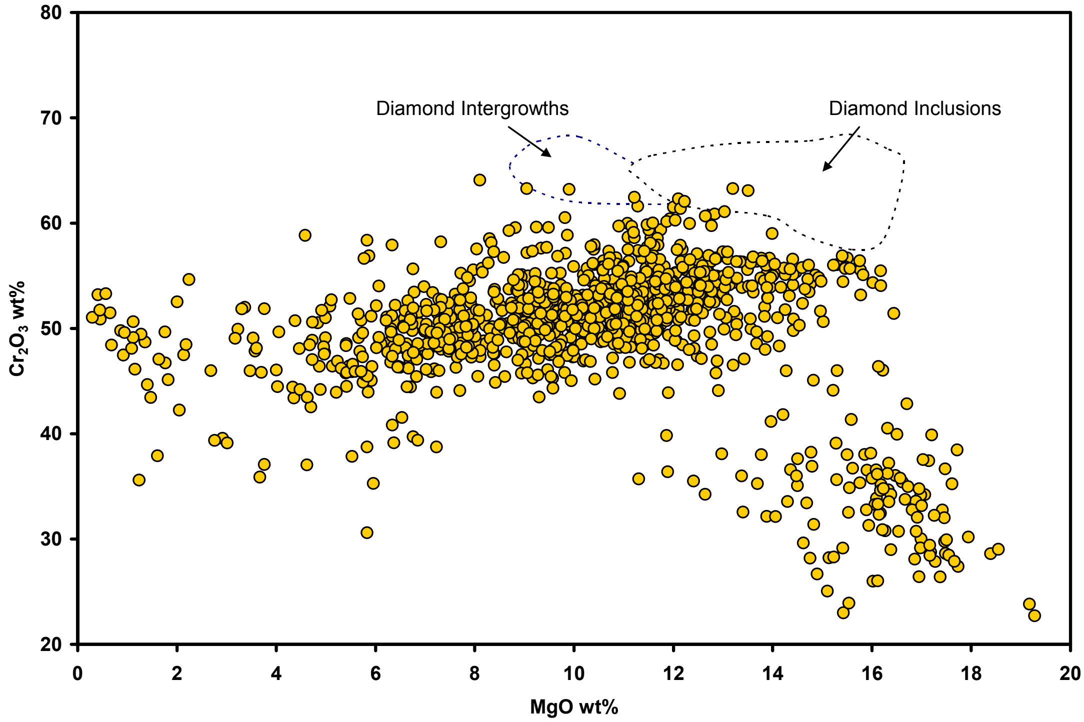

Figure 14. MgO versus Cr_2O_3 binary plot of chromite grains recovered from the study area (*after* Fipke et al. 1995).

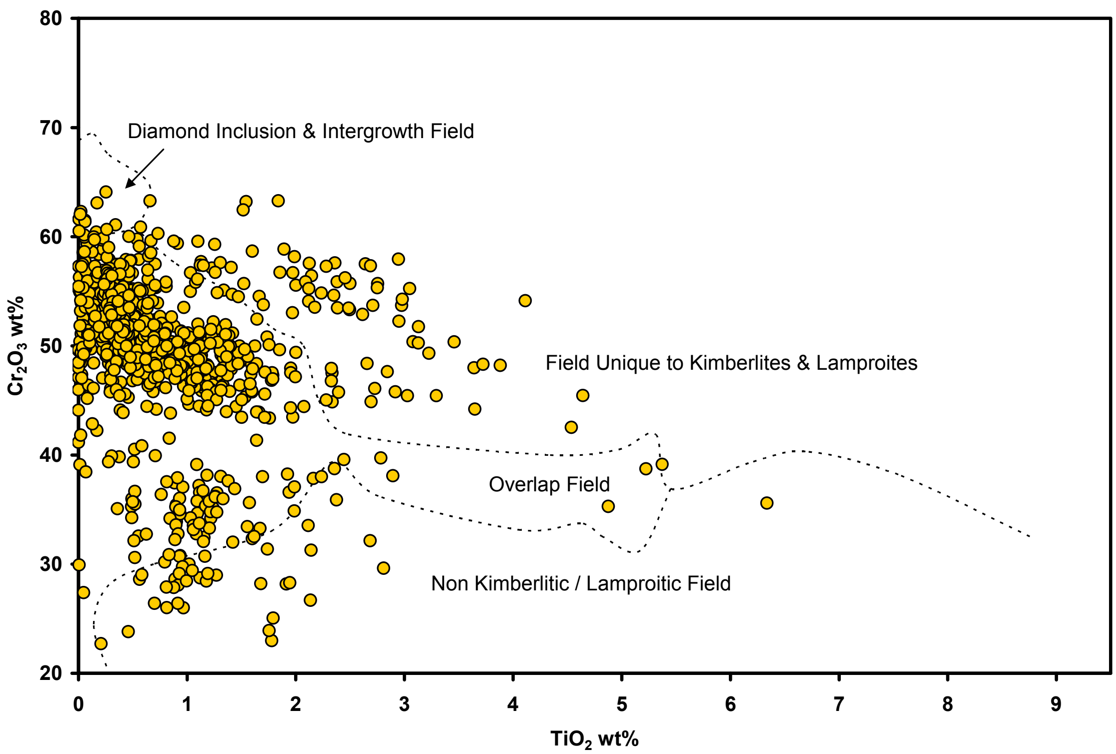

Figure 15. TiO_2 versus Cr_2O_3 binary plot of chromite grains recovered from the study area (*after* Fipke et al. 1995).

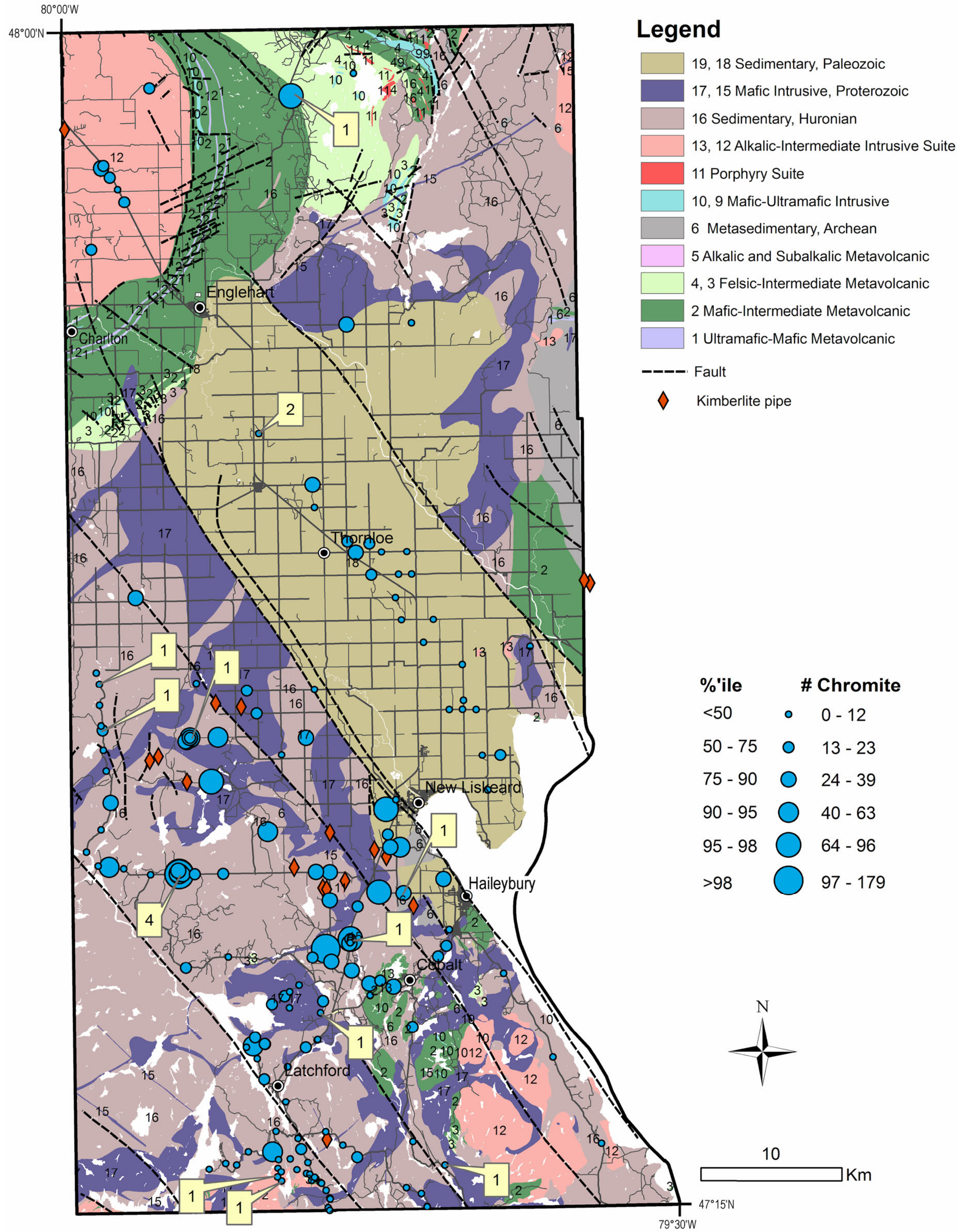

Figure 16. Regional distribution of chromite grains. Annotation with numbers indicates chromite grains classified into the diamond inclusion and intergrowth field (*see* Figures 14, 15). Bedrock geology *after* OGS (1991) and Ayer et al. (2006).

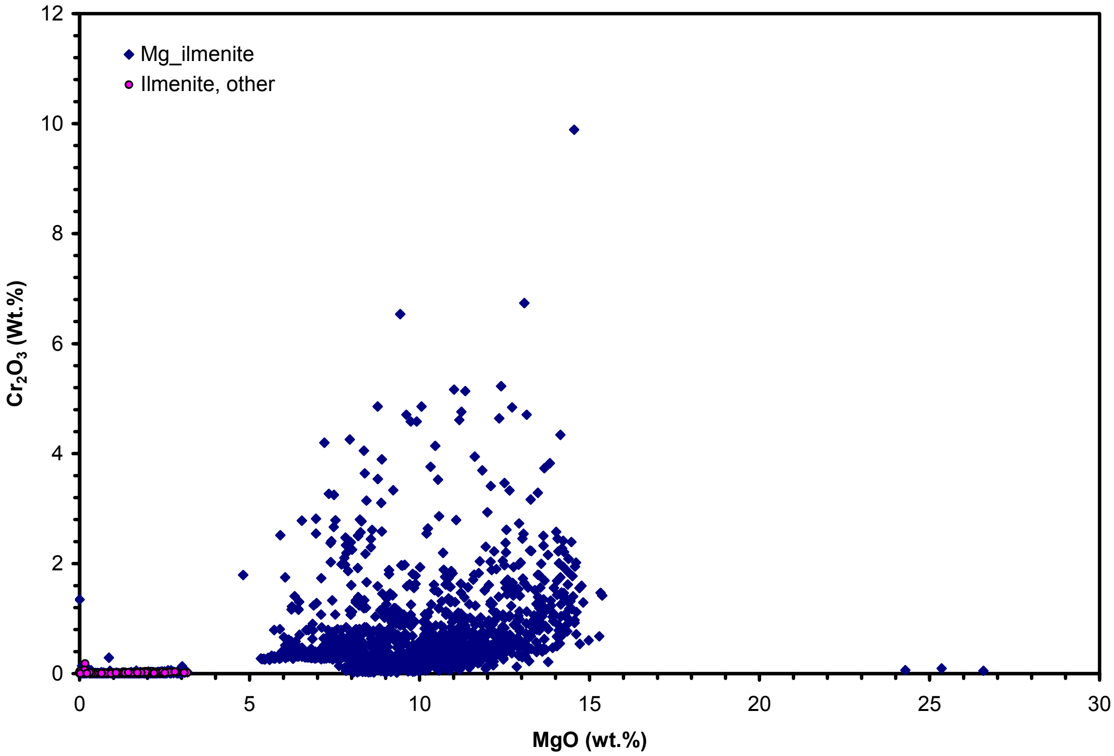

Figure 17. MgO versus Cr_2O_3 binary plot of ilmenite grains.

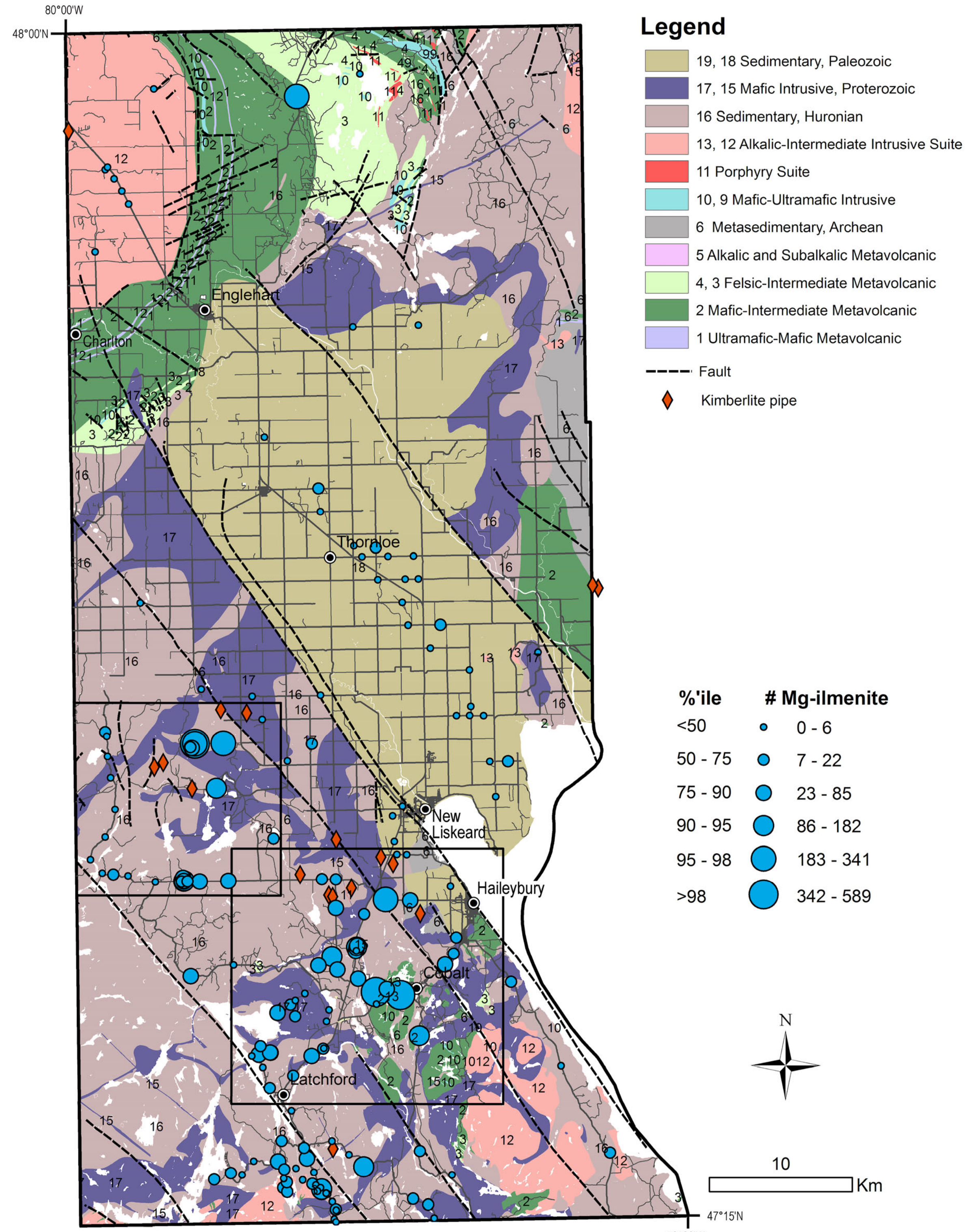

Figure 18. Regional distribution of Mg-ilmenite grains. Bedrock geology *after* OGS (1991) and Ayer et al. (2006). Boxed areas are enlarged in Figures 19 and 20.

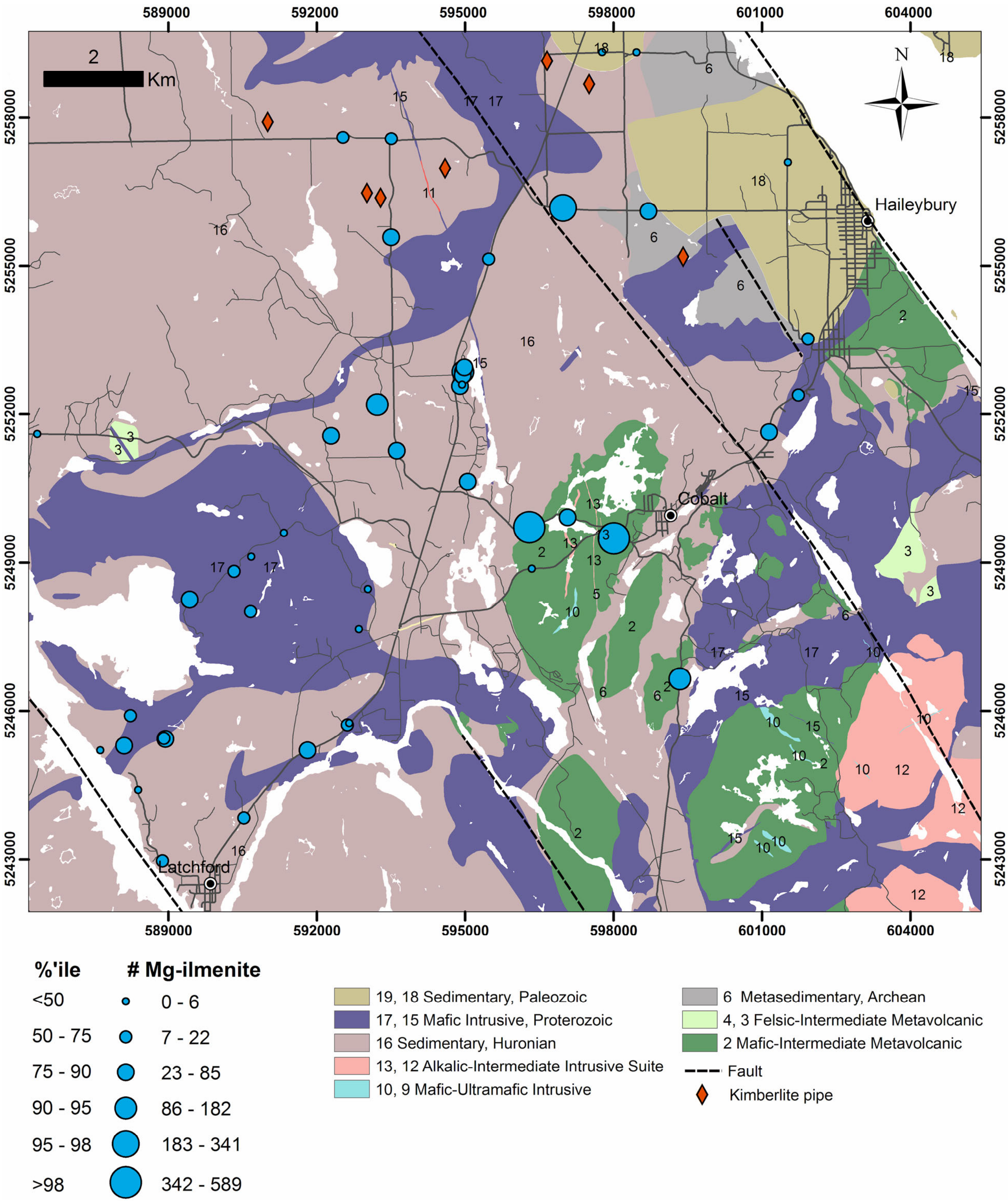

Figure 19. Enlarged view of regional distribution of Mg-ilmenite grains in the Cobalt area (*see* Figure 18 for location).

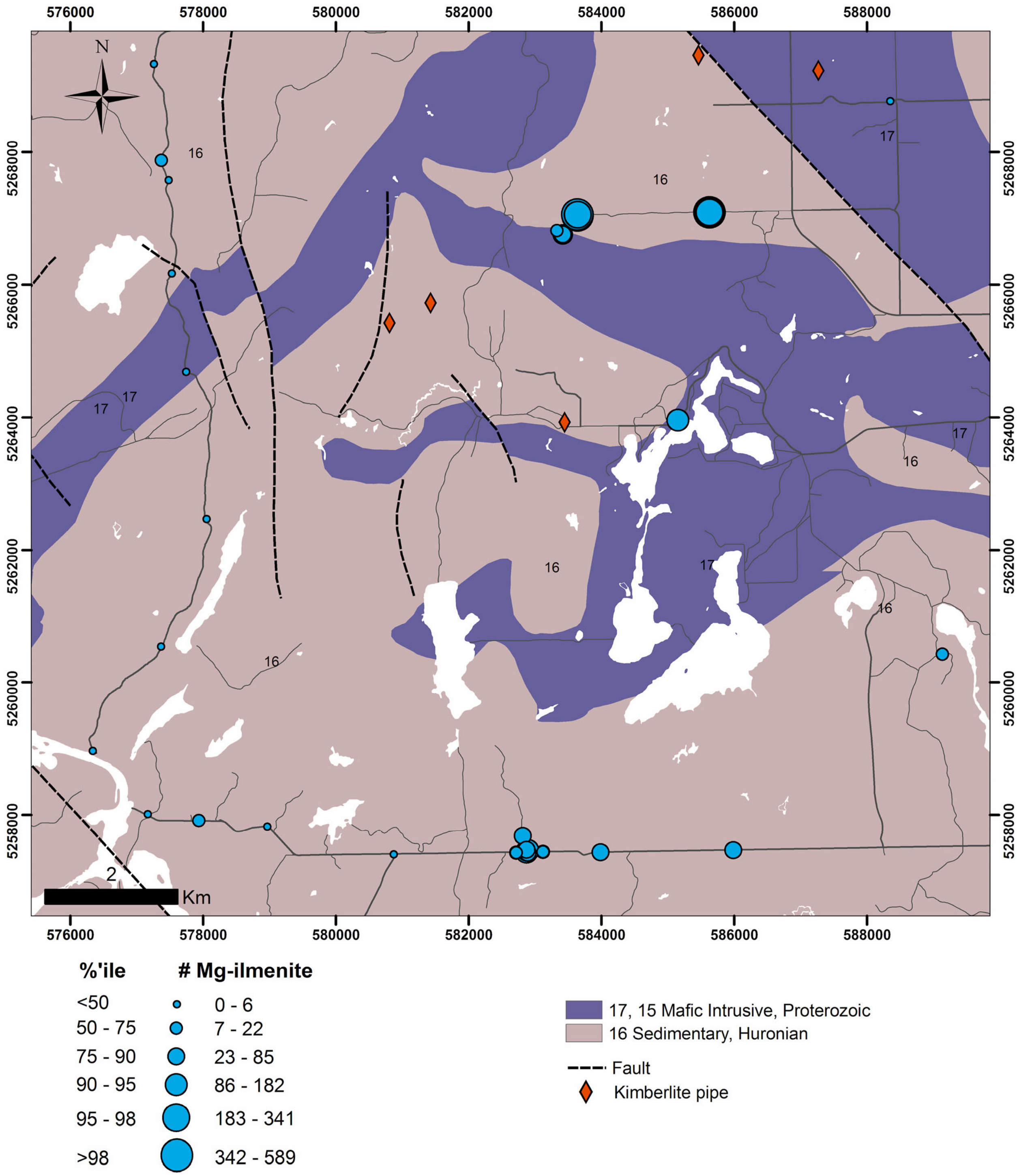

Figure 20. Enlarged view of regional distribution of Mg-ilmenite grains in the western part of the New Liskeard area (*see* Figure 18 for location).

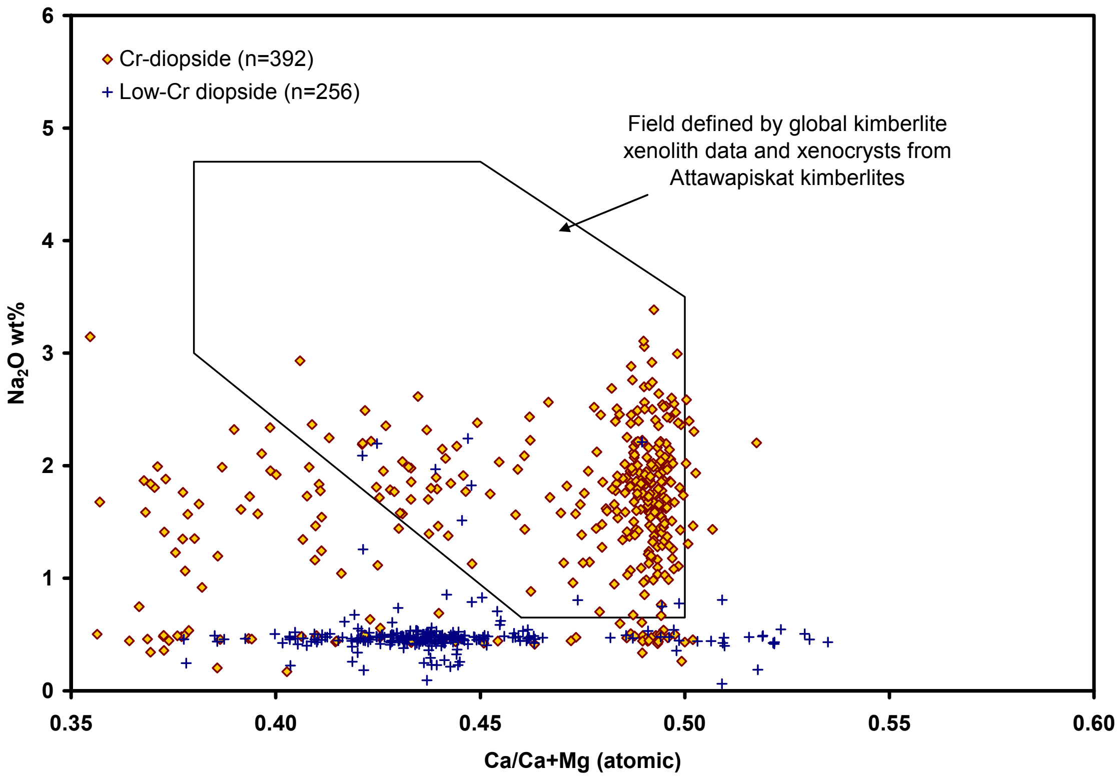

Figure 21. Ca/(Ca+Mg) versus Na_2O classification scheme for clinopyroxene (diopside) grains (*after* Crabtree 2003).

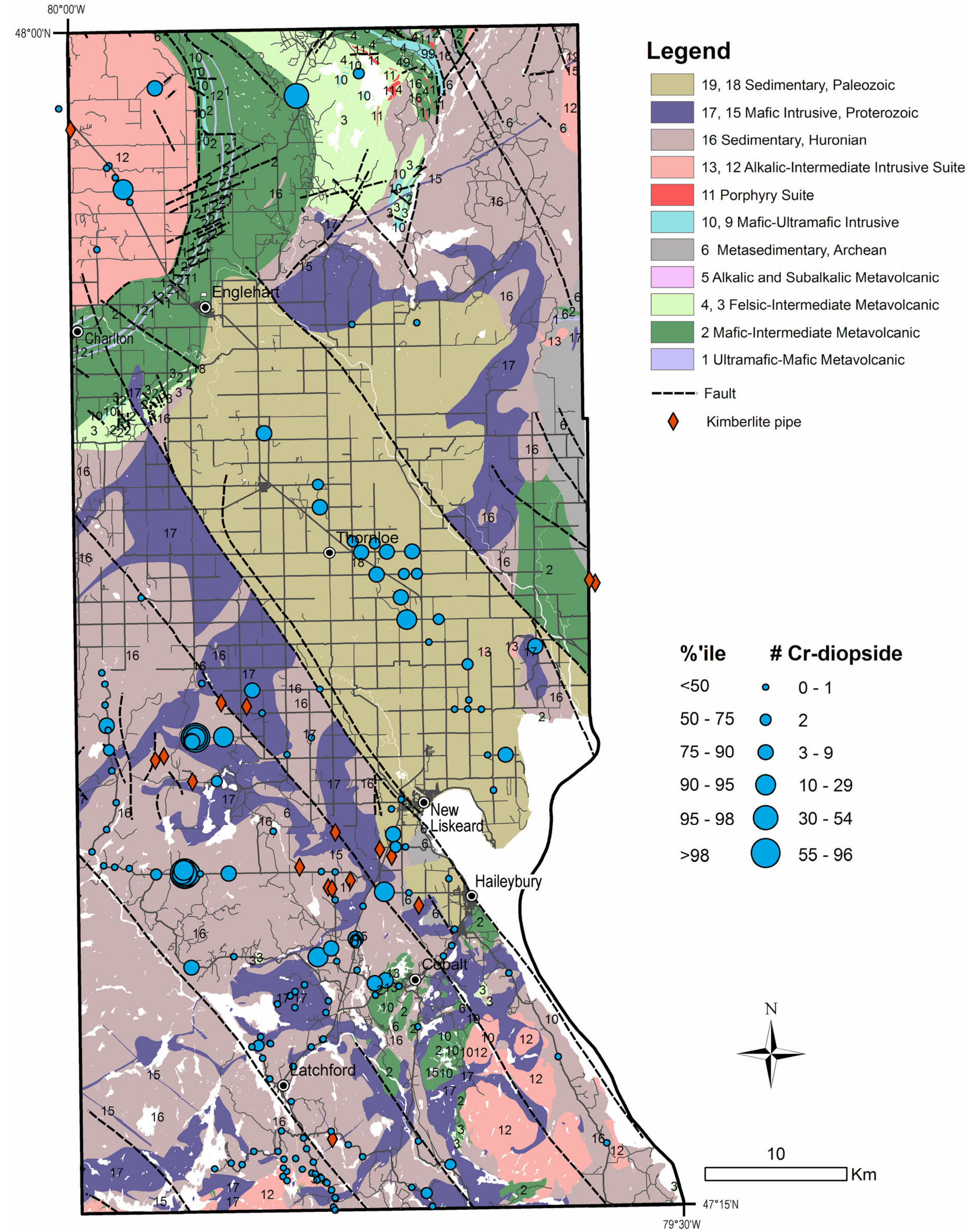

Figure 22. Regional distribution of Cr-diopside grains. Bedrock geology *after* OGS (1991) and Ayer et al. (2006).

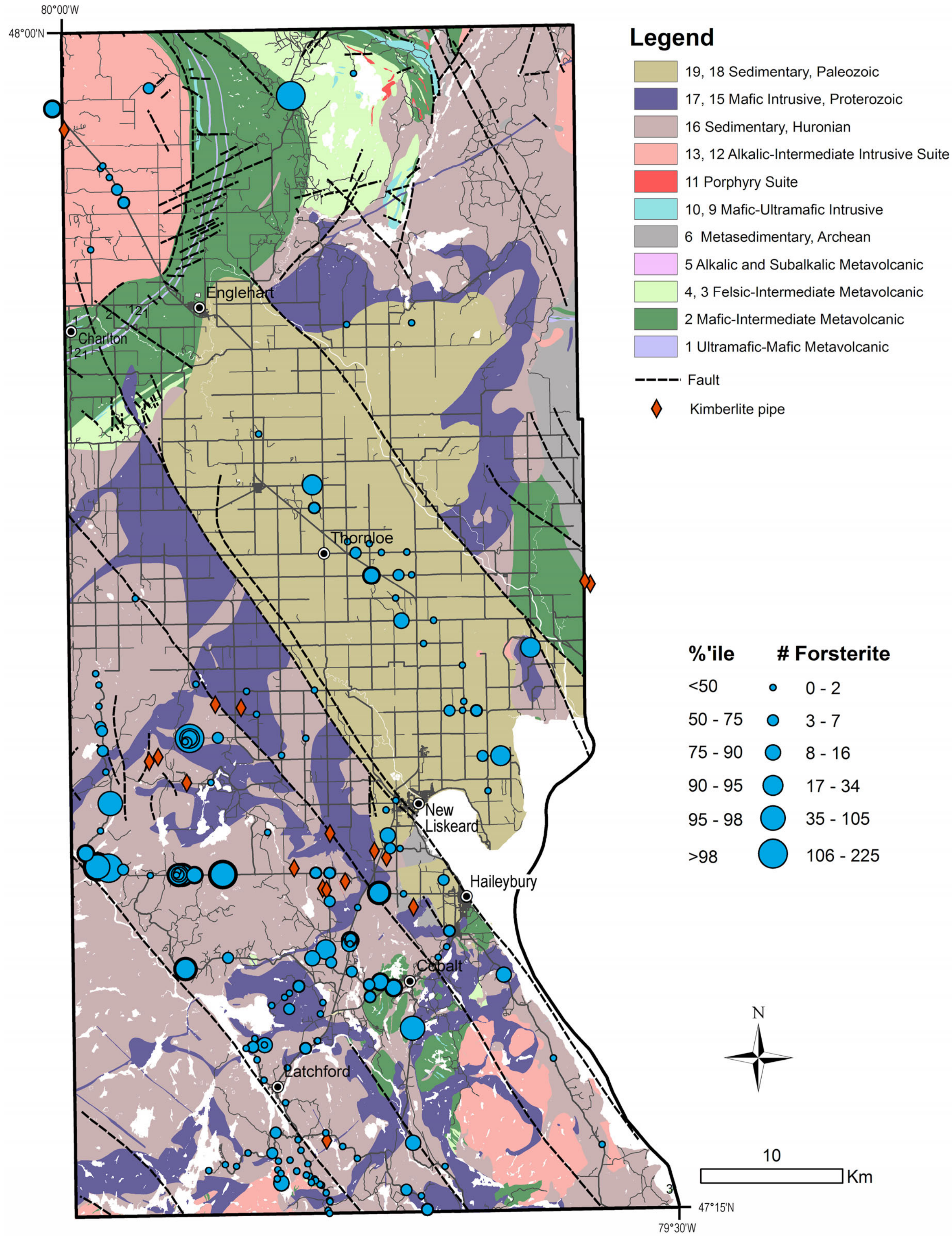

Figure 23. Regional distribution of forsterite (olivine) grains. Bedrock geology *after* OGS (1991) and Ayer et al. (2006).

AREA A

Located about 2 km west of the town centre of Cobalt in the northeast of Coleman Township, Area A includes samples 09CG-59 and 09CG136 which contain anomalous numbers of KIMs (*see* Figure 24; Figure 2 for locations). The mineral compositions consist predominantly of ilmenite and pyrope (*see* Figure 26; Figures 9, 12, 19). In total, 3 G10D and 3 G4D garnets were recovered from the samples collected in this area (*see* Table 5 and Figures 9, 12), suggesting a high potential of the source areas for diamonds. On a binary plot of MgO vs. Cr_2O_3, ilmenite grains from the 2 samples fall within the same area, suggesting a possible single source or 2 sources with similar mineralogy (Figure 27). This is further evidenced by a geochemical similarity among the pyrope garnets at these 2 sites (Figure 28).

Sample 09CG-59 came from a noncalcareous, stone-rich sandy till no more than 0.5 m thick on argillite bedrock with striae oriented at 215° crosscut by younger striae oriented at 200°. Sample 09CG-136 was obtained at the base of a noncalcareous sandy till with abundant argillite boulders, 2 to 4 m thick in a road cut. The bedrock is not exposed here but striae on polished bedrock at sample site 09CG-58 (*see* Figure 2 for location), about 0.8 km to the south, are oriented at 225° crosscut by striae at 210°. As such, the anomalous concentrations of KIM grains in this area are probably related to source(s) in the up-ice direction to the northeast and north-northeast.

The nearest known kimberlite is the Peddie pipe located about 6 km to the north-northeast in Bucke Township (*see* Figure 24 and Figure 2 for locations). McClenaghan, Kjarsgaard and Kjarsgaard (2002) demonstrated a faint, southeast-aligned dispersal train from this pipe based on elevated numbers of olivine and ilmenite grains. As such, the Peddie pipe can be excluded from being the source of the anomalous KIMs in Area A. Previous till sampling conducted between Highway 11 and the Peddie pipe in Bucke Township has returned high KIM counts in numerous samples within a dispersal train that extends southward for 6 km from just west of the Peddie pipe to the southern boundary of Bucke Township (Contact Diamond Corporation 2003). The samples in Area A have a similar mineral composition to those collected by Contact Diamond Corporation (2003) being dominated by ilmenite and pyrope but with negligible Cr-diopside grains (*see* Figure 26). This suggests that the mineral anomalies in Area A may be related to this large dispersal train. Based on mineral compositions, it has been suggested that this dispersal feature is not sourced by the Bucke and Gravel pipes which are 9 km to the north of Area A, but derived from an unknown pipe (Averill 1996).

AREA B

Area B is located 5.5 km east of Mowat Landing on Municipal Road in the eastern part of Barr Township (*see* Figure 24 and Figure 2 for locations). After anomalous numbers of KIM grains were counted from a sample collected in 2007, this area was resampled to confirm this anomaly. Area B contains 7 samples within a radius of 250 m and all have anomalous concentrations of pyrope and chromite grains (*see* Figure*s* 10, 13, 16 and Figure 2 for sample locations). The samples were collected from a noncalcareous stony to sandy till containing numerous argillite boulders, with a thickness of no greater than 2 m. Measurements of striae in the vicinity indicate an ice flow direction of 190° (Baker, Gao and Perttunen 2010). There were a dozen G3D, G4D and G5D garnets recovered from the heavy mineral concentrates, notably, from samples 08CG17, 19 and 18, as well as 07CG734, and, in addition, chromites in the diamond inclusion and intergrowth field are present in the latter 2 samples (*see* Tables 5, 6 and Figures 10, 13, 16). This suggests a source area or kimberlite pipe that contains diamond-bearing chromite harzburgitic peridotite and eclogite/pyroxenite.

The samples have a similar mineral composition dominated by pyrope garnets with a moderate level of ilmenite (*see* Figure 26). Their composition differs from the known kimberlite pipes 95-1 and 96-1, located about 8 km to the north in Lundy Township, where ilmenite predominates in the heavy mineral concentrates of the pipes (Contact Diamond Corporation 2003). Diamondiferous pipe 95-2, about 6 km to the north in the eastern part of Lundy Township, is rich in pyrope garnet but has limited ilmenite. It has a distinct dispersal feature and the till samples in the immediate down-ice direction have a mineral composition similar to that of this pipe (Contact Diamond Corporation 2003). The presence of moderate numbers of ilmenite grains suggests that the KIMs in the samples of Area B came from an unknown kimberlite pipe to the north.

The similar KIM composition among these closely clustered samples suggests a single source or kimberlite pipe. The geochemical data reflect the nature of this unknown kimberlite pipe (Figures 29 to 32). On the binary plot of CaO vs. Cr_2O_3, more than 20 grains are tightly clustered together in the G10 field (Figure 29). Because all of them are from a single sample (08CG-18), they probably result from the break up of a single large garnet or a single piece of xenolith. The ilmenite grains, in general, have low concentrations of Cr_2O_3 (less than 0.8 weight %) (Figure 30), but exhibit compositional ranges of the ilmenite grains in the regional samples (*see* Figure 17). Abundant chromites exist in the samples in Area B, but only a small portion of them were analyzed. The scatter plots (Figures 31, 32) show several grains within or bordering the diamond inclusion and intergrowth field, further suggesting a diamondiferous source rock.

AREA C

Located at the border of Hudson and Lundy Townships, Area C includes several samples that contain anomalous concentrations of KIMs (*see* Figure 24 and Figure 2 for locations). The samples have a similar mineral composition and are dominated by ilmenite with a moderate number of pyrope garnets (*see* Figure 26). In this area, 9 G4D pyroxenitic/eclogitic garnets and 1 chromite in the diamond intergrowth field were recovered, suggesting a high potential of the source rocks to host diamonds (*see* Tables 5, 6 and Figures 13, 16).

Known kimberlite pipes MR 8 and MR6 occur about 4 km to the northeast (*see* Figure 24 and Figure 2). A dispersal train in till has been identified previously extending south of MR8 (Contact Diamond Corporation 2003). About 2 km east of Area C, sample 08CG-35 appears to lie within this dispersal train. This sample contains 2 G10D garnets, suggesting potential diamondiferous source rocks that may occur close by (*see* Table 5; Figure 10). The mineral composition of the samples in Area C appears similar to those of the aforementioned dispersal train dominated by ilmenite with a moderate number of pyrope garnets. As such, it is possible that the anomalous KIMs in Area C are related to this dispersal train. However, the possibility that they came from a different source(s) cannot be excluded. Future comparison with the mineralogical and geochemical compositions of these known kimberlite pipes would be useful for gaining insights into the origin of this anomaly and its relationship to MR 8 and MR6. The geochemical data of Area C were plotted together with sample 08CG-35 and shown in Figures 33 to 35.

AREA D

Located in the centre of Bucke Township, Area D has a single sample 09CG-63 that contains anomalous concentrations of KIMs dominated by pyrope and ilmenite (*see* Figures 24, 26). This sample contains 1 G10D and 1 G4D garnets, suggesting a diamondiferous source rock (*see* Table 5; Figures 9, 12). It was collected from the base of a silty sand till with a moderate amount of stones, 0.5 to 1 m thick and resting on Proterozoic tillite bedrock. Measurements of striae indicate an ice flow direction of 210° crosscut by striae of 190°.

There are 3 known kimberlite pipes within a 3 km radius of this site, namely Gravel, Bucke and OPAP to the north and northwest (*see* Figure 26; Figure 2 for locations). OPAP has low concentrations of KIMs and negligible ilmenite grains (Sage 2000). As such, it can be excluded as being the source of the KIMs in this sample. Both the Bucke and Gravel are rich in pyrope and ilmenite (McClenaghan, Gauvreau and Kjarsgaard 2009). The proximity plus a similar mineral composition seems to suggest a link between sample 09CG-63 and these 2 pipes.

The binary charts in Figures 36 and 37 show the mineral chemical composition of sample 09CG-63 plotted against the Bucke and Gravel pipes. The chart of MgO vs. Cr_2O_3 for ilmenite shows a scatter plot trend that differs from that of the Bucke pipe (*see* Figure 36). The Gravel pipe has 2 prominent clusters of ilmenite grains centered at 0.5 and 2.5 weight % Cr_2O_3 (*see* Figure 36). In comparison, sample 09CG-63 lacks ilmenite grains in the upper cluster of this pipe, therefore suggesting a possible different source. However, this remains to be confirmed because of the small number of ilmenite grains analyzed in this sample (n=55).

The binary plot of CaO vs. Cr_2O_3 for the pyrope garnets from the aforementioned sites show a similar scatter plot trend with a predominance of lherzolitic garnets (*see* Figure 37). This is not surprising, because the till samples in the report area all show a similar trend in pyrope composition (*see* Figure 6). Sample 09CG-63 has several garnets along the border between the G1 and G12 fields, whereas the same area on the plot is barren for both the Bucke and Gravel pipes (*see* Figure 37). In addition, the sample has fewer garnets in the G10 field compared to the pipes (*see* Figure 37). The sample size of 09CG-63 appears adequate statistically (n=146). As such, the geochemical difference would further point to an unknown kimberlite pipe responsible for the anomalous KIMs in this sample.

AREA E

Area E is defined by a single sand and gravel sample, 09CG-113, that is rich in KIM grains (*see* Figure 24). The KIM assemblage contains large counts of ilmenite, olivine and pyrope garnet grains but a low number of chromites (*see* Figure 25; Appendix 9). This sample yielded a chromite grain that is located in the diamond inclusion and intergrowth field, suggesting a diamondiferous source rock (*see* Table 6, Figure 16). It was collected from the upper part of a large esker, the Munro Esker (*see* Figure 3), which has a depth of over 15 m at the sampling site. In the Kirkland Lake region, the Munro Esker runs southwards along a pathway adjacent to a swarm of kimberlite pipes including A1, A4 and B-30 located more than 30 km north of Area E (Baker 2000; Ayer et al. 2006). Kimberlite boulders collected from gravel pits in the Munro Esker south of these pipes show high concentrations of olivine, chromite and ilmenite grains, matching the KIM composition of the A1 pipe (Kjarsgaard et al. 2004). A boulder (Group II) barren of chromite grains is thought to come from an unknown pipe in the adjacent area (Kjarsgaard et al. 2004). Sample 09CG-113 appears to have a similar mineral composition with this boulder. Olivine is a relatively soft mineral which can easily be abraded during fluvial transport and its relative abundance with respect to other KIM grains is reduced with increasing distance of transport. The abundance of olivine grains in the KIM assemblage of this sample would suggest that they may not come from the same kimberlite pipe responsible for the kimberlite boulder located more than 20 km to the north. Unlike the boulder, sample 09CG-113 contains a moderate number of chromites (*see* Table 9; Figure 25). Such a difference in mineral composition favours an interpretation for a different source area.

Despite the abundant KIMs, only a small portion of them were analyzed (Figures 38, 39). Although the sample size is small (n=53), the ilmenite grains on a binary chart show elevated values of Cr_2O_3 at 7 weight % MgO. In contrast, those from the kimberlite boulders or pipes to the north are, as Kjarsgaard et al. (2004) described, located in a field with MgO exceeding 8 weight %. Pyrope garnets (n=106) from this sample are frequently clustered at 4 weight % Cr_2O_3 and some are located in the eclogitic or G3 field on the binary plot of CaO vs. Cr_2O_3 (*see* Figure 39). In contrast, those from the aforementioned Group II boulder are clustered at 2 weight % Cr_2O_3 and less, and eclogitic garnets are absent (Kjarsgaard et al. 2004). Although heavy minerals can be brought into an esker from various sources, such a difference in mineral composition can probably be interpreted as being from an unknown kimberlite pipe located somewhere between this site and the Group II kimberlite boulder located more than 20 km to the north.

Metamorphic/Magmatic Massive Sulphide Indicator Minerals

Metamorphic/magmatic massive sulphide indicator minerals (MMSIM®) are a group of stable heavy minerals typically derived, as Averill (1999) suggests, from volcanogenic massive sulphide (VMS) and magmatic Ni-Cu sulphide deposits, as well as from skarn and greisen rocks (Table 10). Common MMSIM® grains associated with VMS deposits include gahnite, chalcopyrite, red-rutile, staurolite, spinel, kyanite, Mn-epidote, orthopyroxene and sillimanite, whereas those with magmatic Ni-Cu deposits include Cr-rich phases such as Cr-diopside, chromite and Cr-rutile. It is noteworthy that anomalous counts of chromite in the drift material may indicate potential high-grade chromite mineralization in mafic and ultramafic igneous rocks as in the case of the McFaulds Lake (“Ring of Fire”) area in the James Bay Lowland (Crabtree 2003).

The metamorphic/magmatic massive sulphide indicator minerals occur in nonmineralized rocks; nonkimberlitic olivine, chromite and diopside derived from mafic to ultramafic rocks are also common in drift material sampled in northern Ontario (Averill 1999; Crabtree 2003). These minerals become significant only if other diagnostic minerals such as sulphides of the ore phases co-exist with them. However, sulphide heavy minerals are easily weathered and, with exception of chalcopyrite and, to a lesser degree, sphalerite, they are uncommonly preserved in the till and stream sediments (Barnett and Averill 2010). This often renders the use of MMSIM® for assessment of potential mineralization difficult. Gahnite is often enriched in zinc deposits during ore formation and stable in the subsequent secondary environment (Averill 1999; Crabtree 2003). Its coexistence with other MMSIM® in drift sediments may be linked to significant volcanogenic massive sulphide (VMS) type mineralization.

The counts of MMSIM® are listed in Appendix 10. The counts of low-Cr diopside grains in this table differ slightly from those in the KIM data set where they are classified as MMSIM® or pseudo KIMs (*see* Appendix 6). As well, some picked ilmenite and chromite grains were reclassified as rutile and spinel on the basis of the microprobe data (*see* Table 7). For this reason, the number of low-Cr diopside grains from the KIM data set was used instead and the MMSIM® data set was adjusted to include the reclassified rutile and spinel grains. Also, chromite data from the KIM data set (*see* Appendix 9) was included here as part of the MMSIM® data set (*see* Figure 16).

Although some low-Cr diopside grains are of kimberlitic origin, most of them likely come from nonkimberlitic sources such as ultramafic to mafic rocks (*see* Figure 21). Such mineral grains are abundant in the Precambrian bedrock terrain in the northern and southwestern parts of the study area. It was unexpected to find large concentrations of low-Cr diopside grains in the lake Timiskaming graben basin (Figure 40). This feature is probably related to glacial dispersion from mafic and ultramafic rocks situated in the Precambrian bedrock terrain north and northeast of the basin. Abundance of low-Cr diopside grains may indicate significant magmatic Ni-Cu mineralization in such igneous terrains (Averill 1999). Future work in this region is recommended.

Table 9. Samples containing more than 100 KIM grains (0.25-2.0 mm) based on adjusted KIM counts (*see* Appendix 9).

Sample	GP	GO	DC	IM	CR	FO	Total	Low-Cr diopside
08CG-32	77	46	96	589	30	33	871	100
09-CG-113	119	53	48	291	78	225	814	310
07CG-564	56	35	51	308	23	129	601	0
09-CG-063	106	124	16	197	75	34	551	40
09-CG-059	55	59	0	358	24	16	512	14
07CG-734	113	41	59	93	179	13	499	20
09-CG-136	48	56	4	349	26	7	490	43
08CG-17	98	72	53	109	134	23	489	31
08CG-15	131	58	88	53	103	29	462	50
08CG-31	31	13	31	348	26	10	459	10
08CG-30	61	61	26	244	42	8	442	51
08CG-35	39	6	11	327	46	3	432	41
08CG-18	168	55	52	25	53	6	359	28
08CG-24	92	44	54	15	28	34	267	49
07CG-754	12	2	9	101	106	19	249	3
08CG-10-3	8	9	5	139	64	13	238	29
09-CG-140	5	1	2	132	73	1	214	32
08CG-22	8	3	1	10	43	133	198	37
09-CG-086	16	19	0	146	16	0	198	9
08CG-19	70	45	15	21	35	1	187	20
09-CG-065	10	2	5	26	18	104	165	113
09-CG-143	11	9	0	89	19	35	163	20
08CG-33	11	10	3	84	30	3	141	27
09-CG-137	3	14	0	78	31	4	130	24
09-CG-039	9	20	1	88	12	0	130	8
09-CG-069	3	1	0	55	50	4	113	40
08CG-23	1	0	0	0	6	105	112	3
08CG-16	32	13	10	26	27	1	109	18
07CG-729	7	5	9	40	17	30	108	16

Table 10. Indicator minerals commonly associated with base metal mineralizations (*after* Averill 1999). Shaded areas indicate an association between mineral and type of deposit.

Indicator Mineral	**VMS**	**Magmatic Ni-Cu**	**Skarn**	**Greisen**	**Other occurrence**
Sillimanite	■				High grade metamorphic
Kyanite	■				High grade metamorphic
Corundum	■				High grade metamorphic
Anthopyllite	■				High grade metamorphic
Mg-spinel	■				High grade metamorphic
Sapharine	■				High grade metamorphic
Staurolite	■				High grade metamorphic
Dumortierite	■				
Mn-epidote	■				
Spessartine	■				Metavolcanics
Gahnite	■				
Franklinite	■				
Willemite	■				
Barite	■				
Cinnabar	■				
Loellingite	■				
Native Au	■		■		
Orthopyroxene	■	■			High grade metamorphic
Cr-rutile	■	■			
Chalcopyrite	■	■	■	■	
Tourmaline	■			■	
Olivine (Forsterite)		■	■		Mafic igneous
Hercynite		■			
Low-Cr diopside		■			Mafic Igneous
Chromite		■			Mafic Igneous
Uvarovite		■			
Loellingite		■			
Rammelsbergite		■			
Sperrylite		■			
PGE alloys		■			
Olivine (kneb)			■		
Vesuvianite			■		
Johannsenite			■		
Grossular			■		
Scheelite			■		
Topaz				■	
Fluorite				■	
Cassiterite				■	
Wolframite				■	

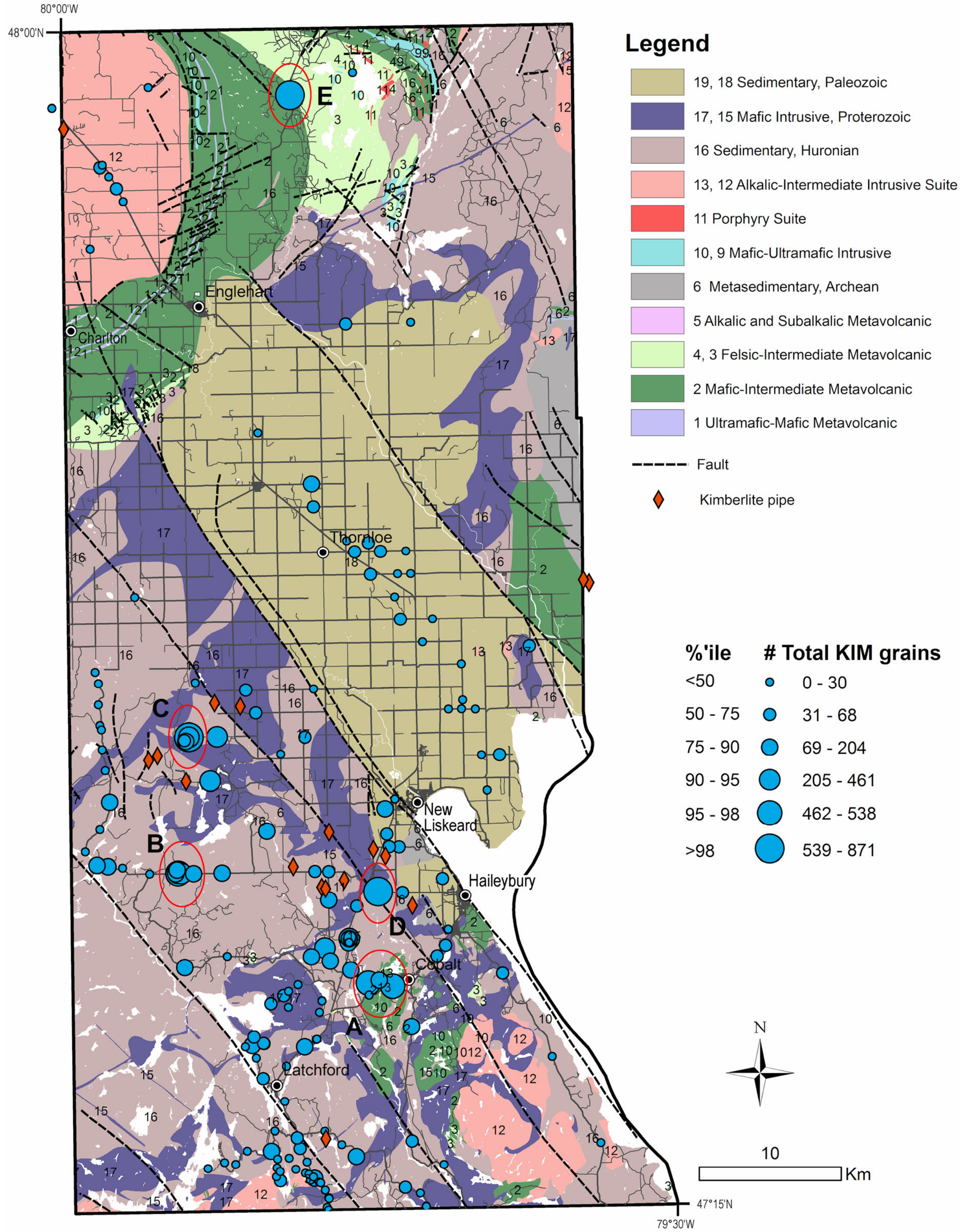

Figure 24. Regional distribution of total KIM grains. Highlighted areas are sites for further discussion in the text. Bedrock geology *after* OGS (1991) and Ayer et al. (2006).

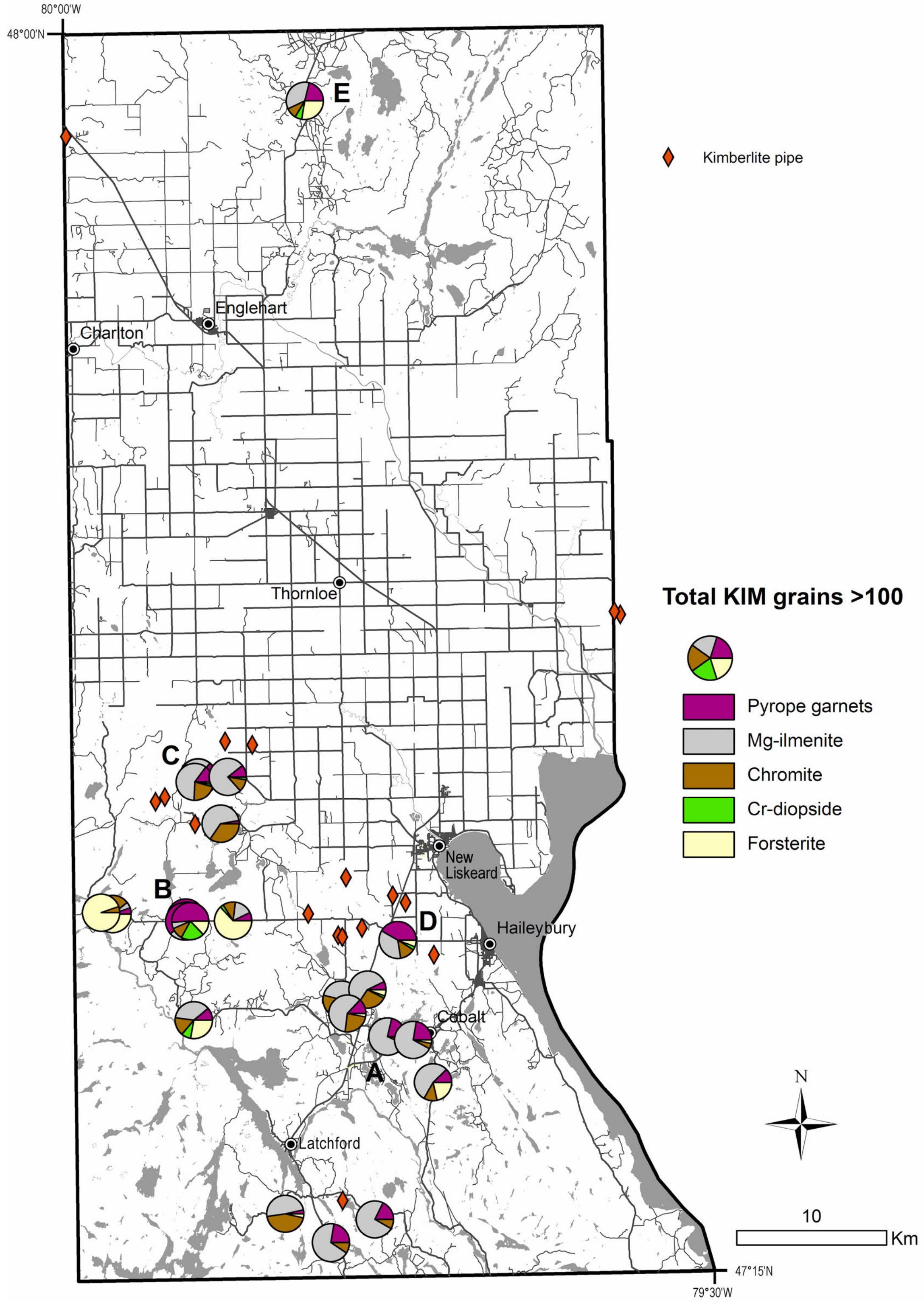

Figure 25. Regional distribution of samples containing more than 100 KIM grains, with pie charts showing mineral compositions.

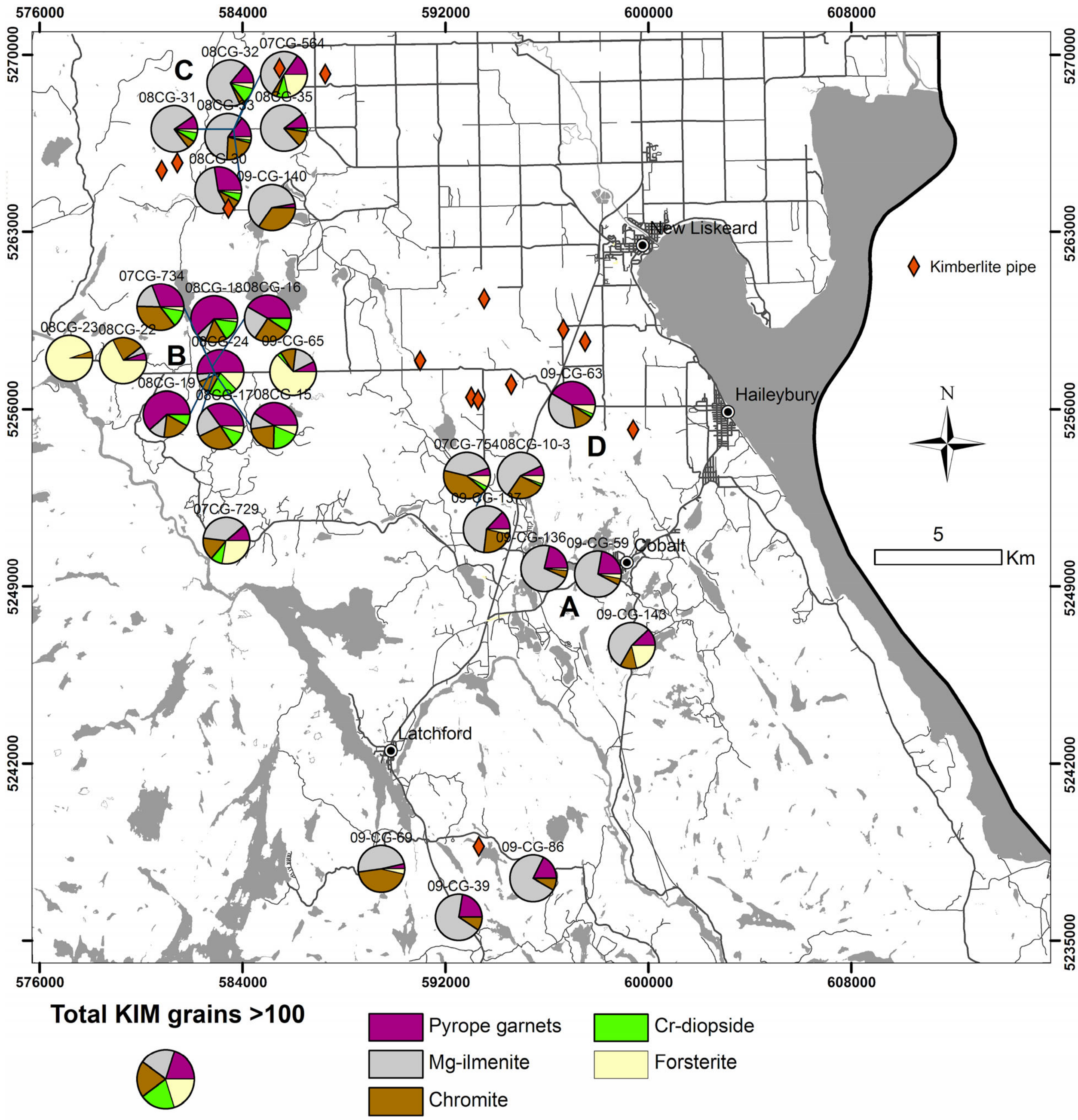

Figure 26. Enlarged view of regional distribution of samples containing more than 100 KIM grains, with pie charts showing mineral compositions in the Cobalt area.

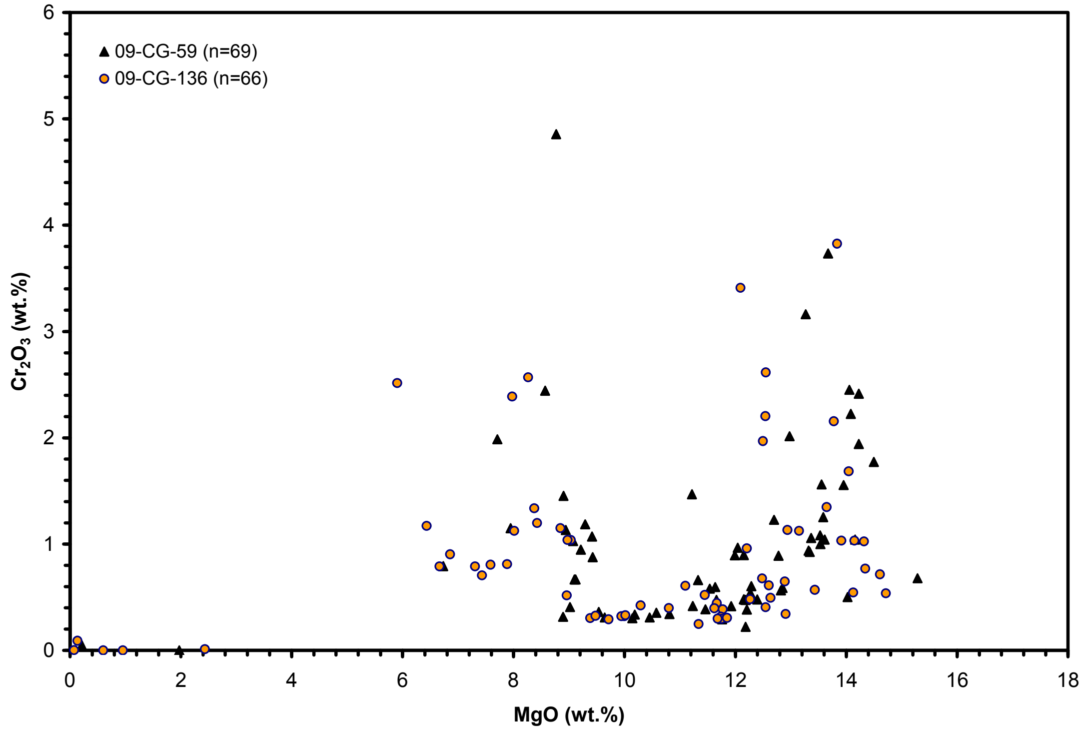

Figure 27. MgO versus Cr_2O_3 binary plot of ilmenite grains recovered from samples 09-CG-59 and 09-CG-136 in Area A.

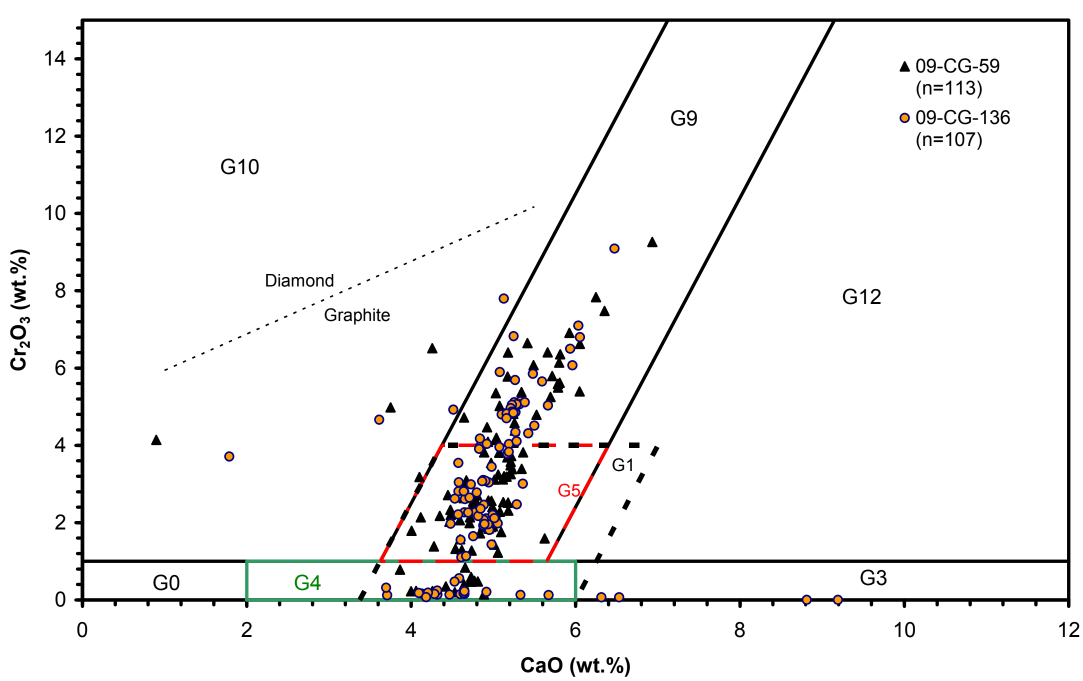

Figure 28. CaO versus Cr_2O_3 binary plot of pyrope garnets recovered from samples 09-CG-59 and 09-CG-136 in Area A (*after* Grütter et al. 2004).

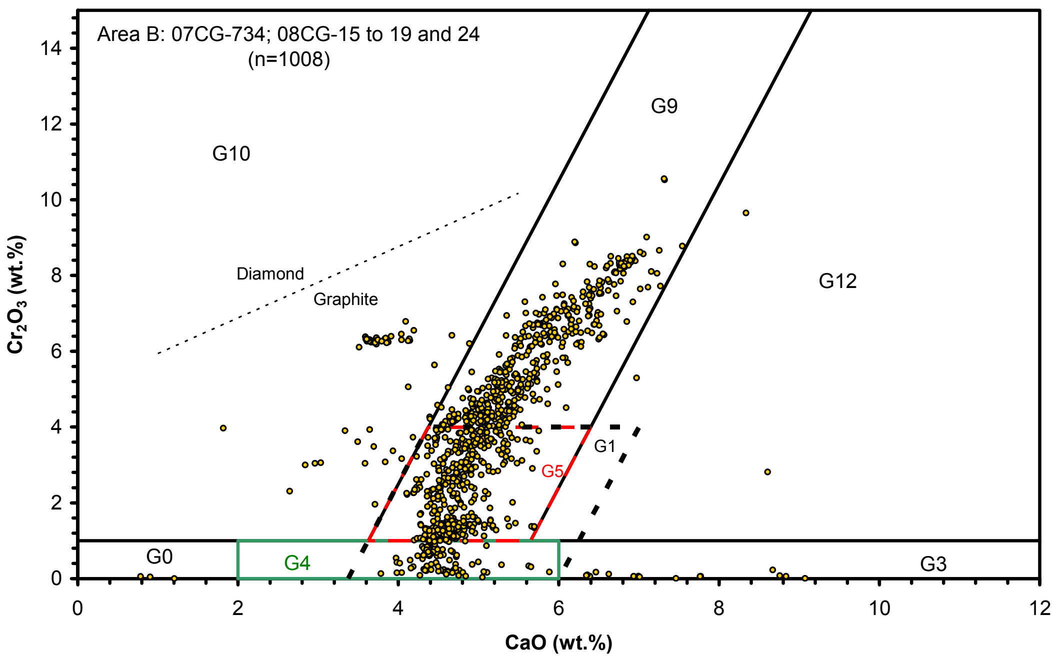

Figure 29. CaO versus Cr_2O_3 binary plot of pyrope garnets recovered from samples 07CG-734, 08CG-15 to 19 and 24 in Area B (*after* Grütter et al. 2004).

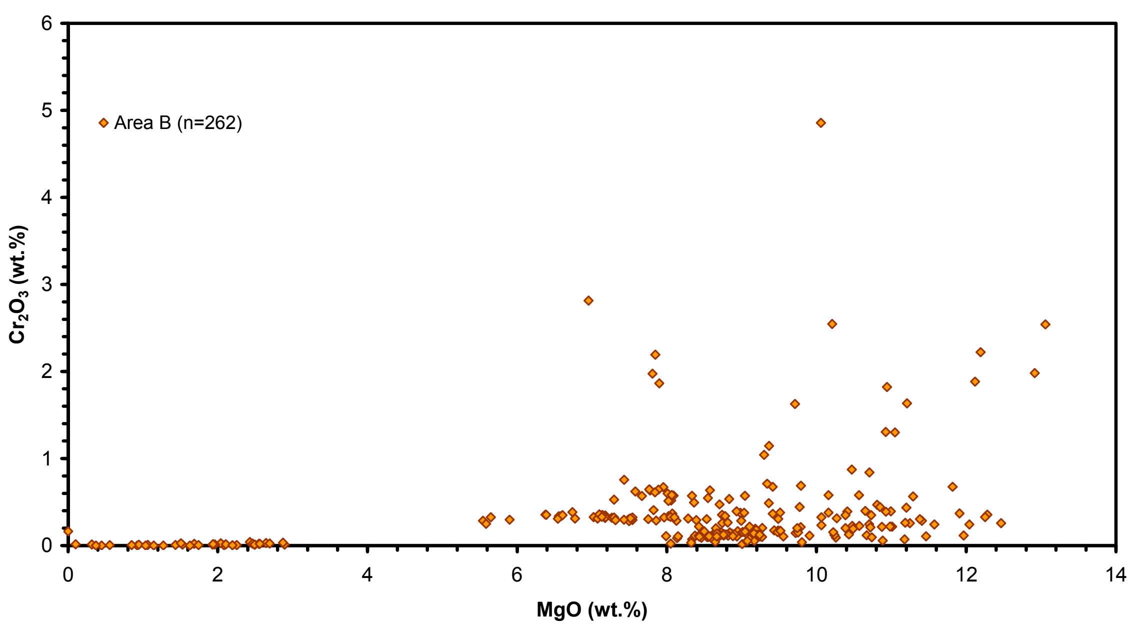

Figure 30. MgO versus Cr_2O_3 binary plot of ilmenite grains recovered from samples 07CG-734, 08CG-15 to 19 and 24 (Area B).

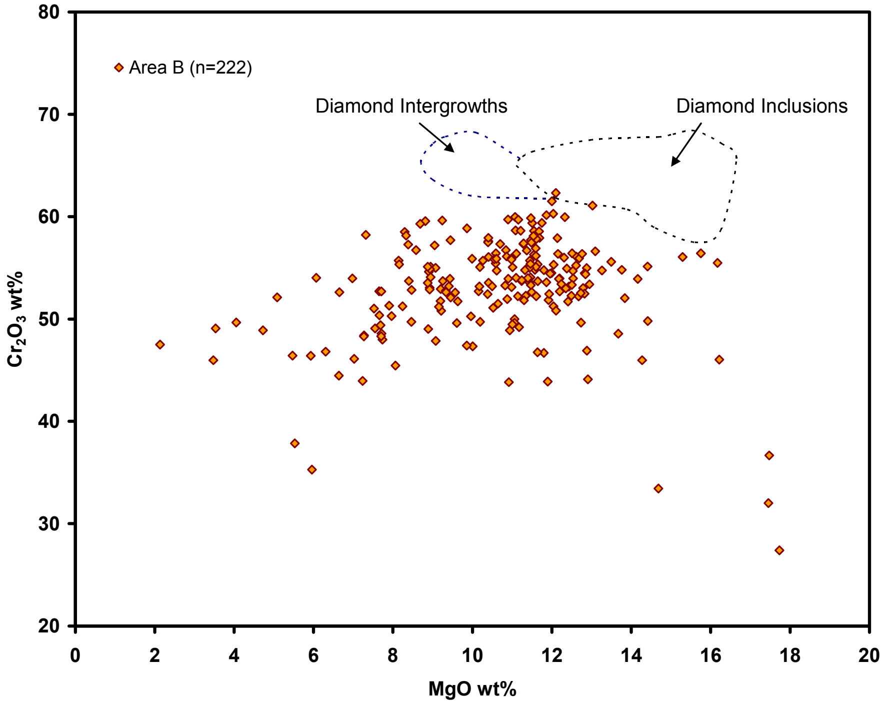

Figure 31. MgO versus Cr_2O_3 binary plot of chromite grains recovered from samples 07CG-734, 08CG-15 to 19 and 24 in Area B (*after* Fipke et al. 1995).

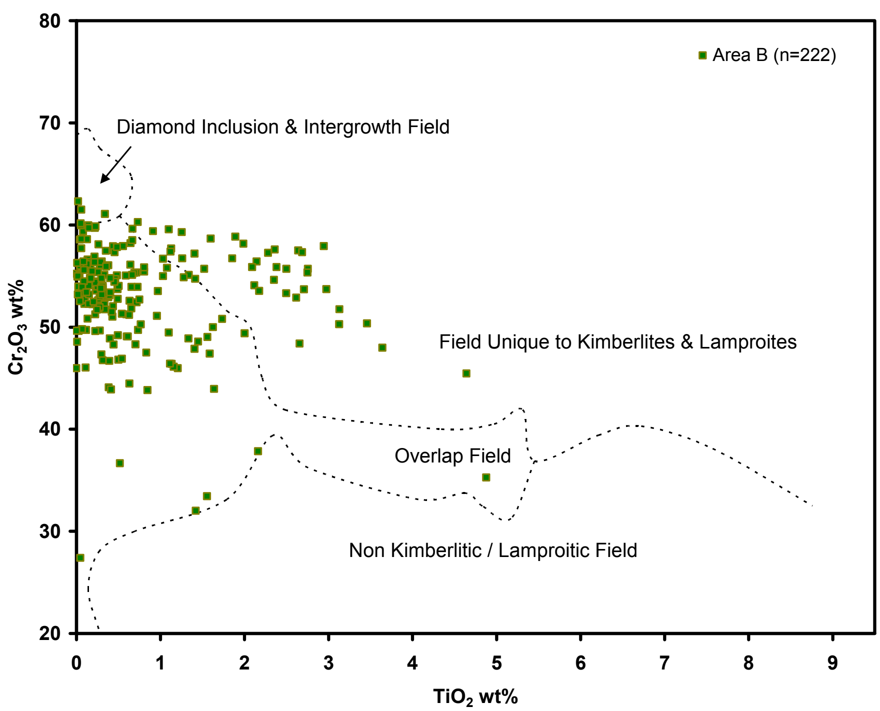

Figure 32. TiO_2 versus Cr_2O_3 binary plot of chromite grains recovered from samples 07CG-734, 08CG-15 to 19 and 24 in Area B (*after* Fipke et al. 1995).

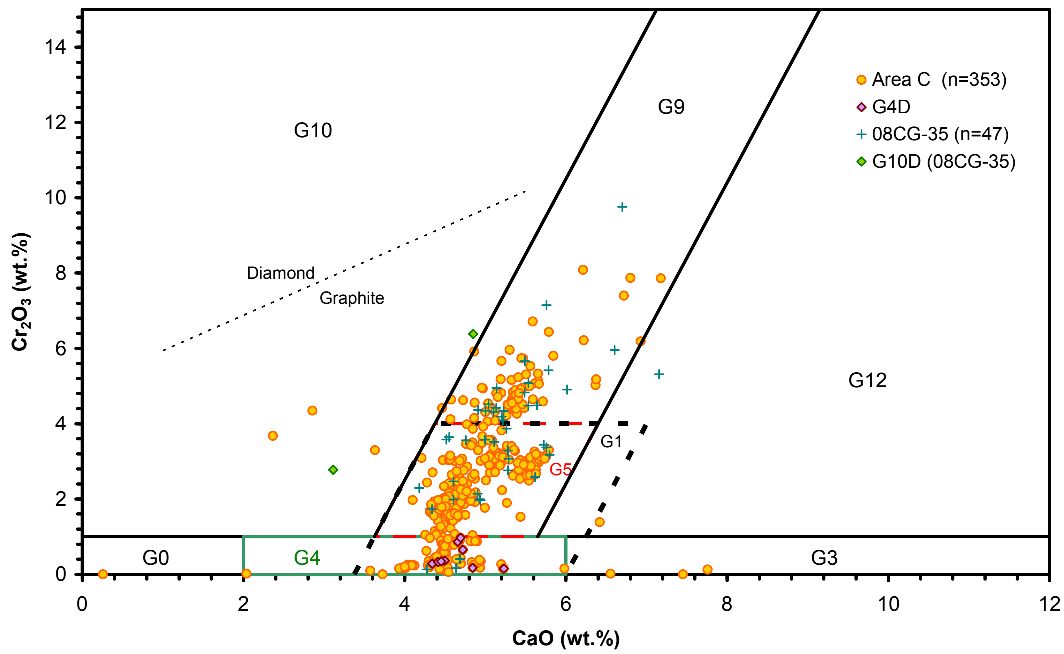

Figure 33. CaO versus Cr_2O_3 binary plot of pyrope garnets recovered from samples 07CG-564, 08CG-30 to 34 in Area C, as well as a nearby sample 08CG-35 (*after* Grütter et al. 2004).

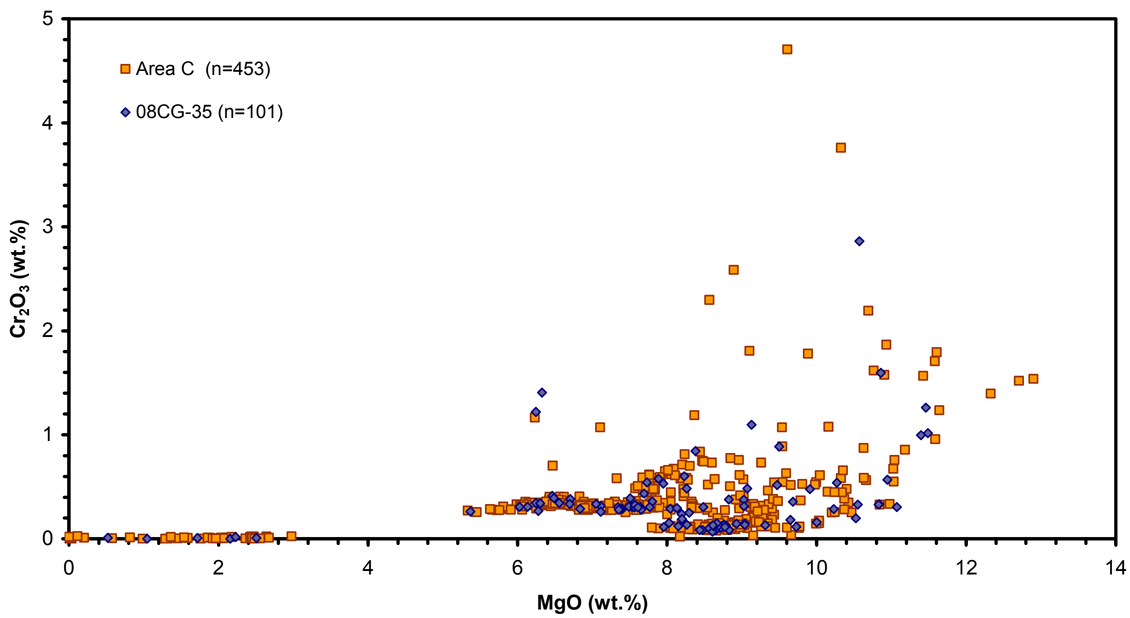

Figure 34. MgO versus Cr_2O_3 binary plot of ilmenite grains recovered from samples 07CG-564, 08CG-30 to 34 in Area C, as well as a nearby sample 08CG-35.

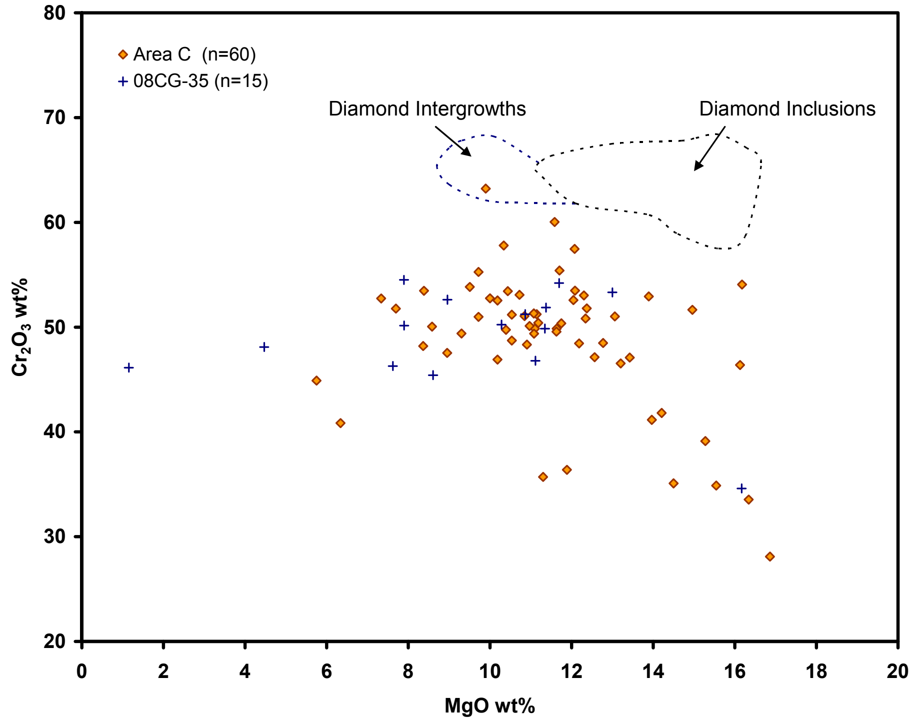

Figure 35. MgO versus Cr_2O_3 binary plot of chromite grains recovered from samples 07CG-564, 08CG-30 to 34 in Area C, as well as a nearby sample 08CG-35 (*after* Fipke et al. 1995).

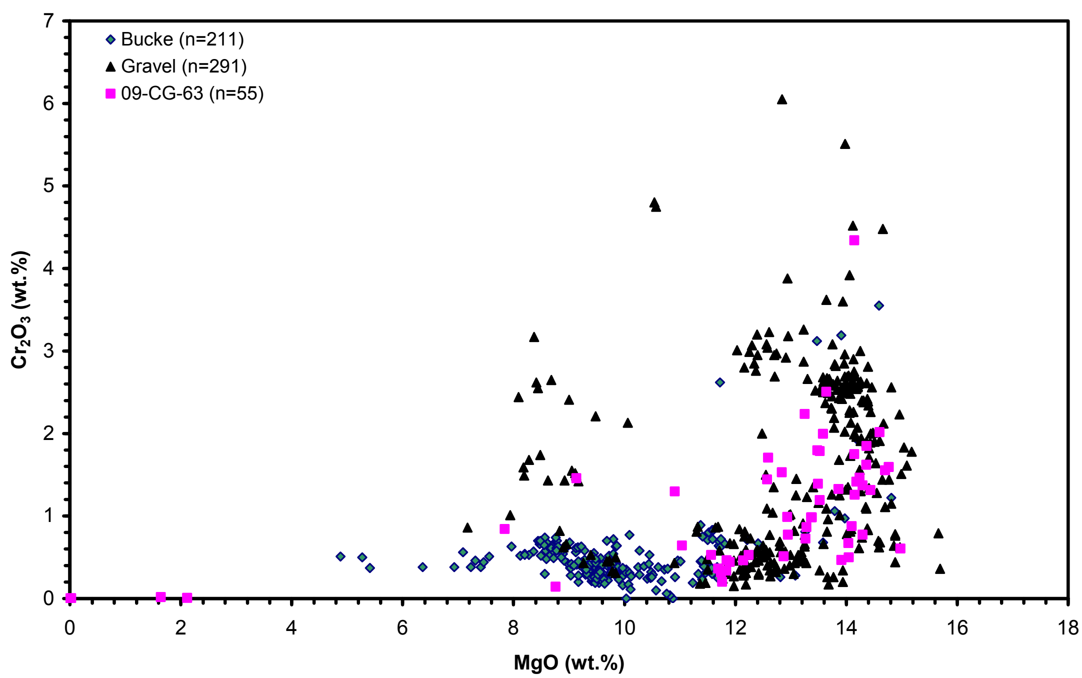

Figure 36. MgO versus Cr_2O_3 binary plot of ilmenite grains recovered from sample 09-CG-63 in Area D, the Gravel and Bucke kimberilte pipes. Geochemical data of the kimberlite pipes *from* McClenaghan et al. (2009).

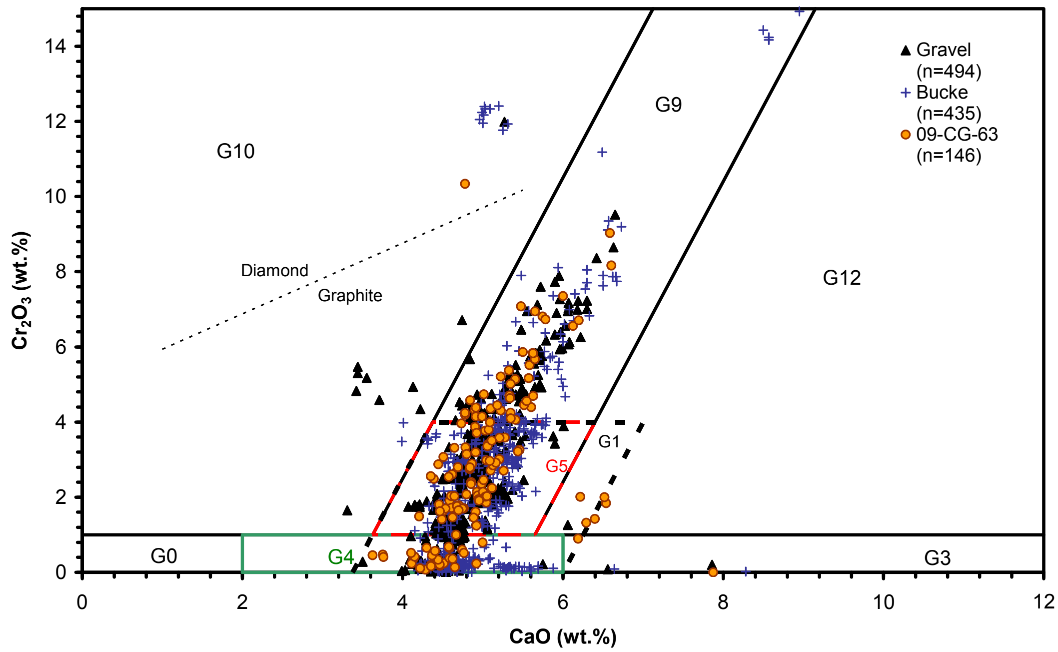

Figure 37. CaO versus Cr_2O_3 binary plot of pyrope garnets recovered from sample 09-CG-63 in Area D, the Gravel and Bucke kimberlite pipes (*after* Grütter et al. 2004). Geochemical data of the kimberlite pipes *from* McClenaghan et al. (2009).

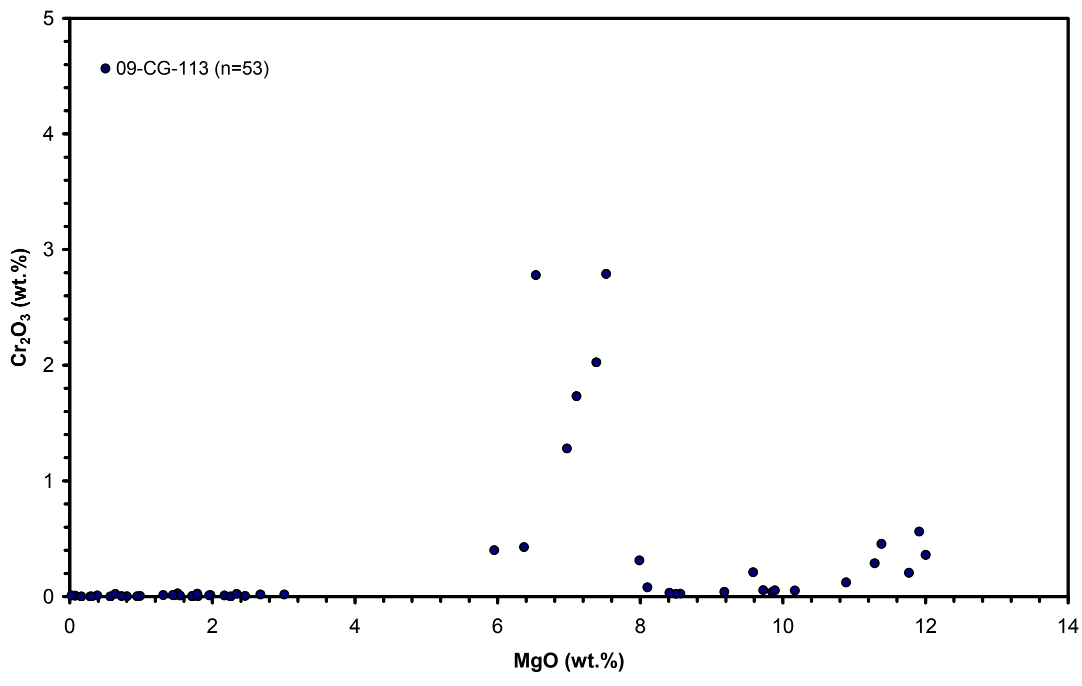

Figure 38. MgO versus Cr_2O_3 binary plot of ilmenite grains recovered from sample 09-CG-113 in Area E.

Chalcopyrite grains were recovered in some samples with counts ranging from 1 to 29 grains (Figure 41). Samples containing relatively large counts of this mineral tend to occur in the Precambrian bedrock terrain bordering the Lake Timiskaming graben to the west, and are likely derived from Proterozoic mafic intrusive rocks (*see* Figure 41). In addition, low-Cr diopside, chromite and other minerals also exist in these samples (*see* Table 11; Figure 40). In comparison, samples collected elsewhere in the Precambrian bedrock terrain contain low counts of such mineral (*see* Figure 41). Therefore, those with anomalous concentrations of chalcopyrite grains may indicate the presence of rich sulphide deposits in mafic intrusive rocks in the up-ice direction. In the Lake Timiskaming graben basin, several samples contain relatively elevated concentrations of chalcopyrite grains (up to 5) (*see* Figure 41). This trend seems consistent with the presence of low-Cr diopside grains and the interpretation for potential magmatic nickel and/or copper deposits in this region as discussed above (*see* Figure 40).

In a recent study, abundant Cr-andradite garnets (up to 2000 grains) were recovered in till samples in the Lac des Iles area and a possible link of this mineral to PGE mineralization was proposed (Barnett and Averill 2010). In the study area, Cr-andradite garnets were found in some samples with counts ranging from 1 to 17 (Figure 42). Compared with the Lac de Iles area, these counts are significantly lower, providing limited information on PGE (platinum group elements) potential for the report area. On the other hand, in that study by Barnett and Averill (2010), no significant concentrations of Cr-andradite garnets have been recorded in the bedrock that hosts the known PGE mineralization. As such, cautions should be taken when such a correlation is used in mineral prospecting for PGEs.

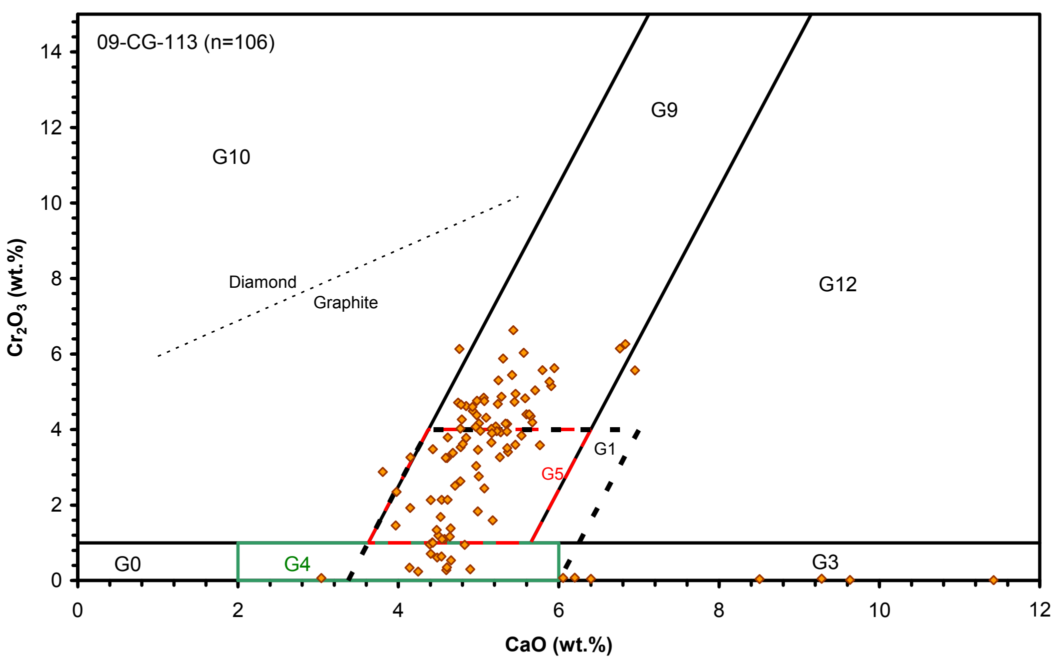

Figure 39. CaO versus Cr_2O_3 binary plot of pyrope garnets recovered from sample 09-CG-113 in Area E (*after* Grütter et al. 2004).

Table 11. Samples containing chalcopyrite (Cpy) grains.

Sample Number	Cpy	Pyrite	Spinel	low-Cr diopside NM	Cr-andradite	Corundum	Red Rutile	Chromite	Grossular	Goethite	Staurolite
08CG-37	29			53				22			
08CG-43	21			3				6			
09-CG-63	9	15	0	40	1	0	0	75			
08CG-54	5			155				23			
09-CG-059	4	15	0	14	0	0	0	24			1
09-CG-058	4	5	0	22	0	0	0	7			
08CG-55	4			56				20			
08CG-46	4			34				5			
07CG-023	4	8	1	30	1	0	1	12	1		2
08CG-53	3			22				5			
07CG-128B	3			13				3			
07CG-040	3	4	0	20	1	1	1	11			5
09-CG-142	2	0	0	10	0	0	0	11		1	
09-CG-134	2	15	0	32	0	0	0	21			3
09-CG-110	2	20	0	9	0	0	2	33			
08CG-42	2			61				11			
08CG-41	2			50				6			
08CG-39	2			32				12			
09-CG-072	1	2	0	53	2	0	0	12			
09-CG-071	1	0	0	13	1	0	0	7			
09-CG-060	1	0	0	60	0	0	0	14			
09-CG-055	1	15	0	101	0	0	0	36			1
09-CG-048	1	1	0	63	0	0	0	22			
09-CG-028	1	0	0	4	0	0	0	12			
08CG-44	1			40				35			
08CG-38	1			40				27			
08CG-12	1			7				11			
07CG-615	1			20				81			
07CG-552	1			17				9			
07CG-057	1	0	0	62	0	0	0	14			6
07CG-024	1	1	0	28	0	0	1	6			6

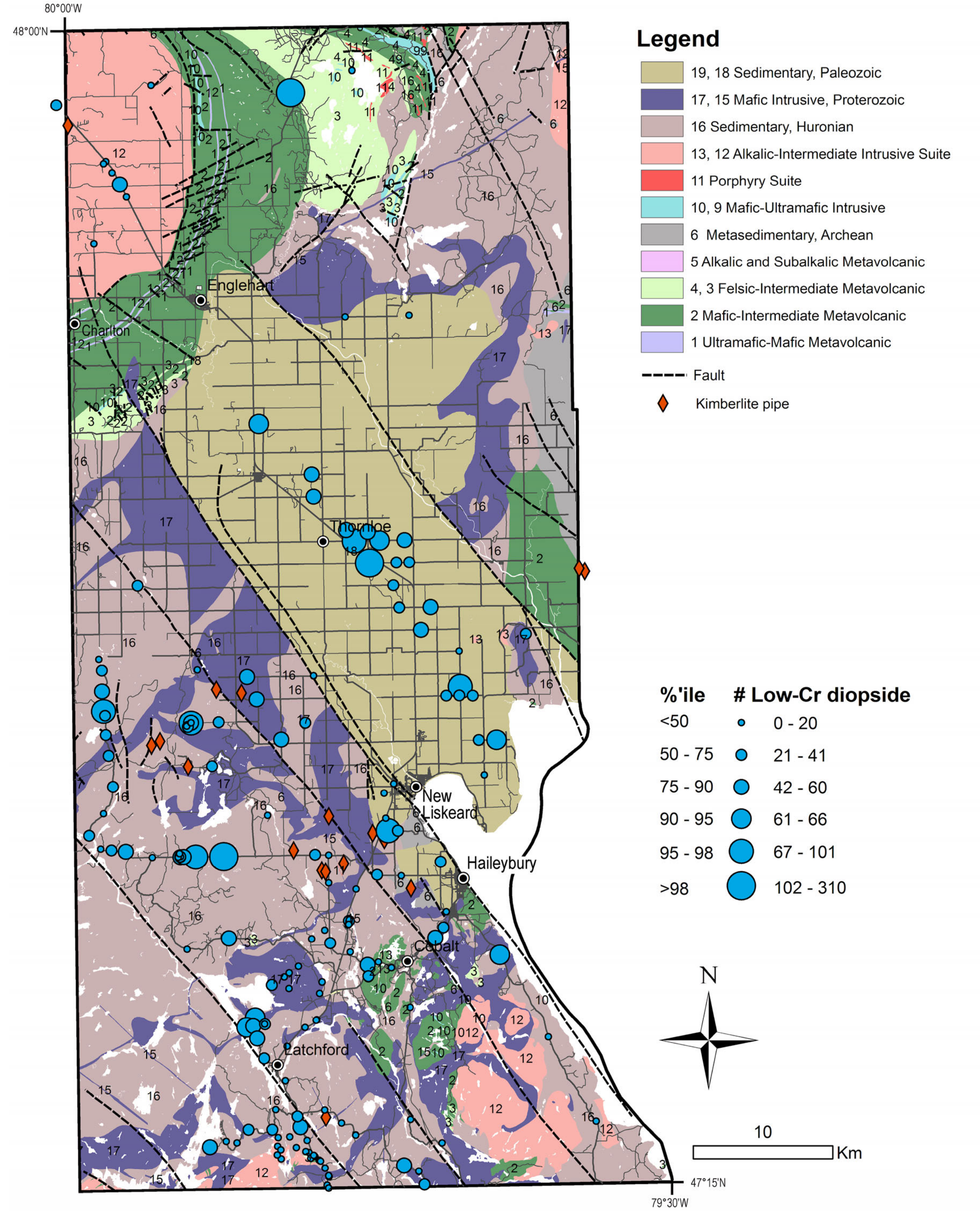

Figure 40 Regional distribution of low-Cr diopside grains. Bedrock geology *after* OGS (1991) and Ayer et al. (2006).

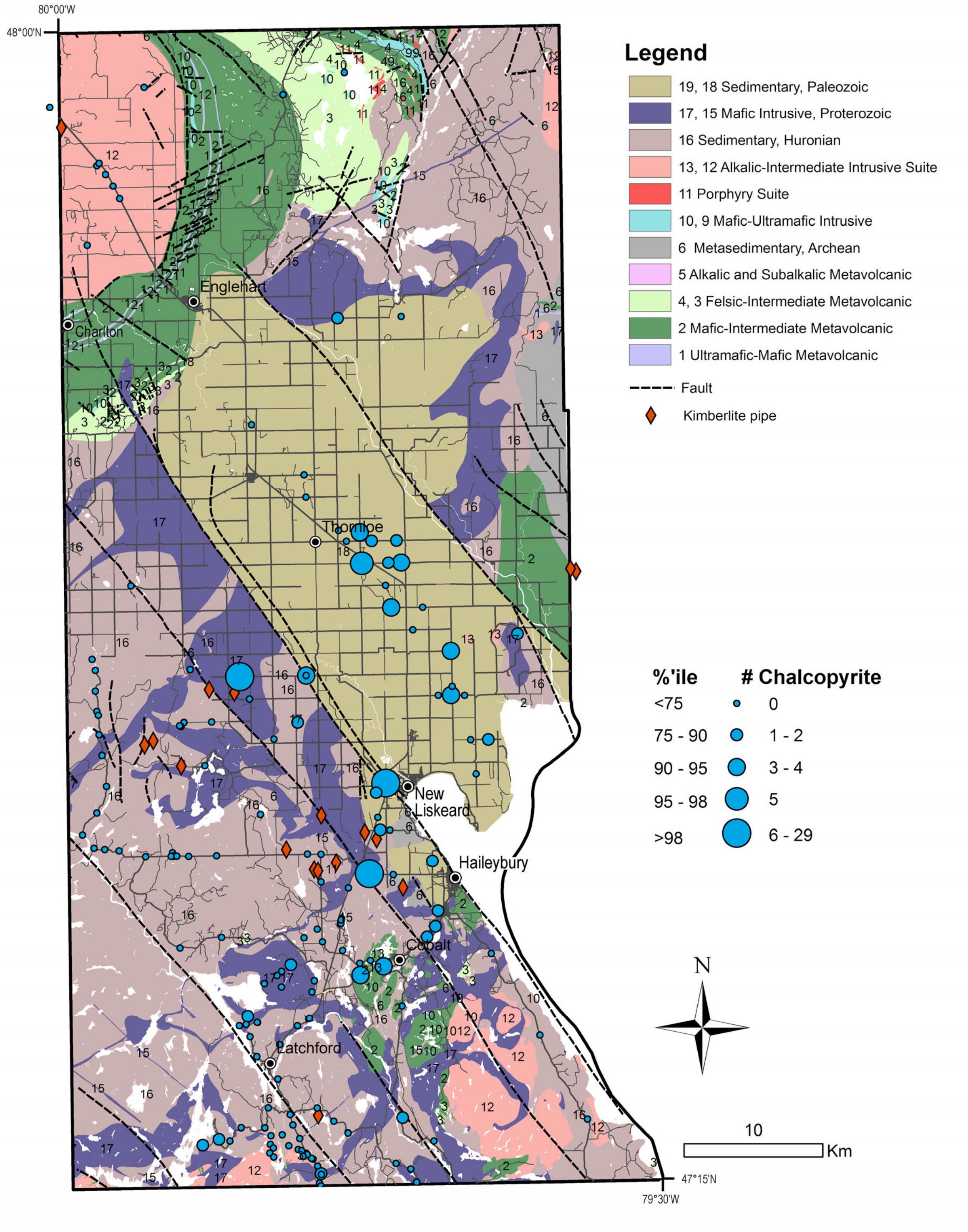

Figure 41. Regional distribution of chalcopyrite grains. Bedrock geology *after* OGS (1991) and Ayer et al. (2006).

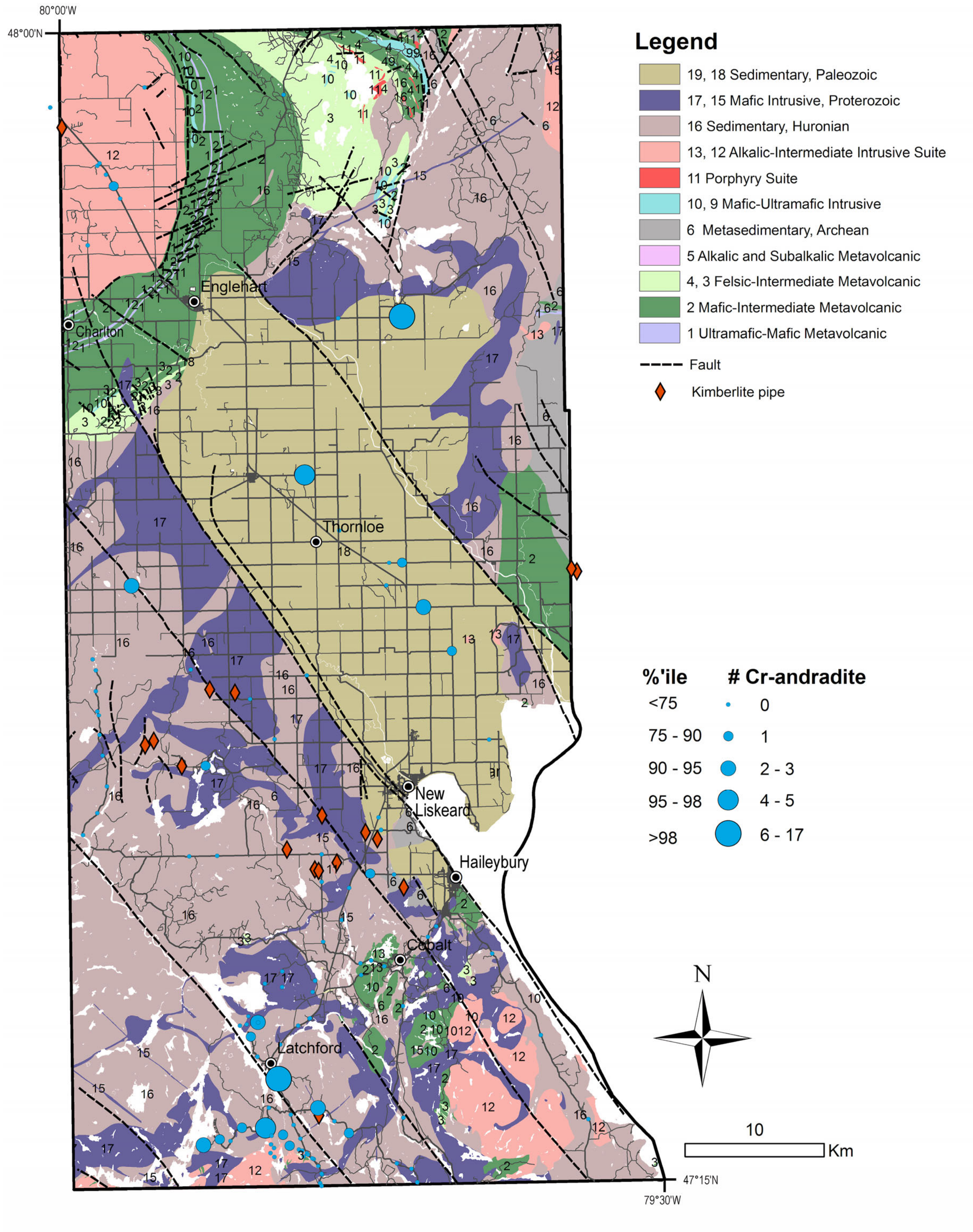

Figure 42. Regional distribution of Cr-andradite grains. Bedrock geology *after* OGS (1991) and Ayer et al. (2006).

Conclusions

More than 1700 gold and 14 000 KIM grains were counted or estimated from 151 till and 16 glaciofluvial sand and gravel samples. Some individual samples contain greater than 20 gold grains (up to 58), which are above the regional background concentration. Relatively high proportions of pristine gold grains were found in some samples, suggesting a proximity to source areas. There are quite a few samples that contain anomalous concentrations of KIM grains with 871 grains being recovered from one site. The KIM assemblages are dominated by ilmenite and pyrope garnet grains. Some samples contain harzburgitic G10D, pyroxenitic/lherzolitic and pyroxenitic/eclogitic G5D, G4D and G3D garnets, as well as chromites classified into the diamond inclusion and intergrowth field, indicating potential diamondiferous source areas in the up-ice direction. Most of the anomalies do not appear to be sourced by the known pipes, suggesting a good potential for finding new kimberlite pipes in the report area. The presence of large numbers of low-Cr diopside in conjunction with chalcopyrite grains suggests the potential for magmatic nickel and/or copper mineralization in this region.

Acknowledgments

The author wishes to thank Dan Belanger, Congxi Chen, Melissa Chiang, Ewen Cuthiell, Andrew Day, Charles Kadors, Alyne Lalonde, Brian Packer and Eric Rock for providing valuable field assistance. Overburden Drilling Management undertook the heavy mineral processing and the Geoscience Laboratories of the Ontario Geological Survey conducted the microprobe analyses. David Crabtree, Gary Grabowski, Remy Huneault, John Ayer and Ben Berger are acknowledged for their help and assistance. Thanks are also extended to Andy Bajc and Jack Parker for the review of the manuscript and helpful comments.

References

Averill, S.A. 1996. Air photo analysis of kimberlite potential; Assessment File CO-2793 filed by Sudbury Contact Mines Limited in 2003, Kirkland Lake Office, Ministry of Northern Development and Mines, 47p.

——— 1999. The application of heavy indicator mineralogy in mineral exploration; *in* Drift exploration in glaciated terrain, short course manual; Society of Exploration Geochemists, Vancouver, B.C., p.117-132.

Ayer, J.A., Chartrand, J.E., Grabowski, G.P.D., Josey, S., Rainsford, D. and Trowell, N.F. 2006. Geological compilation of the Cobalt–Temagami area, Abitibi greenstone belt; Ontario Geological Survey, Preliminary Map P.3581, scale 1:100 000.

Bajc, A.F. 1996. Regional distribution of gold in till in the Peterlong Lake–Radisson Lake area, southern Abitibi Subprovince; potential exploration targets; Ontario Geological Survey, Open File Report 5941, 57p.

——— 1997. A regional evaluation of gold potential along the western extension of the Larder Lake–Cadillac Break, Matachewan area: results of regional till sampling; Ontario Geological Survey, Open File Report 5957, 50p.

Baker, C.L. 1985. Quaternary geology of the Kirkland Lake area, districts of Cochrane and Timiskaming; Ontario Geological Survey, Open File Report 5553, 144p.

——— 2000. Quaternary geology, Larder Lake area; Ontario Geological Survey, Map 2647, scale 1:50 000.

Baker, C.L., Gao, C. and Perttunen, M. 2010. Quaternary geology of the Cobalt area, northern Ontario; Ontario Geological Survey, Map 2685, scale 1:50 000.

Barnett, P.J. and Averill, S. 2010. Heavy mineral dispersal trains in till in the area of the Lac des Iles PGE deposit, northwestern Ontario, Canada; Geochemistry: Exploration, Environment, Analysis, v.10 no.4, p. 391-399.

Contact Diamond Corporation 2003. Map of till samples and kimberlite indicator minerals in the Cobalt area, scale 1:20 000; Kirkland Lake Resident Geologist's office, Assessment File CO-2973.

Crabtree, D.C. 2003. Preliminary results from the James Bay Lowland indicator mineral sampling program; Ontario Geological Survey, Open File Report 6108, 115p.

Fipke, C.E., Gurney, J.J. and Moore, R.O. 1995. Diamond exploration techniques emphasizing indicator mineral geochemistry and Canadian examples; Geological Survey of Canada, Bulletin 423, 86p.

Gao, C. 2010a. Quaternary geology of the Englehart area, northern Ontario; Ontario Geological Survey, Map 2661, scale 1:50 000.

——— 2010b. Quaternary geology of the New Liskeard area, northern Ontario; Ontario Geological Survey, Map 2657, scale 1:50 000.

——— 2012. Till sample and indicator mineral database for the Cobalt, New Liskeard and Englehart areas, northern Ontario; Ontario Geological Survey, Miscellaneous Release—Data 284.

Gao, C. and Kodors, C. 2009. Update on surficial mapping and till sampling in the Detour Lake and Burntbush areas, northeastern Ontario; *in* Summary of Field Work and Other Activities 2009, Ontario Geological Survey, Open File Report 6240, p.18-1 to 18-6.

Grabowski, G.P.B. and Wilson, A.C. 2005. Sampling lamprophyre dikes for diamonds: Discover Abitibi Initiative; Ontario Geological Survey, Open File Report 6170, 262p.

Griffin, W.L., Ryan, C.G., Gurney, J.J., Sobolev, N.V. and Win, T.T. 1994. Chromite macrocrysts in kimberlites and lamproites: geochemistry and origin; *in* Kimberlites, related rocks and mantle xenoliths; Companhia de Pesquisa de Recursos Minerais, Rio de Janeiro, Brazil, Special Publication 1A, p.366-377.

Grütter, H.S., Gurney, J.J., Menzies, A.H. and Winter, F. 2004. An updated classification scheme for mantle-derived garnet, for use by diamond explorers; Lithos, v.77, p.841-857.

Guindon, D.L. and Reid, J.L. 2005. Regional modern alluvium sampling of the Kirkland Lake–Matachewan area, northeastern Ontario; Ontario Geological Survey, Open File Report 6124, 121p.

Helmstaedt, H.H. 1993. Natural diamond occurrences and tectonic setting of "primary" diamond deposits; *in* Diamonds: Exploration, Sampling and Evaluation; Prospectors and Developers Association of Canada, Toronto, Ontario, 1993 short course proceedings, p.1-72.

Hughes, O.L. 1965. Surficial geology of part of the Cochrane District, Ontario, Canada; *in* International Studies on the Quaternary, the 7th International Quaternary Association (INQUA) Congress, Geological Society of America, Special Paper 84, p.535-565.

Kjarsgaard, I.M., McClenaghan, M.B., Kjarsgaard, B.A. and Heaman, L.M. 2004. Indicator mineralogy of kimberlite boulders from eskers in the Kirkland Lake and Lake Timiskaming areas, Ontario, Canada. Lithos, v.77, p.705– 731.

McCandless, T.E. and Gurney, J.J., 1989. Sodium in garnet and potassium in clinopyroxene: criteria for classifying mantle eclogites. *in* Ross, J. (Ed.), Kimberlites and Related Rocks. Geological Society of Australia Special Publication, v. 14 (2), pp. 827– 832.

McClenaghan, M.B., Gauvreau, D. and Kjarsgaard, B.A. 2009. Mineral chemistry data for kimberlite, surficial sediments and kimberlite boulders from the Lake Timiskaming and Kirkland Lake kimberlite fields, Ontario and Quebec; Geological Survey of Canada, Open File 5833.

McClenaghan, M.B., Kjarsgaard, B.A. and Kjarsgaard, I.M. 2002. Kimberlite indicator mineral content and geochemistry of till around the Peddie kimberlite, Lake Timiskaming, Ontario; Geological Survey of Canada, Open File 4262.

McClenaghan, M.B. and Veillette, J.J. 2001. Ice flow indicators for the New Liskeard-Temagami area, Ontario; Geological Survey of Canada, Open File 3385, map 1:100 000.

Mitchell, R.H. 1986. Kimberlites, mineralogy, geochemistry, and petrology; Plenum Press, New York, 442p.

Morris, T.F., Sage, R.P., Ayer, J.A. and Crabtree, D.C. 2002. A study of clinopyroxene composition: Implications for kimberlite exploration. Geochemistry: Exploration, Environment, Analysis, v.2 no.4, p.321-331.

Nichols, R.S. 1988. Archean geology and silver mineralization controls at Cobalt, Ontario; CIM Bulletin, v.81 no.910, p.40-47.

Ontario Geological Survey 1991. Bedrock geology of Ontario; Ontario Geological Survey, Map 2544, scale: 1:1 000 000.

Reid, J.L. 2002. Regional modern alluvium sampling survey of the Mattawa–Cobalt corridor, northeastern Ontario; Ontario Geological Survey, Open File Report 6088, 235p.

——— 2004. Regional modern alluvium sampling survey of the Cobalt–Elk Lake area, northeastern Ontario; Ontario Geological Survey, Open File Report 6119, 140p.

Russell, D.J. 1984. Paleozoic geology of the Lake Timiskaming area, Timiskaming District; Ontario Geological Survey, Preliminary Map P.2700, scale 1:50 000.

Sage, R.P. 2000. Kimberlites of the Lake Timiskaming Structural Zone: Supplement; Ontario Geological Survey, Open File Report 6018, 123p.

Schulze, D.J. 1997. The significance of eclogite and Cr-poor megacryst garnets in diamond exploration; Exploration and Mining Geology, v.6, p.349-366.

——— 2003. A classification scheme for mantle-derived garnets in kimberlite: a tool for investigating the mantle and exploring for diamonds; Lithos, v.7, p.195-213.

Temex Resources Corporation 2011. News: Temex set to drill Latchford high grade gold project at http://www.newswire.ca/en/story/803683/temex-set-to-drill-latchford-high-grade-gold-project [accessed on Feb 17, 2012].

Veillette, J.J. 1986. Former southwesterly ice flow in the Abitibi–Timiskaming region: implications for the configuration of the Late Wisconsinan ice sheet; Canadian Journal of Earth Sciences, v.23, p.1724-174.

Vincent, J.S. and Hardy, L. 1979. The evolution of glacial lakes Barlow and Ojibway, Quebec and Ontario; Geological Survey of Canada, Bulletin 316, 18p.

This page left intentionally blank.

Appendix 1.

Sample site locations

UTM co-ordinates in North American Datum 1983 (NAD 83), Zone 17

Abbreviations:

UTM: Universal Transverse Mercator

NAD: North American Datum

Sample Number	UTM zone	Easting (NAD 83)	Northing (NAD 83)	Material
07CG-019	17	594757	5280936	Till
07CG-022	17	598146	5276967	Till
07CG-023	17	599274	5278618	Till
07CG-024	17	598358	5278599	Till
07CG-030	17	600817	5275404	Till
07CG-040	17	602854	5272231	Till
07CG-057	17	605539	5265832	Till
07CG-081	17	592291	5284933	Till
07CG-128A	17	592429	5270462	Till
07CG-128B	17	592429	5270462	Till
07CG-141	17	577371	5267877	Till
07CG-143	17	576341	5258966	Till
07CG-244	17	595178	5313936	Till
07CG-294-2	17	572118	5314867	Sand and gravel
07CG-332	17	588500	5288525	Till
07CG-473	17	598464	5259318	Till
07CG-552	17	601933	5253521	Till
07CG-564	17	583641	5267057	Till
07CG-615	17	597479	5262013	Till
07CG-651-2	17	592289	5251559	Sand and gravel
07CG-682-7	17	594895	5252566	Sand and gravel
07CG-699-2	17	594987	5252943	Sand and gravel
07CG-709	17	594953	5252782	Sand and gravel
07CG-716	17	594940	5252599	Till
07CG-723	17	586352	5251597	Till
07CG-729	17	583356	5250811	Till
07CG-733	17	578967	5257820	Till
07CG-734	17	582892	5257463	Till
07CG-737-3	17	595054	5250628	Sand and gravel
07CG-749	17	601633	5236900	Till
07CG-754	17	593226	5252189	Sand and gravel
08CG-10-3	17	594955	5252854	Sand and gravel
08CG-10-5	17	594955	5252854	Sand and gravel
08CG-11	17	590330	5248823	Till
08CG-12	17	591336	5249595	Till
08CG-15	17	582889	5257427	Till
08CG-16	17	582815	5257683	Till
08CG-17	17	582874	5257437	Till
08CG-18	17	582872	5257473	Till
08CG-19	17	582718	5257426	Till
08CG-21	17	580874	5257402	Till
08CG-22	17	577936	5257915	Till

Sample Number	UTM zone	Easting (NAD 83)	Northing (NAD 83)	Material
08CG-23	17	577169	5258008	Sand and gravel
08CG-24	17	583121	5257440	Till
08CG-27	17	589138	5260423	Sand and gravel
08CG-28	17	592530	5257595	Till
08CG-30	17	583643	5267057	Till
08CG-31	17	583638	5267062	Till
08CG-32	17	583642	5267045	Till
08CG-33	17	583420	5266757	Till
08CG-34	17	583330	5266815	Till
08CG-35	17	585627	5267093	Till
08CG-37	17	587652	5270371	Till
08CG-38	17	591829	5267053	Till
08CG-39	17	607638	5273495	Till
08CG-41	17	598935	5280216	Till
08CG-42	17	597148	5280181	Till
08CG-43	17	598162	5262696	Till
08CG-44	17	601525	5257095	Till
08CG-45	17	602939	5269686	Till
08CG-46	17	602869	5269054	Till
08CG-47	17	603833	5269036	Till
08CG-48	17	604267	5265819	Till
08CG-49	17	604662	5263372	Till
08CG-51	17	601938	5269032	Till
08CG-52	17	600114	5273781	Till
08CG-53	17	598556	5275376	Till
08CG-54	17	596436	5278559	Till
08CG-55	17	596299	5280795	Till
08CG-56	17	595335	5280151	Till
08CG-57	17	592425	5283317	Till
09-CG-012	17	592851	5247658	Till
09-CG-014	17	593035	5248467	Till
09-CG-016	17	590676	5249120	Till
09-CG-017	17	590661	5248013	Till
09-CG-019	17	592620	5245720	Till
09-CG-020	17	592659	5245759	Till
09-CG-021	17	591813	5245207	Till
09-CG-022	17	590529	5243837	Till
09-CG-024	17	590407	5241366	Till
09-CG-026	17	593400	5233875	Till
09-CG-027	17	593532	5234480	Till
09-CG-028	17	593507	5234542	Till
09-CG-029	17	593257	5235082	Till
09-CG-035	17	593503	5233684	Till
09-CG-036	17	592928	5235589	Till
09-CG-037	17	592827	5235652	Till
09-CG-038	17	592436	5236014	Till

Sample Number	**UTM zone**	**Easting (NAD 83)**	**Northing (NAD 83)**	**Material**
09-CG-039	17	592520	5235922	Till
09-CG-040	17	591278	5238782	Till
09-CG-041	17	591968	5237074	Till
09-CG-042	17	591484	5238032	Till
09-CG-043	17	588392	5244408	Till
09-CG-044	17	589432	5248253	Till
09-CG-045	17	588882	5242972	Till
09-CG-046	17	588108	5245301	Till
09-CG-047	17	587623	5245208	Till
09-CG-048	17	588233	5245907	Till
09-CG-049	17	588941	5245435	Till
09-CG-050	17	588912	5245450	Till
09-CG-051	17	591870	5236282	Till
09-CG-052	17	592221	5235788	Till
09-CG-053	17	592104	5236204	Till
09-CG-054	17	597598	5260214	Till
09-CG-055	17	597771	5259323	Till
09-CG-058	17	596350	5248875	Till
09-CG-059	17	598008	5249485	Till
09-CG-060	17	601145	5251635	Till
09-CG-062	17	598708	5256104	Till
09-CG-063	17	596980	5256172	Till
09-CG-065	17	585987	5257467	Till
09-CG-066	17	583987	5257433	Till
09-CG-067	17	593509	5257572	Till
09-CG-068	17	589709	5239270	Till
09-CG-069	17	589473	5237833	Till
09-CG-070	17	587763	5237836	Till
09-CG-071	17	586160	5237010	Till
09-CG-072	17	584998	5236595	Till
09-CG-073	17	586943	5236898	Till
09-CG-074	17	589897	5237279	Till
09-CG-075	17	590718	5237341	Till
09-CG-076	17	591192	5236559	Till
09-CG-078	17	589856	5236652	Till
09-CG-079	17	590080	5236397	Till
09-CG-080	17	589819	5236029	Till
09-CG-081	17	590103	5235748	Till
09-CG-084	17	593228	5239249	Till
09-CG-085	17	594424	5238309	Till
09-CG-086	17	595452	5237460	Till
09-CG-090	17	598907	5235281	Till
09-CG-091	17	599964	5234870	Till
09-CG-092	17	600382	5233948	Till
09-CG-100	17	576685	5301508	Till
09-CG-101	17	577372	5307238	Till

Sample Number	UTM zone	Easting (NAD 83)	Northing (NAD 83)	Material
09-CG-102	17	578539	5305755	Till
09-CG-103	17	577989	5306596	Till
09-CG-104	17	580769	5312878	Till
09-CG-106	17	573981	5311439	Till
09-CG-108	17	577534	5307404	Till
09-CG-109	17	579013	5304852	Till
09-CG-110	17	594689	5296241	Till
09-CG-111	17	599271	5296355	Sand and gravel
09-CG-113	17	590770	5312352	Sand and gravel
09-CG-115	17	595476	5255138	Till
09-CG-116	17	590114	5265848	Till
09-CG-118	17	588352	5268769	Till
09-CG-119	17	584092	5270884	Sand and gravel
09-CG-120	17	579818	5276920	Sand and gravel
09-CG-121	17	577035	5271619	Till
09-CG-122	17	577256	5270819	Till
09-CG-123	17	577260	5269330	Till
09-CG-124	17	577482	5267578	Till
09-CG-125	17	577530	5266170	Till
09-CG-126	17	577746	5264686	Till
09-CG-127	17	578055	5262466	Till
09-CG-128	17	577369	5260535	Till
09-CG-129	17	605768	5250417	Till
09-CG-132	17	609256	5244532	Till
09-CG-133	17	612683	5238452	Till
09-CG-134	17	601737	5252386	Till
09-CG-135	17	597070	5249910	Till
09-CG-136	17	596296	5249709	Till
09-CG-137	17	593617	5251259	Till
09-CG-139	17	593506	5255579	Till
09-CG-140	17	585152	5263960	Sand and gravel
09-CG-142	17	599379	5238567	Till
09-CG-143	17	599341	5246649	Till

This page left intentionally blank.

Appendix 3.

Summary of gold grain counts

UTM co-ordinates in North American Datum 1983 (NAD 83), Zone 17

Abbreviations:

UTM: Universal Transverse Mercator

NAD: North American Datum

HMC: Heavy Mineral Concentrate

g: grams

PPB parts per billion

	Number of Visible Gold Grains					Calculated PPB Visible Gold			
Sample Number	**Total**	**Reshaped**	**Modified**	**Pristine**	**Nonmag HMC (g)**	**Total**	**Reshaped**	**Modified**	**Pristine**
07CG-019	6	5	0	1	43.70	180	180	0	<1
07CG-022	1	0	1	0	24.40	1	0	1	0
07CG-023	7	7	0	0	57.90	12	12	0	0
07CG-024	21	16	4	1	55.40	66	61	5	<1
07CG-030	10	10	0	0	44.10	39	39	0	0
07CG-040	5	5	0	0	50.70	13	13	0	0
07CG-057	4	4	0	0	55.90	18	18	0	0
07CG-081	16	11	1	4	55.00	31	30	<1	1
07CG-128A	3	3	0	0	29.40	14	14	0	0
07CG-128B	6	6	0	0	34.40	32	32	0	0
07CG-141	3	3	0	0	79.20	4	4	0	0
07CG-143	20	19	1	0	22.60	138	135	4	0
07CG-244	9	7	2	0	31.60	33	21	13	0
07CG-294-2	3	3	0	0	41.20	20	20	0	0
07CG-332	2	2	0	0	30.80	2	2	0	0
07CG-473	6	6	0	0	49.20	7	7	0	0
07CG-552	5	5	0	0	35.60	36	36	0	0
07CG-564	2	2	0	0	36.00	1	1	0	0
07CG-615	1	1	0	0	54.00	4	4	0	0
07CG-651-2	1	1	0	0	42.40	9	9	0	0
07CG-682-7	1	1	0	0	42.40	<1	<1	0	0
07CG-699-2	2	2	0	0	30.80	4028	4028	0	0
07CG-709	0	0	0	0	43.20	0	0	0	0
07CG-716	4	3	1	0	46.00	1	1	<1	0
07CG-723	2	2	0	0	54.40	10	10	0	0
07CG-729	2	1	1	0	38.40	7	5	2	0
07CG-733	4	3	1	0	49.60	13	9	4	0
07CG-734	5	2	3	0	36.00	154	87	67	0
07CG-737-3	1	1	0	0	20.80	341	341	0	0
07CG-749	1	1	0	0	42.00	<1	<1	0	0
07CG-754	1	0	1	0	30.80	<1	0	<1	0
08CG-10-3	0	0	0	0	49.20	0	0	0	0
08CG-10-5	0	0	0	0	20.40	0	0	0	0
08CG-11	9	5	3	1	46.00	25	24	1	1
08CG-12	6	4	2	0	42.80	48	47	1	0
08CG-15	0	0	0	0	33.20	0	0	0	0
08CG-16	2	1	1	0	43.20	2	2	1	0
08CG-17	7	0	2	5	25.20	189	0	16	173
08CG-18	4	0	1	3	19.60	162	0	1	160
08CG-19	21	19	1	1	42.40	133	128	<1	5
08CG-21	7	6	0	1	48.00	93	89	0	4

	Number of Visible Gold Grains					Calculated PPB Visible Gold			
Sample Number	Total	Reshaped	Modified	Pristine	Nonmag HMC (g)	Total	Reshaped	Modified	Pristine
08CG-22	3	1	1	1	30.40	14	1	1	12
08CG-23	3	1	2	0	16.80	8	5	3	0
08CG-24	15	13	2	0	44.80	40	38	2	0
08CG-27	3	3	0	0	44.00	3	3	0	0
08CG-28	5	4	1	0	26.80	8	5	3	0
08CG-30	13	13	0	0	51.60	40	40	0	0
08CG-31	24	21	3	0	42.00	160	158	2	0
08CG-32	16	15	1	0	44.00	38	38	1	0
08CG-33	3	3	0	0	37.60	16	16	0	0
08CG-34	23	22	1	0	80.40	89	88	1	0
08CG-35	13	13	0	0	82.80	115	115	0	0
08CG-37	11	11	0	0	44.40	964	964	0	0
08CG-38	1	1	0	0	38.40	<1	<1	0	0
08CG-39	26	25	0	1	72.80	215	215	0	1
08CG-41	8	8	0	0	48.40	210	210	0	0
08CG-42	9	8	1	0	59.20	11	11	<1	0
08CG-43	4	4	0	0	56.80	11	11	0	0
08CG-44	7	7	0	0	58.80	176	176	0	0
08CG-45	8	7	1	0	48.40	11	11	<1	0
08CG-46	10	8	2	0	41.60	62	57	5	0
08CG-47	38	34	1	3	59.60	121	111	<1	10
08CG-48	28	26	2	0	61.20	132	132	<1	0
08CG-49	5	5	0	0	49.20	31	31	0	0
08CG-51	21	17	2	2	51.20	71	70	<1	1
08CG-52	5	5	0	0	66.80	45	45	0	0
08CG-53	26	15	6	5	71.60	73	68	3	1
08CG-54	5	3	2	0	56.00	11	7	4	0
08CG-55	5	4	1	0	73.60	7	6	1	0
08CG-56	9	9	0	0	57.60	55	55	0	0
08CG-57	10	9	1	0	51.60	39	39	<1	0
09-CG-100	11	6	4	1	50.00	20	14	4	2
09-CG-101	11	9	2	0	47.60	18	16	2	0
09-CG-102	10	5	1	4	43.60	193	183	9	1
09-CG-103	5	5	0	0	36.40	33	33	0	0
09-CG-104	0	0	0	0	43.60	0	0	0	0
09-CG-106	13	12	1	0	44.40	46	45	1	0
09-CG-108	27	18	6	3	87.60	112	100	13	<1
09-CG-109	41	30	7	4	59.60	152	139	9	4
09-CG-110	43	22	8	13	38.80	68	43	9	16
09-CG-111	10	3	4	3	34.40	239	222	13	3
09-CG-113	3	0	0	3	68.80	10	0	0	10
09-CG-115	8	5	0	3	43.20	847	837	0	10
09-CG-116	3	0	1	2	34.00	1	0	<1	1
09-CG-118	12	8	4	0	61.20	14	12	2	0

	Number of Visible Gold Grains					Calculated PPB Visible Gold			
Sample Number	Total	Reshaped	Modified	Pristine	Nonmag HMC (g)	Total	Reshaped	Modified	Pristine
09-CG-119	0	0	0	0	30.00	0	0	0	0
09-CG-012	10	9	1	0	44.80	59	57	2	0
09-CG-120	1	1	0	0	58.40	<1	<1	0	0
09-CG-121	8	7	1	0	52.00	19	19	<1	0
09-CG-122	10	10	0	0	59.20	35	35	0	0
09-CG-123	5	5	0	0	60.80	74	74	0	0
09-CG-124	9	9	0	0	47.60	38	38	0	0
09-CG-125	11	9	0	2	59.60	37	34	0	3
09-CG-126	9	4	4	1	49.60	31	5	19	8
09-CG-127	15	14	1	0	50.00	78	78	<1	0
09-CG-128	0	0	0	0	34.40	0	0	0	0
09-CG-129	13	11	1	1	46.80	76	71	4	<1
09-CG-132	6	1	3	2	42.80	103	4	83	16
09-CG-133	2	2	0	0	38.80	10	10	0	0
09-CG-134	8	7	1	0	50.40	15	15	<1	0
09-CG-135	35	18	10	7	39.60	625	261	20	344
09-CG-136	14	9	4	1	53.20	44	35	9	<1
09-CG-137	13	11	2	0	37.60	131	128	3	0
09-CG-139	4	4	0	0	34.80	22	22	0	0
09-CG-014	12	11	1	0	60.80	244	243	1	0
09-CG-140	2	2	0	0	45.20	4	4	0	0
09-CG-142	31	11	10	10	58.00	202	168	19	16
09-CG-143	15	8	0	7	48.00	52	39	0	14
09-CG-016	1	1	0	0	43.20	15	15	0	0
09-CG-017	8	5	2	1	36.80	90	88	1	1
09-CG-019	5	4	1	0	30.80	1165	1162	3	0
09-CG-020	10	7	2	1	44.80	43	34	5	4
09-CG-021	11	10	0	1	58.80	85	83	0	1
09-CG-022	5	4	1	0	34.40	26	24	2	0
09-CG-024	10	9	0	1	36.40	41	40	0	1
09-CG-026	16	11	4	1	44.00	606	566	25	15
09-CG-027	57	40	9	8	39.60	907	842	37	28
09-CG-028	29	16	12	1	42.00	332	277	53	2
09-CG-029	18	14	2	2	42.40	64	60	1	2
09-CG-035	0	0	0	0	53.60	0	0	0	0
09-CG-036	2	0	2	0	39.60	1	0	1	0
09-CG-037	9	9	0	0	38.80	2333	2333	0	0
09-CG-038	6	5	1	0	42.00	33	31	2	0
09-CG-039	4	2	0	2	46.00	20	16	0	5
09-CG-040	9	4	4	1	59.60	46	42	3	1
09-CG-041	9	6	2	1	37.20	33	32	1	<1
09-CG-042	5	2	3	0	34.40	14	11	3	0
09-CG-043	26	17	9	0	46.00	153	146	7	0
09-CG-044	5	3	2	0	42.00	13	8	5	0

	Number of Visible Gold Grains					Calculated PPB Visible Gold			
Sample Number	**Total**	**Reshaped**	**Modified**	**Pristine**	**Nonmag HMC (g)**	**Total**	**Reshaped**	**Modified**	**Pristine**
09-CG-045	30	24	4	2	54.80	66	61	4	2
09-CG-046	7	4	0	3	35.60	10	6	0	4
09-CG-047	10	7	1	2	74.00	22	19	<1	3
09-CG-048	5	4	1	0	40.80	24	23	1	0
09-CG-049	3	3	0	0	42.00	5	5	0	0
09-CG-050	3	3	0	0	49.60	321	321	0	0
09-CG-051	30	25	3	2	65.20	74	66	5	3
09-CG-052	10	8	0	2	41.60	41	39	0	3
09-CG-053	8	5	3	0	42.40	23	20	3	0
09-CG-054	13	11	2	0	57.20	200	193	7	0
09-CG-055	4	4	0	0	63.60	23	23	0	0
09-CG-058	58	36	13	9	68.40	195	179	14	2
09-CG-059	15	10	4	1	77.60	11	7	2	2
09-CG-060	14	13	1	0	36.00	70	69	1	0
09-CG-062	4	4	0	0	45.60	5	5	0	0
09-CG-063	12	8	2	2	59.20	14	14	<1	<1
09-CG-065	50	34	10	6	47.20	122	91	24	7
09-CG-066	12	6	3	3	41.20	59	38	14	7
09-CG-067	12	9	3	0	59.60	14	11	3	0
09-CG-068	15	15	0	0	39.20	49	49	0	0
09-CG-069	12	4	1	7	41.60	166	159	<1	7
09-CG-070	7	3	2	2	48.40	22	17	4	1
09-CG-071	12	8	1	3	62.00	135	123	1	11
09-CG-072	7	6	1	0	52.00	184	181	4	0
09-CG-073	8	6	1	1	36.80	19	13	5	1
09-CG-074	8	5	2	1	44.00	4	2	2	1
09-CG-075	15	14	0	1	48.40	50	50	0	1
09-CG-076	9	9	0	0	40.40	22	22	0	0
09-CG-078	11	11	0	0	48.40	13	13	0	0
09-CG-079	11	11	0	0	40.00	302	302	0	0
09-CG-080	6	4	1	1	37.60	22	16	5	1
09-CG-081	5	5	0	0	33.20	7	7	0	0
09-CG-084	7	4	3	0	37.60	22	16	6	0
09-CG-085	5	3	2	0	31.20	63	45	18	0
09-CG-086	13	11	1	1	50.80	25	25	<1	<1
09-CG-090	7	6	1	0	44.80	16	16	1	0
09-CG-091	10	5	2	3	40.80	96	94	1	1
09-CG-092	11	6	2	3	45.60	314	305	6	3

This page left intentionally blank.

Appendix 6.

Summary of kimberlite indicator minerals (KIM) counts

Abbreviations:

CR: Chromite

DC: Cr-diopside; distinctly emerald green (paler emerald green low-Cr diopside picked separately)

FO: Forsterite

GO: Orange mantle garnet, which includes both eclogitic pyrope-almandine (G3) and Cr-poor megacrystic pyrope (G1/G2) varieties, and may include unchecked (by SEM) grains of common crustal garnet

GP: Purple to red peridotitic garnet (G9/10 Cr-pyrope)

IM: Mg-ilmenite, which may include unchecked (by SEM) grains of common crustal ilmenite lacking diagnostic inclusions or crystal faces

SEM: Scanning Electronic Microscope

Sample Number	Selected PseudoKIMs			KIM Count																				
	2.0 to 1.0 mm	1.0 to 0.5 mm	0.5 to 0.25 mm		2.0 to 1.0 mm						1.0 to 0.5 mm						0.5 to 0.25 mm						
	Low-Cr diopside	Low-Cr diopside	Low-Cr diopside	Total	GP	GO	DC	IM	CR	FO	GP	GO	DC	IM	CR	FO	GP	GO	DC	IM	CR	FO	Total
07CG-019	0	4	50	54	0	0	0	0	0	0	0	0	0	1	0	0	7	0	2	0	15	0	25
07CG-022	0	1	23	24	0	0	0	0	0	0	1	0	0	0	0	0	2	3	3	0	14	2	25
07CG-023	0	0	30	30	0	0	0	0	0	0	1	0	0	0	0	0	2	1	2	2	12	2	22
07CG-024	0	2	26	28	0	0	0	0	0	0	0	0	0	0	0	0	3	1	2	4	7	3	20
07CG-030	0	0	45	45	0	0	0	0	0	0	0	0	0	0	0	0	1	0	2	4	9	2	18
07CG-040	0	0	20	20	0	0	0	0	0	0	0	0	0	0	0	1	2	1	2	1	12	0	19
07CG-057	0	6	56	62	0	0	0	0	0	0	0	1	1	2	0	10	8	2	2	6	13	13	58
07CG-081	0	1	60	61	0	0	0	0	0	0	1	1	0	1	1	3	10	2	3	1	38	15	76
07CG-128A	0	2	18	20	0	0	0	0	0	0	0	0	0	0	0	0	1	0	1	1	9	1	13
07CG-128B	0	1	12	13	0	0	0	0	0	0	0	0	0	0	0	0	3	0	0	0	3	0	6
07CG-141	0	8	59	67	0	0	0	0	0	0	0	1	1	0	0	2	3	1	2	2	9	1	22
07CG-143	0	1	35	36	0	0	0	0	0	0	0	0	0	0	0	4	1	2	1	0	5	9	22
07CG-244	0	0	6	6	0	0	0	0	0	0	1	0	0	0	0	0	7	2	2	0	12	0	24
07CG-294-2	0	0	7	7	0	0	0	0	0	0	0	0	1	0	0	0	2	0	0	0	12	1	16
07CG-332	0	1	60	61	0	0	0	0	0	0	1	0	0	0	0	0	5	4	5	2	11	0	28
07CG-473	0	1	30	31	0	0	0	0	0	0	0	0	0	0	2	0	1	0	1	0	50	1	55
07CG-552	0	1	14	15	0	0	0	1	0	0	1	0	0	2	1	2	3	3	1	2	11	5	32
07CG-564	0	0	0	0	0	1	0	13	0	0	10	5	11	59	4	29	40	40	40	250	19	100	621
07CG-615	0	1	19	20	0	0	0	0	0	0	0	0	0	0	1	0	2	1	0	1	80	0	85
07CG-651-2	0	2	11	13	0	0	0	0	0	0	5	1	4	10	0	9	0	3	6	40	24	2	104
07CG-682-7	0	0	11	11	0	0	0	5	3	1	1	0	0	13	6	5	2	2	0	40	40	3	121
07CG-699-2	0	0	8	8	0	0	0	2	0	2	5	0	0	11	0	0	1	2	1	25	10	1	60
07CG-709	0	3	9	12	0	0	0	0	0	0	3	2	2	23	0	3	1	2	0	29	2	4	71
07CG-716	0	0	0	0	0	0	0	0	0	0	1	0	0	0	0	0	2	0	2	6	4	0	15
07CG-723	0	5	40	45	0	0	0	0	0	0	0	0	0	0	0	2	0	0	0	2	12	1	17
07CG-729	0	0	16	16	0	0	0	3	2	3	2	2	0	7	4	10	6	3	9	40	40	17	148
07CG-733	0	1	50	51	0	0	0	0	0	0	0	1	0	1	0	1	3	4	0	15	10	2	37

Sample Number	Selected PseudoKIMs				KIM Count																		
	2.0 to 1.0 mm	1.0 to 0.5 mm	0.5 to 0.25 mm		2.0 to 1.0 mm						1.0 to 0.5 mm						0.5 to 0.25 mm						
	Low-Cr diopside	Low-Cr diopside	Low-Cr diopside	Total	GP	GO	DC	IM	CR	FO	GP	GO	DC	IM	CR	FO	GP	GO	DC	IM	CR	FO	Total
07CG-734	0	10	10	20	3	0	0	6	1	0	30	14	9	50	60	7	80	30	50	40	120	6	506
07CG-737-3	0	1	7	8	0	0	0	1	0	0	1	1	0	36	0	2	1	2	0	37	23	2	106
07CG-749	0	0	13	13	0	0	0	0	0	0	1	1	0	1	0	1	1	1	2	10	7	1	26
07CG-754	0	0	3	3	0	0	0	0	0	1	3	2	1	9	0	9	8	1	8	100	120	9	271
08CG-10-3	0	4	25	29	0	0	0	3	0	0	1	2	1	43	0	2	9	12	4	100	60	11	248
08CG-10-5	0	1	9	10	0	0	0	7	0	0	1	0	0	21	0	5	1	2	1	40	14	7	99
08CG-11	0	5	9	14	0	0	0	0	0	0	0	0	0	1	0	0	4	1	1	23	17	2	49
08CG-12	0	1	6	7	0	0	0	0	0	0	0	0	0	1	0	0	2	1	0	5	10	6	25
08CG-15	0	5	45	50	2	0	0	2	1	0	26	3	18	18	21	13	117	45	70	40	80	16	472
08CG-16	0	1	17	18	0	0	0	1	0	0	2	1	1	6	5	0	31	11	9	20	21	1	109
08CG-17	0	6	25	31	0	0	2	4	0	1	24	30	15	45	44	10	73	43	36	80	70	12	489
08CG-18	0	7	21	28	2	0	0	1	0	0	41	7	8	10	15	5	131	37	44	21	31	1	354
08CG-19	0	0	20	20	0	2	1	0	0	0	4	5	4	3	5	0	68	36	10	20	28	1	187
08CG-21	0	1	10	11	0	0	0	0	0	0	0	1	0	1	0	0	4	3	2	4	4	0	19
08CG-22	0	5	32	37	0	0	0	0	0	2	3	1	0	3	3	31	5	2	1	8	39	100	198
08CG-23	0	2	1	3	0	0	0	0	0	0	1	0	0	0	1	5	0	0	0	0	5	100	112
08CG-24	0	4	45	49	0	0	0	0	0	0	10	5	5	1	7	3	84	42	49	21	14	31	272
08CG-27	0	0	4	4	0	0	0	1	0	0	0	0	0	4	0	1	3	0	1	5	60	1	76
08CG-28	0	1	40	41	0	0	0	0	0	0	0	0	0	1	0	1	3	3	0	9	25	6	48
08CG-30	1	0	50	51	1	0	0	10	0	1	15	8	15	80	6	4	56	46	11	150	40	3	446
08CG-31	0	0	10	10	0	1	1	4	0	0	5	7	2	60	0	7	24	7	28	300	10	3	459
08CG-32	0	0	100	100	0	0	0	12	0	0	13	5	16	80	2	10	60	50	80	500	25	23	876
08CG-33	0	2	25	27	0	0	0	2	0	0	6	1	0	28	0	0	8	6	3	60	25	3	142
08CG-34	0	0	11	11	0	0	0	0	0	0	1	1	1	2	1	0	9	0	4	11	25	0	55
08CG-35	0	1	40	41	0	0	0	3	0	0	8	1	2	80	0	2	29	8	9	250	40	1	433
08CG-37	0	3	50	53	0	0	0	0	0	0	1	0	1	0	0	0	3	1	3	6	22	0	37
08CG-38	0	0	40	40	0	0	0	0	0	0	0	0	0	2	0	0	2	0	1	7	27	2	41
08CG-39	0	2	30	32	0	0	0	0	0	0	2	0	0	0	1	6	13	1	5	3	10	11	52
08CG-41	0	0	50	50	0	0	0	0	0	0	0	0	0	0	0	0	6	0	5	1	6	0	18
08CG-42	0	1	60	61	0	0	0	0	0	0	0	0	0	1	0	0	10	1	8	4	11	1	36
08CG-43	0	1	2	3	0	0	0	0	0	0	0	0	0	0	0	0	2	1	0	1	6	0	10
08CG-44	0	0	40	40	0	0	0	0	0	0	1	0	0	0	1	1	9	1	0	1	34	3	51
08CG-45	0	6	80	86	0	0	0	0	0	0	1	0	0	0	0	0	3	0	1	0	9	2	16
08CG-46	0	2	32	34	0	0	0	0	0	0	0	0	0	0	0	0	2	2	0	3	5	2	14

Sample Number	Selected PseudoKIMs			KIM Count																			
	2.0 to 1.0 mm	1.0 to 0.5 mm	0.5 to 0.25 mm		2.0 to 1.0 mm						1.0 to 0.5 mm						0.5 to 0.25 mm						
	Low-Cr diopside	Low-Cr diopside	Low-Cr diopside	Total	GP	GO	DC	IM	CR	FO	GP	GO	DC	IM	CR	FO	GP	GO	DC	IM	CR	FO	Total
08CG-47	0	0	30	30	0	0	0	0	0	0	0	0	0	0	0	0	2	1	1	0	8	5	17
08CG-48	0	1	30	31	0	0	0	0	0	0	0	0	0	0	0	0	0	0	0	2	2	3	7
08CG-49	0	0	20	20	0	0	0	0	0	0	0	0	0	0	1	0	1	0	0	0	1	0	3
08CG-51	0	1	40	41	0	0	0	0	0	0	0	0	0	1	0	2	2	1	0	2	9	2	19
08CG-52	0	1	50	51	0	0	0	0	0	0	0	1	0	0	0	2	9	3	1	0	8	0	24
08CG-53	0	0	22	22	0	0	0	0	0	0	2	0	3	0	0	1	12	1	11	0	5	7	42
08CG-54	0	5	150	155	0	0	0	0	0	0	1	0	0	0	0	1	8	1	3	4	25	12	55
08CG-55	0	6	50	56	0	0	0	0	0	0	2	0	0	3	0	2	5	1	2	11	19	0	45
08CG-56	0	1	101	101	0	0	0	0	0	0	0	0	2	0	0	1	4	3	5	0	40	2	57
08CG-57	0	3	53	53	0	0	0	1	0	0	1	1	1	0	1	2	8	7	7	4	7	3	43
09-CG-012	0	1	7	8	0	0	0	0	0	0	0	0	0	0	0	0	0	0	0	1	9	0	10
09-CG-014	0	0	4	4	0	0	0	0	0	0	0	0	0	0	0	0	2	0	0	3	18	0	23
09-CG-016	0	0	1	1	0	0	0	0	0	0	0	0	0	0	0	0	2	0	1	0	9	0	12
09-CG-017	0	0	9	9	0	0	0	2	0	0	0	0	0	0	0	0	5	1	1	8	4	3	24
09-CG-019	0	0	0	0	0	0	0	0	0	0	0	0	0	2	0	0	1	0	1	7	10	0	21
09-CG-020	0	0	9	9	0	0	0	0	0	0	0	0	0	1	0	0	0	0	0	0	5	0	6
09-CG-021	0	1	19	20	0	0	0	2	0	0	2	0	0	4	0	0	6	2	0	60	16	6	98
09-CG-022	0	0	17	17	0	0	0	1	0	0	0	0	0	1	0	0	5	0	0	17	2	1	27
09-CG-024	0	0	10	10	0	0	0	0	0	0	2	0	0	0	0	1	0	1	0	1	7	1	13
09-CG-026	0	0	3	3	0	0	0	0	0	0	0	0	0	0	0	0	1	0	0	0	2	0	3
09-CG-027	0	0	9	9	0	0	0	0	0	0	0	0	0	0	0	0	2	2	0	1	5	0	10
09-CG-028	0	0	4	4	0	0	0	0	0	0	0	0	0	2	0	0	0	0	0	8	12	2	24
09-CG-029	0	0	6	6	0	0	0	0	0	0	0	0	0	1	0	0	2	1	0	4	5	0	13
09-CG-035	0	0	0	0	0	0	0	0	0	0	0	0	0	0	0	0	0	0	0	0	0	0	0
09-CG-036	0	1	4	5	0	0	0	0	0	0	0	0	0	1	0	0	3	0	0	2	1	0	7
09-CG-037	0	0	13	13	0	0	0	0	0	0	1	0	0	0	0	0	1	0	1	2	3	0	8
09-CG-038	0	0	4	4	0	0	0	0	0	0	0	0	0	1	1	0	3	1	1	3	2	0	12
09-CG-039	0	1	7	8	0	0	0	0	0	0	2	1	0	11	1	0	8	17	1	75	14	0	130
09-CG-040	0	0	24	24	0	0	0	1	0	0	0	0	0	4	0	0	3	6	0	11	9	1	35
09-CG-041	0	0	11	11	0	0	0	1	0	0	0	0	0	1	0	0	2	1	0	2	3	0	10
09-CG-042	0	2	40	42	0	0	0	0	0	0	1	0	0	5	0	0	5	0	0	17	20	0	48
09-CG-043	0	1	50	51	0	0	0	0	0	0	0	0	0	1	0	0	2	0	1	4	10	2	20
09-CG-044	0	1	28	29	0	0	0	0	0	0	0	0	0	7	0	1	2	1	0	20	19	0	50
09-CG-045	0	2	22	24	0	0	0	0	0	0	1	0	0	1	0	0	2	1	1	8	18	1	33

Sample Number	Selected PseudoKIMs			KIM Count																			
	2.0 to 1.0 mm	1.0 to 0.5 mm	0.5 to 0.25 mm		2.0 to 1.0 mm						1.0 to 0.5 mm						0.5 to 0.25 mm						
	Low-Cr diopside	Low-Cr diopside	Low-Cr diopside	Total	GP	GO	DC	IM	CR	FO	GP	GO	DC	IM	CR	FO	GP	GO	DC	IM	CR	FO	Total
09-CG-046	0	3	50	53	0	0	0	0	0	0	0	0	0	7	1	2	5	1	2	28	43	4	93
09-CG-047	0	2	60	62	0	0	0	0	0	0	1	0	0	0	0	0	6	7	1	2	4	0	21
09-CG-048	0	3	60	63	0	0	0	0	0	0	1	0	0	2	3	0	0	2	0	13	20	0	41
09-CG-049	0	0	40	40	0	0	0	1	0	0	0	1	0	10	1	1	5	1	0	18	21	8	67
09-CG-050	0	0	12	12	0	0	0	1	0	0	0	0	0	12	1	0	4	3	1	8	21	0	51
09-CG-051	0	1	8	9	0	0	0	0	0	0	2	0	0	0	1	0	2	2	1	8	9	0	25
09-CG-052	0	0	6	6	0	0	0	0	0	0	0	1	0	0	3	0	0	3	1	3	9	0	20
09-CG-053	0	1	17	18	0	0	0	0	0	0	0	0	0	0	0	0	2	1	0	6	7	2	18
09-CG-054	0	0	17	17	0	0	0	0	0	0	1	0	0	0	1	4	2	0	3	1	23	6	41
09-CG-055	0	1	100	101	0	0	0	0	0	0	0	0	0	0	2	0	4	1	2	4	39	3	55
09-CG-058	0	0	22	22	0	0	0	0	0	0	0	0	0	0	0	0	1	0	0	0	7	6	14
09-CG-059	0	1	13	14	1	1	0	7	0	0	11	7	0	56	1	2	67	27	0	300	19	14	513
09-CG-060	0	0	60	60	0	0	0	0	0	0	0	0	0	4	1	0	3	3	0	21	13	0	45
09-CG-062	0	0	19	19	0	0	0	0	0	0	1	0	0	1	1	1	3	2	1	25	30	1	66
09-CG-063	0	0	40	40	0	1	0	6	0	0	10	20	0	100	4	8	100	100	16	100	80	26	571
09-CG-065	0	13	100	113	0	0	0	2	0	0	2	1	0	7	0	24	7	3	5	17	20	80	168
09-CG-066	0	1	80	81	0	1	0	0	0	0	3	0	0	5	0	2	8	2	0	21	17	14	73
09-CG-067	0	0	7	7	0	0	0	1	0	0	0	0	0	7	0	0	1	2	0	15	28	7	61
09-CG-068	0	1	13	14	0	0	0	0	0	0	0	0	0	1	0	0	2	2	0	11	9	4	29
09-CG-069	0	0	40	40	0	0	0	0	0	0	1	0	0	12	0	2	2	1	0	46	47	2	113
09-CG-070	0	0	21	21	0	0	0	0	0	0	0	0	0	0	0	0	1	3	0	1	11	0	16
09-CG-071	0	1	12	13	0	0	0	0	0	0	1	0	0	1	0	0	1	0	1	8	8	1	21
09-CG-072	0	3	50	53	0	0	0	0	0	0	0	0	0	2	1	0	0	2	1	5	15	1	27
09-CG-073	0	0	13	13	0	0	0	0	0	0	0	0	0	0	0	0	1	1	0	1	5	0	8
09-CG-074	0	0	10	10	0	0	0	0	0	0	0	0	0	1	0	0	1	0	0	5	9	1	17
09-CG-075	0	0	12	12	0	0	0	0	0	0	0	0	0	2	0	0	2	1	0	4	1	0	10
09-CG-076	0	0	8	8	0	0	0	0	0	0	0	0	0	1	0	1	0	0	0	1	8	0	11
09-CG-078	0	0	9	9	0	0	0	0	0	0	0	0	0	0	0	0	1	0	0	4	9	1	15
09-CG-079	0	0	7	7	0	0	0	0	0	0	0	0	0	4	0	0	0	0	1	4	3	0	12
09-CG-080	0	0	4	4	0	0	0	0	0	0	0	0	0	1	0	0	4	1	0	13	4	0	23
09-CG-081	0	0	7	7	0	0	0	0	0	0	0	0	0	1	0	0	3	2	0	8	8	11	33
09-CG-084	0	0	1	1	0	0	0	0	0	0	0	0	0	0	0	0	0	2	1	3	6	0	12
09-CG-085	0	0	0	0	0	0	0	0	0	0	0	0	0	0	0	0	1	0	0	0	2	0	3
09-CG-086	0	0	9	9	0	0	0	0	0	0	1	0	0	5	0	0	23	11	0	150	14	0	204

Sample Number	Selected PseudoKIMs			KIM Count																			
	2.0 to 1.0 mm	1.0 to 0.5 mm	0.5 to 0.25 mm		2.0 to 1.0 mm						1.0 to 0.5 mm						0.5 to 0.25 mm						
	Low-Cr diopside	Low-Cr diopside	Low-Cr diopside	Total	GP	GO	DC	IM	CR	FO	GP	GO	DC	IM	CR	FO	GP	GO	DC	IM	CR	FO	Total
09-CG-090	0	2	40	42	0	0	0	1	0	0	0	1	0	1	0	0	1	5	0	13	6	4	32
09-CG-091	0	0	16	16	0	0	0	0	0	0	1	0	0	0	0	0	1	0	2	8	8	1	21
09-CG-092	0	1	25	26	0	0	0	0	0	0	0	0	0	1	0	1	1	1	0	2	9	6	21
09-CG-100	0	0	3	3	0	0	0	0	0	0	0	0	1	0	0	0	0	0	0	0	13	0	14
09-CG-101	0	0	8	8	0	0	0	0	0	0	0	0	0	0	1	1	1	0	0	1	34	0	38
09-CG-102	0	2	40	42	0	0	0	0	0	0	2	1	1	1	1	1	15	1	9	0	4	3	39
09-CG-103	0	0	1	1	0	0	0	1	0	0	1	0	0	0	1	0	2	0	1	0	19	0	25
09-CG-104	0	2	16	18	0	0	0	0	0	0	0	0	0	0	0	0	3	4	4	0	16	3	30
09-CG-106	0	1	23	24	0	0	0	0	0	0	0	0	0	0	0	1	4	0	1	1	9	12	28
09-CG-108	0	0	10	10	0	0	0	0	0	0	2	0	0	0	0	0	3	3	1	0	21	0	30
09-CG-109	0	0	18	18	0	0	0	0	0	0	0	0	0	0	0	1	2	1	1	4	15	4	28
09-CG-110	0	0	9	9	0	0	0	0	0	0	0	0	0	0	1	0	5	1	0	3	32	0	42
09-CG-111	0	0	8	8	0	0	0	0	0	0	0	0	0	1	1	0	1	1	0	3	11	0	18
09-CG-113	0	10	300	310	0	1	1	1	0	2	24	10	10	16	13	23	100	40	37	300	40	200	818
09-CG-115	0	0	4	4	0	0	0	1	0	0	0	0	0	1	0	0	0	0	0	8	23	0	33
09-CG-116	0	0	60	60	0	0	0	0	0	0	1	0	0	0	0	1	5	1	1	2	5	0	16
09-CG-118	0	3	51	54	0	0	0	0	0	0	0	0	0	0	0	0	7	4	0	2	24	1	38
09-CG-119	0	0	2	2	0	0	0	0	0	0	0	0	0	0	1	0	3	0	1	1	7	0	13
09-CG-120	0	0	30	30	0	0	0	0	0	0	1	0	0	1	1	0	1	0	0	2	23	1	30
09-CG-121	0	1	16	17	0	0	0	0	0	0	0	0	0	0	0	0	5	2	1	0	7	1	16
09-CG-122	0	0	26	26	0	0	0	0	0	0	0	0	0	0	0	0	1	1	0	0	11	0	13
09-CG-123	0	0	60	60	0	0	0	0	0	0	0	1	0	0	0	0	0	1	1	0	4	0	7
09-CG-124	0	0	26	26	0	0	0	0	0	0	0	0	0	2	1	1	2	2	1	0	16	2	27
09-CG-125	0	0	40	40	0	0	0	0	0	0	1	0	0	0	0	1	3	0	2	0	14	2	23
09-CG-126	0	0	30	30	0	0	0	0	0	0	0	0	0	0	0	0	2	0	1	1	7	0	11
09-CG-127	0	3	24	27	0	0	0	0	0	0	0	0	0	0	1	8	2	0	0	6	33	40	90
09-CG-128	0	1	15	16	0	0	0	0	0	0	1	0	0	0	1	0	2	0	0	0	1	1	6
09-CG-129	0	3	63	63	0	0	0	0	0	0	0	0	0	1	1	1	2	1	0	7	11	8	32
09-CG-132	0	0	6	6	0	0	0	0	0	0	0	0	1	0	0	0	1	1	0	2	5	0	10
09-CG-133	0	0	3	3	0	0	0	0	0	0	1	0	0	2	0	1	3	1	0	12	6	0	26
09-CG-134	0	0	32	32	0	0	0	1	0	0	0	0	0	1	1	0	3	0	0	17	21	1	45
09-CG-135	0	0	15	15	0	0	0	1	0	0	0	2	0	5	3	0	3	6	4	35	9	12	80
09-CG-136	0	3	40	43	0	0	0	4	0	0	10	6	1	41	1	1	69	23	3	300	31	6	496
09-CG-137	0	0	24	24	0	0	0	1	0	0	0	1	0	19	0	2	4	12	0	60	30	2	131

Sample Number	Selected PseudoKIMs			KIM Count																			
	2.0 to 1.0 mm	1.0 to 0.5 mm	0.5 to 0.25 mm		2.0 to 1.0 mm						1.0 to 0.5 mm						0.5 to 0.25 mm						
	Low-Cr diopside	Low-Cr diopside	Low-Cr diopside	Total	GP	GO	DC	IM	CR	FO	GP	GO	DC	IM	CR	FO	GP	GO	DC	IM	CR	FO	Total
09-CG-139	0	1	15	16	0	0	0	0	0	0	2	0	1	5	0	3	5	1	0	28	25	1	71
09-CG-140	2	1	29	32	0	0	0	1	1	0	2	0	0	31	5	1	3	1	2	70	100	0	217
09-CG-142	0	0	10	10	0	0	0	0	0	0	0	0	0	1	1	1	4	0	0	10	10	7	34
09-CG-143	0	0	20	20	0	0	0	1	0	1	2	1	0	8	1	7	15	2	0	80	18	27	163

This page left intentionally blank.

Appendix 9.

Summary of adjusted kimberlite indicator minerals (KIM) counts and sample calculations

Abbreviations:

CR: Chromite

DC: Cr-diopside; distinctly emerald green (paler emerald green low-Cr diopside picked separately)

FO: Forsterite

GO: Orange mantle garnet, which includes both eclogitic pyrope-almandine (G3) and Cr-poor megacrystic pyrope (G1/G2) varieties, and may include unchecked (by SEM) grains of common crustal garnet

GP: Purple to red peridotitic garnet (G9/10 Cr-pyrope)

IM: Mg-ilmenite, which may include unchecked (by SEM) grains of common crustal ilmenite lacking diagnostic inclusions or crystal faces

SEM: Scanning Electronic Microscope

Sample Number	Original (2.0 to 0.25 mm)	Adjusted (2.0 to 0.25 mm)	Original KIMs (2.0 to 0.25 mm)							Adjusted (2.0 to 0.25 mm)						
	Low-Cr diopside	Low-Cr diopside	GP	GO	DC	IM	CR	FO	Total	GP	GO	DC	IM	CR	FO	Total
07CG-019	54	54	7	0	2	1	15	0	25	7	0	2	3	13	0	25
07CG-022	24	24	3	3	3	0	14	2	25	3	3	3	3	12	2	26
07CG-023	30	30	3	1	2	2	12	2	22	2	2	2	3	12	2	23
07CG-024	28	28	3	1	2	4	7	3	20	3	1	2	5	6	3	20
07CG-030	45	45	1	0	2	4	9	2	18	1	0	2	12	8	2	25
07CG-040	20	20	2	1	2	1	12	1	19	2	1	2	3	11	1	20
07CG-057	62	62	8	3	3	8	13	23	58	8	7	3	8	14	23	63
07CG-081	61	60	11	3	3	2	39	18	76	11	3	2	15	35	18	84
07CG-128A	20	20	1	0	1	1	9	1	13	1	1	1	6	7	1	17
07CG-128B	13	13	3	0	0	0	3	0	6	3	0	0	0	3	0	6
07CG-141	67	68	3	2	3	2	9	3	22	3	2	3	9	7	3	27
07CG-143	36	36	1	2	1	0	5	13	22	1	2	1	0	5	13	22
07CG-244	6	6	8	2	2	0	12	0	24	8	4	2	0	12	0	26
07CG-294-2	7	7	2	0	1	0	12	1	16	2	0	1	0	11	1	15
07CG-332	61	61	6	4	5	2	11	0	28	6	3	5	0	9	0	23
07CG-473	31	31	1	0	1	0	52	1	55	1	0	1	1	50	1	54
07CG-552	15	17	4	3	1	5	12	7	32	3	3	1	7	9	7	30
07CG-564	0	0	50	46	51	322	23	129	621	56	35	51	308	23	129	601
07CG-615	20	20	2	1	0	1	81	0	85	2	1	0	1	81	0	85
07CG-651-2	13	13	5	4	10	50	24	11	104	4	5	10	50	19	11	99
07CG-682-7	11	11	3	2	0	58	49	9	121	3	1	0	57	29	9	99
07CG-699-2	8	8	6	2	1	38	10	3	60	6	2	1	25	12	3	49
07CG-709	12	12	4	4	2	52	2	7	71	4	4	2	27	6	7	50
07CG-716	0	0	3	0	2	6	4	0	15	3	0	2	5	4	0	14
07CG-723	45	45	0	0	0	2	12	3	17	0	0	0	3	9	3	15
07CG-729	16	16	8	5	9	50	46	30	148	7	5	9	40	17	30	108

Sample Number	Original (2.0 to 0.25 mm)	Adjusted (2.0 to 0.25 mm)	Original KIMs (2.0 to 0.25 mm)							Adjusted (2.0 to 0.25 mm)						
	Low-Cr diopside	Low-Cr diopside	GP	GO	DC	IM	CR	FO	Total	GP	GO	DC	IM	CR	FO	Total
07CG-733	51	51	3	5	0	16	10	3	37	2	6	0	1	5	3	17
07CG-734	20	20	113	44	59	96	181	13	506	113	41	59	93	179	13	499
07CG-737-3	8	8	2	3	0	74	23	4	106	2	2	0	64	24	4	96
07CG-749	13	16	2	2	2	11	7	2	26	2	1	2	6	6	2	19
07CG-754	3	3	11	3	9	109	120	19	271	12	2	9	101	106	19	249
08CG-10-3	29	29	10	14	5	146	60	13	248	8	9	5	139	64	13	238
08CG-10-5	10	10	2	2	1	68	14	12	99	1	3	1	67	14	12	98
08CG-11	14	14	4	1	1	24	17	2	49	4	1	1	21	20	2	49
08CG-12	7	7	2	1	0	6	10	6	25	2	1	0	5	11	6	25
08CG-15	50	50	145	48	88	60	102	29	472	131	58	88	53	103	29	462
08CG-16	18	18	33	12	10	27	26	1	109	32	13	10	26	27	1	109
08CG-17	31	31	97	73	53	129	114	23	489	98	72	53	109	134	23	489
08CG-18	28	28	174	44	52	32	46	6	354	168	55	52	25	53	6	359
08CG-19	20	20	72	43	15	23	33	1	187	70	45	15	21	35	1	187
08CG-21	11	11	4	4	2	5	4	0	19	4	3	2	5	4	0	18
08CG-22	37	37	8	3	1	11	42	133	198	8	3	1	10	43	133	198
08CG-23	3	3	1	0	0	0	6	105	112	1	0	0	0	6	105	112
08CG-24	49	49	94	47	54	22	21	34	272	92	44	54	15	28	34	267
08CG-27	4	4	3	0	1	10	60	2	76	2	1	1	11	60	2	77
08CG-28	41	41	3	3	0	10	25	7	48	2	4	0	10	25	7	48
08CG-30	51	51	72	54	26	240	46	8	446	61	61	26	244	42	8	442
08CG-31	10	10	29	15	31	364	10	10	459	31	13	31	348	26	10	459
08CG-32	100	100	73	55	96	592	27	33	876	77	46	96	589	30	33	871
08CG-33	27	27	14	7	3	90	25	3	142	11	10	3	84	30	3	141
08CG-34	11	11	10	1	5	13	26	0	55	10	1	5	12	27	0	55
08CG-35	41	41	37	9	11	333	40	3	433	39	6	11	327	46	3	432
08CG-37	53	53	4	1	4	6	22	0	37	4	1	4	6	22	0	37
08CG-38	40	40	2	0	1	9	27	2	41	2	0	1	9	27	2	41
08CG-39	32	32	15	1	5	3	11	17	52	15	1	5	2	12	17	52
08CG-41	50	50	6	0	5	1	6	0	18	6	0	5	1	6	0	18
08CG-42	61	61	10	1	8	5	11	1	36	8	3	8	5	11	1	36
08CG-43	3	3	2	1	0	1	6	0	10	2	1	0	1	6	0	10
08CG-44	40	40	10	1	0	1	35	4	51	10	1	0	1	35	4	51

Sample Number	Original (2.0 to 0.25 mm)	Adjusted (2.0 to 0.25 mm)	Original KIMs (2.0 to 0.25 mm)							Adjusted (2.0 to 0.25 mm)						
	Low-Cr diopside	Low-Cr diopside	GP	GO	DC	IM	CR	FO	Total	GP	GO	DC	IM	CR	FO	Total
08CG-45	86	86	4	0	1	0	9	2	16	4	0	1	0	9	2	16
08CG-46	34	34	2	2	0	3	5	2	14	2	2	0	3	5	2	14
08CG-47	30	30	2	1	1	0	8	5	17	2	1	1	0	8	5	17
08CG-48	31	31	0	0	0	2	2	3	7	0	0	0	2	2	3	7
08CG-49	20	20	1	0	0	0	2	0	3	0	1	0	0	2	0	3
08CG-51	41	41	2	1	0	3	9	4	19	2	1	0	3	9	4	19
08CG-52	51	51	9	4	1	0	8	2	24	9	4	1	0	8	2	24
08CG-53	22	22	14	1	14	0	5	8	42	15	1	14	0	5	8	43
08CG-54	155	155	9	1	3	4	25	13	55	9	1	3	6	23	13	55
08CG-55	56	56	7	1	2	14	19	2	45	6	1	2	13	20	2	44
08CG-56	101	101	4	3	7	0	40	3	57	3	3	7	3	37	3	56
08CG-57	53	53	9	8	8	5	8	5	43	7	7	8	5	8	5	40
09-CG-100	3	3	0	0	1	0	13	0	14	0	0	1	0	13	0	14
09-CG-101	8	8	1	0	0	1	35	1	38	1	0	0	1	35	1	38
09-CG-102	42	42	17	2	10	1	5	4	39	17	2	10	1	5	4	39
09-CG-103	1	1	3	0	1	1	20	0	25	3	0	1	1	20	0	25
09-CG-104	18	18	3	4	4	0	16	3	30	3	4	4	1	15	3	30
09-CG-106	24	24	4	0	1	1	9	13	28	4	0	1	1	9	13	28
09-CG-108	10	10	5	3	1	0	21	0	30	5	3	1	1	20	0	30
09-CG-109	18	18	2	1	1	4	15	5	28	2	0	1	3	16	5	27
09-CG-110	9	9	5	1	0	3	33	0	42	5	1	0	3	33	0	42
09-CG-111	8	8	1	1	0	4	12	0	18	1	1	0	4	11	0	17
09-CG-113	310	310	124	51	48	317	53	225	818	119	53	48	291	78	225	814
09-CG-115	4	4	0	0	0	10	23	0	33	0	0	0	10	23	0	33
09-CG-116	60	60	6	1	1	2	5	1	16	6	1	1	2	5	1	16
09-CG-118	54	54	7	4	0	2	24	1	38	6	4	0	5	21	1	37
09-CG-119	2	2	3	0	1	1	8	0	13	2	0	1	1	8	0	12
09-CG-012	8	8	0	0	0	1	9	0	10	0	0	0	1	9	0	10
09-CG-120	30	30	2	0	0	3	24	1	30	2	0	0	3	24	1	30
09-CG-121	17	17	5	2	1	0	7	1	16	5	2	1	0	7	1	16
09-CG-122	26	26	1	1	0	0	11	0	13	1	1	0	0	11	0	13
09-CG-123	60	60	0	2	1	0	4	0	7	0	2	1	0	3	0	6
09-CG-124	26	26	2	2	1	2	17	3	27	2	2	1	3	16	3	27
09-CG-125	40	40	4	0	2	0	14	3	23	4	0	2	2	12	3	23

Sample Number	Original (2.0 to 0.25 mm)	Adjusted (2.0 to 0.25 mm)	Original KIMs (2.0 to 0.25 mm)							Adjusted (2.0 to 0.25 mm)						
	Low-Cr diopside	Low-Cr diopside	GP	GO	DC	IM	CR	FO	Total	GP	GO	DC	IM	CR	FO	Total
09-CG-126	30	30	2	0	1	1	7	0	11	2	0	1	1	7	0	11
09-CG-127	27	27	2	0	0	6	34	48	90	2	0	0	5	35	48	90
09-CG-128	16	16	3	0	0	0	2	1	6	3	0	0	0	2	1	6
09-CG-129	63	63	2	1	0	8	12	9	32	2	1	0	8	12	9	32
09-CG-132	6	6	1	1	1	2	5	0	10	0	2	1	2	4	0	9
09-CG-133	3	3	4	1	0	14	6	1	26	4	1	0	14	5	1	25
09-CG-134	32	32	3	0	0	19	22	1	45	2	1	0	19	21	1	44
09-CG-135	15	15	3	8	4	41	12	12	80	3	8	4	34	16	12	77
09-CG-136	43	43	79	29	4	345	32	7	496	48	56	4	349	26	7	490
09-CG-137	24	24	4	13	0	80	30	4	131	3	14	0	78	31	4	130
09-CG-139	16	16	7	1	1	33	25	4	71	2	4	1	30	28	4	69
09-CG-014	4	4	2	0	0	3	18	0	23	2	0	0	3	18	0	23
09-CG-140	32	32	5	1	2	102	106	1	217	5	1	2	132	73	1	214
09-CG-142	10	10	4	0	0	11	11	8	34	3	1	0	11	11	8	34
09-CG-143	20	20	17	3	0	89	19	35	163	11	9	0	89	19	35	163
09-CG-016	1	1	2	0	1	0	9	0	12	2	0	1	0	9	0	12
09-CG-017	9	9	5	1	1	10	4	3	24	5	1	1	10	4	3	24
09-CG-019	0	0	1	0	1	9	10	0	21	1	0	1	9	10	0	21
09-CG-020	9	9	0	0	0	1	5	0	6	0	0	0	2	4	0	6
09-CG-021	20	20	8	2	0	66	16	6	98	8	2	0	57	15	6	88
09-CG-022	17	17	5	0	0	19	2	1	27	4	1	0	17	4	1	27
09-CG-024	10	10	2	1	0	1	7	2	13	2	1	0	1	7	2	13
09-CG-026	3	3	1	0	0	0	2	0	3	1	0	0	0	2	0	3
09-CG-027	9	9	2	2	0	1	5	0	10	1	3	0	1	5	0	10
09-CG-028	4	4	0	0	0	10	12	2	24	0	0	0	10	12	2	24
09-CG-029	6	6	2	1	0	5	5	0	13	1	2	0	6	4	0	13
09-CG-035	0	0	0	0	0	0	0	0	0	0	0	0	0	0	0	0
09-CG-036	5	5	3	0	0	3	1	0	7	3	0	0	3	1	0	7
09-CG-037	13	13	2	0	1	2	3	0	8	2	0	1	2	3	0	8
09-CG-038	4	4	3	1	1	4	3	0	12	3	1	1	4	3	0	12
09-CG-039	8	8	10	18	1	86	15	0	130	9	20	1	88	12	0	130
09-CG-040	24	24	3	6	0	16	9	1	35	3	4	0	16	9	1	33
09-CG-041	11	11	2	1	0	4	3	0	10	2	1	0	4	2	0	9
09-CG-042	42	42	6	0	0	22	20	0	48	6	0	0	23	18	0	47

Sample Number	Original (2.0 to 0.25 mm)	Adjusted (2.0 to 0.25 mm)	Original KIMs (2.0 to 0.25 mm)							Adjusted (2.0 to 0.25 mm)						
	Low-Cr diopside	Low-Cr diopside	GP	GO	DC	IM	CR	FO	Total	GP	GO	DC	IM	CR	FO	Total
09-CG-043	51	51	2	0	1	5	10	2	20	2	0	1	6	8	2	19
09-CG-044	29	29	2	1	0	27	19	1	50	1	2	0	27	19	1	50
09-CG-045	24	24	3	1	1	9	18	1	33	3	1	1	9	18	1	33
09-CG-046	53	53	5	1	2	35	44	6	93	5	1	2	29	48	6	91
09-CG-047	62	62	7	7	1	2	4	0	21	8	3	1	2	4	0	18
09-CG-048	63	63	1	2	0	15	23	0	41	1	1	0	16	22	0	40
09-CG-049	40	40	5	2	0	29	22	9	67	5	2	0	30	20	9	66
09-CG-050	12	12	4	3	1	21	22	0	51	4	2	1	23	18	0	48
09-CG-051	9	9	4	2	1	8	10	0	25	1	5	1	8	9	0	24
09-CG-052	6	6	0	4	1	3	12	0	20	1	3	1	4	11	0	20
09-CG-053	18	18	2	1	0	6	7	2	18	2	1	0	6	7	2	18
09-CG-054	17	17	3	0	3	1	24	10	41	3	0	3	1	23	10	40
09-CG-055	101	101	4	1	2	4	41	3	55	4	1	2	4	36	3	50
09-CG-058	22	22	1	0	0	0	7	6	14	1	0	0	0	7	6	14
09-CG-059	14	14	79	35	0	363	20	16	513	55	59	0	358	24	16	512
09-CG-060	60	60	3	3	0	25	14	0	45	3	3	0	25	14	0	45
09-CG-062	19	19	4	2	1	26	31	2	66	4	2	1	26	27	2	62
09-CG-063	40	40	110	121	16	206	84	34	571	106	124	16	197	75	34	551
09-CG-065	113	113	9	4	5	26	20	104	168	10	2	5	26	18	104	165
09-CG-066	81	81	11	3	0	26	17	16	73	9	5	0	25	17	16	72
09-CG-067	7	7	1	2	0	23	28	7	61	1	2	0	9	27	7	46
09-CG-068	14	14	2	2	0	12	9	4	29	1	2	0	13	7	4	27
09-CG-069	40	40	3	1	0	58	47	4	113	3	1	0	55	50	4	113
09-CG-070	21	21	1	3	0	1	11	0	16	1	3	0	2	9	0	15
09-CG-071	13	13	2	0	1	9	8	1	21	1	0	1	10	7	1	20
09-CG-072	53	53	0	2	1	7	16	1	27	0	2	1	8	12	1	24
09-CG-073	13	13	1	1	0	1	5	0	8	1	0	0	1	5	0	7
09-CG-074	10	10	1	0	0	6	9	1	17	1	0	0	7	7	1	16
09-CG-075	12	12	2	1	0	6	1	0	10	2	1	0	6	1	0	10
09-CG-076	8	8	0	0	0	2	8	1	11	0	0	0	2	7	1	10
09-CG-078	9	9	1	0	0	4	9	1	15	1	0	0	5	8	1	15
09-CG-079	7	7	0	0	1	8	3	0	12	0	0	1	8	3	0	12
09-CG-080	4	4	4	1	0	14	4	0	23	4	1	0	14	4	0	23
09-CG-081	7	7	3	2	0	9	8	11	33	1	4	0	9	8	11	33

Sample Number	Original (2.0 to 0.25 mm)	Adjusted (2.0 to 0.25 mm)	Original KIMs (2.0 to 0.25 mm)							Adjusted (2.0 to 0.25 mm)						
	Low-Cr diopside	Low-Cr diopside	GP	GO	DC	IM	CR	FO	Total	GP	GO	DC	IM	CR	FO	Total
09-CG-084	1	1	0	2	1	3	6	0	12	0	2	1	4	5	0	12
09-CG-085	0	0	1	0	0	0	2	0	3	1	0	0	0	2	0	3
09-CG-086	9	9	24	11	0	155	14	0	204	16	19	0	146	16	0	198
09-CG-090	42	42	1	6	0	15	6	4	32	1	6	0	16	5	4	32
09-CG-091	16	16	2	0	2	8	8	1	21	2	0	2	8	6	1	19
09-CG-092	26	26	1	1	0	3	9	7	21	1	1	0	3	9	7	21

Appendix 9 (continued). Sample calculations to show how adjusted KIM counts were determined.

Case A: less than 20 grains microprobed

Sample 1 has counts of 10 GP and 2 GO grains

Microprobed: 8 GP grains; 0 GO grains

Results of microprobing

- of the 8 GP grains microprobed, there are 5 GP, 2 GO and 1 other grains
- 0 GO grains microprobed

Adjusted GO and GP

GP: 10-2-1=7 or 5+2=7

GO: 2+2=4

Case B: 20 or more grains microprobed

Sample 2 has counts of 200 GP and 100 GO grains

Microprobed: 100 GP grains; 50 GO grains

Results of microprobing

- Of the 100 GP grains microprobed, there are 80 GP, 19 GO, and 1 other grains
- Of the 50 GO grains microprobed, there are 30 GO, 15 GP, and 5 other grains

Adjusted GP and GO

GP: (80/100)x200+(15/50)x100=160+30=190

GO: (30/50)x100+(19/100)x200=60+38=98

GP includes G9, G10, G11, G12, and G5

GO includes G1, G3, and G4

Metric Conversion Table

Conversion from SI to Imperial			Conversion from Imperial to SI		
SI Unit	*Multiplied by*	*Gives*	*Imperial Unit*	*Multiplied by*	*Gives*
		LENGTH			
1 mm	0.039 37	inches	1 inch	**25.4**	mm
1 cm	0.393 70	inches	1 inch	**2.54**	cm
1 m	3.280 84	feet	1 foot	**0.304 8**	m
1 m	0.049 709	chains	1 chain	20.116 8	m
1 km	0.621 371	miles (statute)	1 mile (statute)	**1.609 344**	km
		AREA			
1 cm^2	0.155 0	square inches	1 square inch	**6.451 6**	cm^2
1 m^2	10.763 9	square feet	1 square foot	**0.092 903 04**	m^2
1 km^2	0.386 10	square miles	1 square mile	2.589 988	km^2
1 ha	2.471 054	acres	1 acre	0.404 685 6	ha
		VOLUME			
1 cm^3	0.061 023	cubic inches	1 cubic inch	**16.387 064**	cm^3
1 m^3	35.314 7	cubic feet	1 cubic foot	0.028 316 85	m^3
1 m^3	1.307 951	cubic yards	1 cubic yard	0.764 554 86	m^3
		CAPACITY			
1 L	1.759 755	pints	1 pint	0.568 261	L
1 L	0.879 877	quarts	1 quart	1.136 522	L
1 L	0.219 969	gallons	1 gallon	**4.546 090**	L
		MASS			
1 g	0.035 273 962	ounces (avdp)	1 ounce (avdp)	28.349 523	g
1 g	0.032 150 747	ounces (troy)	1 ounce (troy)	**31.103 476 8**	g
1 kg	2.204 622 6	pounds (avdp)	1 pound (avdp)	**0.453 592 37**	kg
1 kg	0.001 102 3	tons (short)	1 ton(short)	**907.184 74**	kg
1 t	1.102 311 3	tons (short)	1 ton (short)	**0.907 184 74**	t
1 kg	0.000 984 21	tons (long)	1 ton (long)	**1016.046 908 8**	kg
1 t	0.984 206 5	tons (long)	1 ton (long)	**1.016 046 9**	t
		CONCENTRATION			
1 g/t	0.029 166 6	ounce (troy) / ton (short)	1 ounce (troy) / ton (short)	34.285 714 2	g/t
1 g/t	0.583 333 33	pennyweights / ton (short)	1 pennyweight / ton (short)	1.714 285 7	g/t

OTHER USEFUL CONVERSION FACTORS

	Multiplied by	
1 ounce (troy) per ton (short)	31.103 477	grams per ton (short)
1 gram per ton (short)	0.032 151	ounces (troy) per ton (short)
1 ounce (troy) per ton (short)	20.0	pennyweights per ton (short)
1 pennyweight per ton (short)	0.05	ounces (troy) per ton (short)

*Note: Conversion factors in **bold** type are exact. The conversion factors have been taken from or have been derived from factors given in the* Metric Practice Guide for the Canadian Mining and Metallurgical Industries*, published by the Mining Association of Canada in co-operation with the Coal Association of Canada.*

ISSN 0826-9580 (Print)
ISBN 978-1-4435-9957-3 (Print)

ISSN 1916-6117 (online)
ISBN 978-1-4435-9958-0 (PDF)

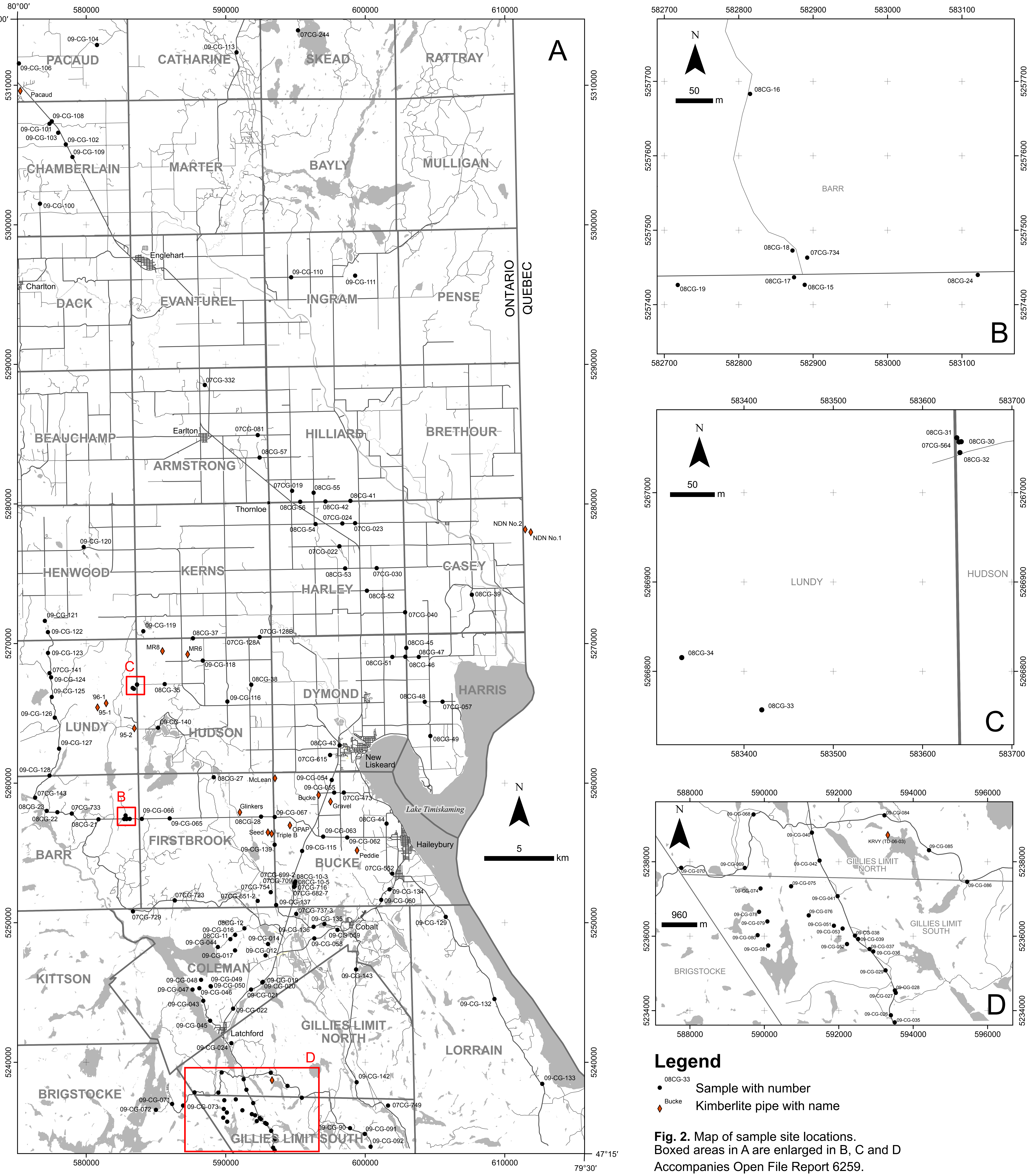

Fig. 2. Map of sample site locations.
Boxed areas in A are enlarged in B, C and D
Accompanies Open File Report 6259.